Overexpression and analysis on posttranslational modification of the Retinoic Acid Related Orphan Receptor α4

Dissertation zur
Erlangung des Doktorgrades
der Naturwissenschaften

vorgelegt beim Fachbereich
Biochemie, Chemie und Pharmazie
der Johann Wolfgang Goethe-Universität
in Frankfurt am Main

von
Adriane Lechtken
aus Erlangen

Frankfurt am Main (2007)
(D30)

Vom Fachbereich Biochemie, Chemie und Pharmazie
der Johann Wolfgang Goethe-Universität als Dissertation angenommen.

Dekan:	Prof. Dr. Harald Schwalbe
Gutachter:	Prof. Dr. Dieter Steinhilber
	Prof. Dr. Oliver Werz
Datum der Disputation:	30.08.2007

“There is a theory which states that if ever anybody discovers exactly what the Universe is for and why it is here, it will instantly disappear and be replaced by something even more bizarre and inexplicable. There is another theory which states that this has already happened.”

(Douglas Adams)

CONTENTS

1 INTRODUCTION

1.1 Nuclear Receptors

Nuclear receptors are ligand-inducible transcription factors that modulate gene expression in response to a wide range of developmental, physiological, and environmental cues. They are involved in numerous processes like growth, cell differentiation, proliferation, homeostasis and apoptosis. In a signal transduction cross-talk, they regulate the activities of major signaling cascades. Ligands for nuclear receptors are small lipophilic molecules such as steroid and thyroid hormones or the active forms of vitamin A (retinoids) and vitamin D. Recently, it was shown that products of the lipid metabolism, such as fatty acids, prostaglandins, or cholesterol derivatives, can regulate gene expression by binding to nuclear receptors. However, for a variety of nuclear receptors ligands still remain to be discovered, some of these "orphans" are discussed to act as constitutively activating transcription factors without binding of a ligand.

Transcriptional regulation results from binding of nuclear receptors to specific DNA motifs, the hormone response elements (HREs), which leads to an activation or suppression of target gene expression. Nuclear receptor activity is controlled by three distinct mechanisms, whereas induction by a small ligand plays the major role. A further mechanism of activation is the covalent posttranslational modification, usually in form of a phosphorylation, acetylation, methylation or ubiquitinylation, regulated by events at the cellular membrane or during the cell cycle. Protein-protein interactions generally occur through contact with other transcription factors including nuclear receptors themselves. All three mechanisms work either individually or in concert with each other to modulate a specific signal. In addition, some nuclear receptors can also mediate rapid nongenomic effects without changes in gene transcription [1].

Evolutionary studies of the nuclear receptor subfamily according to Laudet et al. [2] have led to a subdivision into seven different classes (0-VI). Different receptor families, denoted by their most commonly used trivial names, represent each class. Greek letters identify members of these families, the receptor isoforms. A list of selected known mammalian nuclear receptors and their respectively ligands is presented in Table 1.1.

Class	Receptor	Ligand	Binding
I	TRα, β (Thyroid Hormone Receptor)	thyroid hormone (T_3)	H
	RARα, β, γ (Retinoic Acid Receptor)	retinoic acid	H
	VDR (Vitamin D Receptor)	1-25$(OH)_2$ vitamin D_3	H
	PPARα, β, γ (Peroxisome Proliferator Activated Receptor)	leukotriene B4, eicosanoids, thiazolidinediones, 15-deoxy-12,41-prostaglandine J2, polyunsaturated fatty acids	H
	RevErbα, β (Reverse ErbA)	unknown	M, D
	RZR/RORα, β, γ (Retinoid Z Receptor/ Retinoic Acid Related Orphan receptor)	cholesterol?	M, D
II	RXRα, β, γ (Retinoid X Receptor)	9-cis-retinoic acid	D
III	GR (Glucocorticoid Receptor)	glucocorticoids	D
	AR (Androgen Receptor)	androgens	D
	PR (Progesterone Receptor)	progestins	D
	ERα, β (Estrogene Receptor)	estradiol	D
IV	NGFI-Bα, β, γ (NGF induced clone B)	unknown	M, D, H
V	SF-1/FTZ-F1 (Steroidogenic Factor-1/ Fushi Tarazu Factor-1)	oxysterols	M
VI	GCNF (Germ Cell Nuclear Factor)	unknown	D
0	SHP (Small Heterodimeric Partner)	unknown	H

Table 1.1: Subfamily classes of mammalian nuclear receptors with a selection of family members and their respective ligands. *Character of nuclear receptor binding to hormone response elements (HREs) as indicated (M: monomer; D: homodimer; H: heterodimer) [2,3].*

1.1.1 Structure of Nuclear Receptors

Nuclear receptors exhibit a modular structure with different regions corresponding to autonomous functional domains that can be interchanged between related receptors without loss of function. A typical nuclear receptor is composed of four domains, a variable NH_2-terminal modulatoric A/B domain, a conserved DNA-binding domain (DBD or region C), a linking hinge domain (region D) and a conserved ligand binding domain (LBD or region E). Some receptors also contain a COOH-terminal region F of so far unknown function. A schematical constitution of nuclear receptors is shown in Fig. 1.2.

Fig. 1.2: Schematical construction of a typical nuclear receptor composed of several functional domains: *the modulatoric A/B region containing the ligand-independent AF-1 (activation function-1) transactivation domain, the conserved DNA binding domain C, the variable hinge region D, the ligand binding domain E containing the ligand-dependent transactivation domain AF-2 and region F with unknown function.*

The modulatoric A/B domain is very variable in length and primary sequence. In many cases a transcriptional activation function domain (AF-1) is included, this domain contributes to constitutive ligand-independent activation of the receptor, e. g. after phosphorylation of this site [4]. In contrast, the AF-2 within the C-terminal ligand binding region is responsible for the ligand-dependent transactivation. The strong AF-1 domain within the A/B region of the nuclear receptor PPARα is phosphorylated by MAP kinases (mitogen activated protein kinases) resulting in an enhanced transcriptional activity [5]. By contrast, the activity of PPARγ is decreased after phosphorylation by MAP kinases at the A/B domain [6]. Interestingly, this PPARγ modification reduces ligand binding to the receptor, showing that ligand binding can also be regulated by intramolecular communication between the modulatoric and the ligand-binding domain. The nuclear receptor isoforms that only diverge from their A/B regions are often generated from a single gene by alternative splicing or by the use of different promoters. This is the case for ROR isoforms α1-α4 which are identical in their DBD, hinge region and LBD, but differ in their NH_2-terminal regions. Because of their different A/B domain constitution, RORα isoforms show promoter as well as cell specific activity.

The DNA-binding domain (DBD) enables the receptor to bind to specific response elements located in the promoter region of the receptor target genes. The DBD is the most conserved domain among the nuclear receptor superfamily. This domain comprises two "zinc fingers" that span over 60-70 amino acids, in each zinc finger one zinc ion is coordinated tetrahedrically by four cysteines and both zinc finger modules are fold together to form a compact (Fig. 1.3). The amino acids that are required for recognition of DNA motifs are located at the base of the first zinc finger in a region termed "P box". Further residues at the second zinc finger form the "D box" which is involved in receptor dimerization. The DBD forms two α-helices: the first binds to the major groove of the DNA contacting specific bases, and the second forms a right angle with the first recognition helix [7-9]. C-terminal to the second zinc finger, is the 12-15 amino acids long carboxy-terminal extension (CTE) located, embedding the T box (tandem box) that is necessary for receptor dimerization on the DNA [10] and the A box (adenine box) that serves for recognition of AT regions within a promoter, in case of binding as a monomer [11].

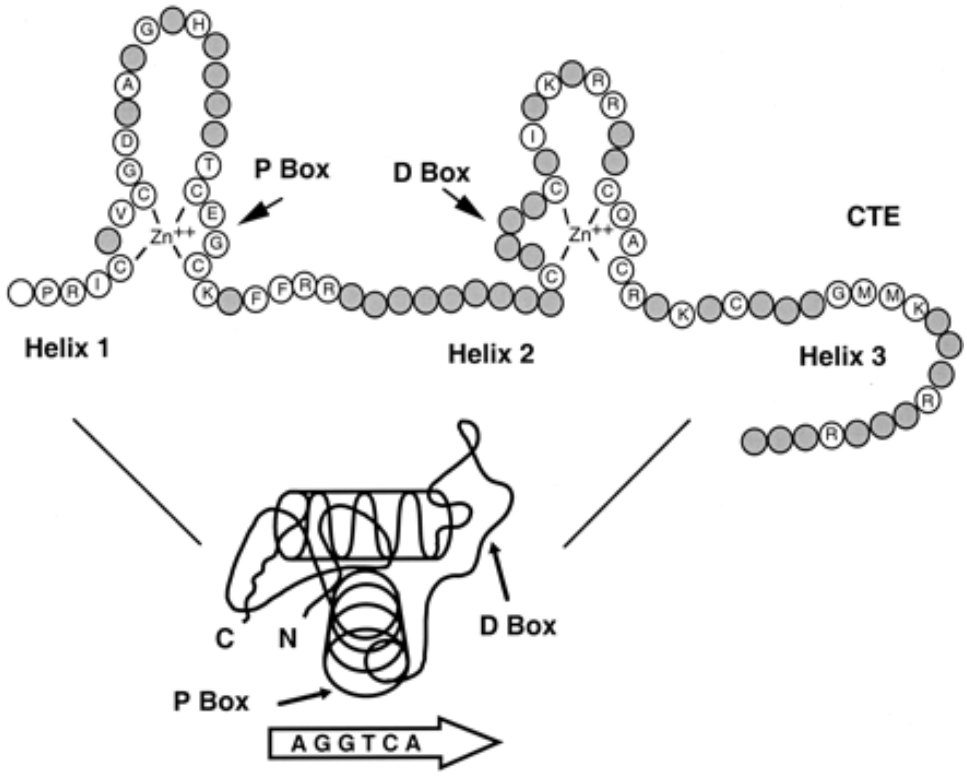

Fig. 1.3: DNA binding domain of nuclear receptors. *Two zinc fingers are formed by four conserved cysteine residues, respectively, that coordinate a zinc ion tetrahedrically. Other conserved residues are designated by the corresponding letter abbreviation. Helix 1 contains the P box involved in the recognition of response element. Residues in the second zinc finger labeled as D box form the dimerization interface. Helix 1 and helix 2 cross at right angles to form the core of the DBD that recognizes a hemi-site of the response element [12].*

The linking hinge region is weakly conserved among the nuclear receptors. It serves as a rotating and arranging hinge between the DBD and the ligand binding domain (LBD), facilitating nuclear receptors to bind as homo- or heterodimers to a repeated nucleotide hexamer sequence [13,14]. In many cases it harbors a nuclear localization signal and residues that are necessary for interaction with nuclear receptor corepressors [15,16].

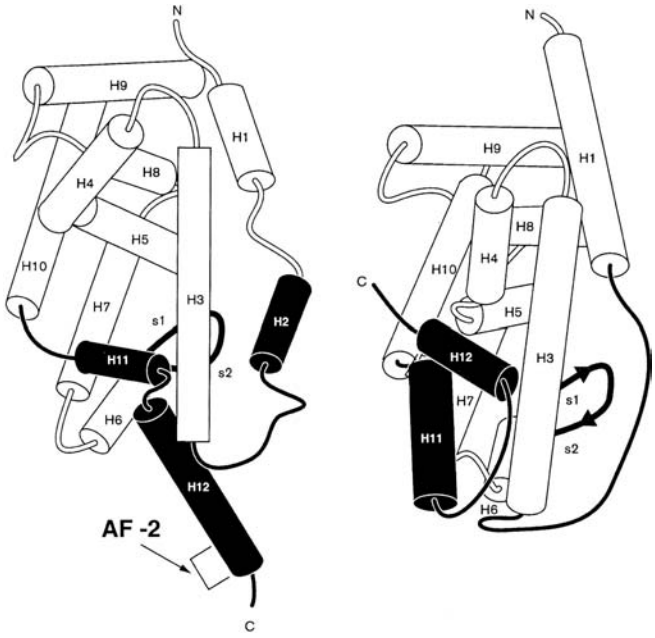

Fig. 1.4: Schematical drawing of the nuclear receptor ligand-binding domain (LBD). *Cylinders represent α–helices that are numbered from 1 to 12. Left: LBD from the crystal structure of unbound RXRα with helix 12 positioned outwards. Right: Ligand-bound LBD of RARγ, helix 12 seals the ligand binding pocket as a lid [17].*

The LBD is formed by 12 conserved α-helical regions numbered from H1 to H12 that are folded into three layers. In the central of these three layers a cavity is created, the ligand binding pocket, where the ligand is accommodated. This domain is mainly hydrophobic and its size varies among the different receptors, thus allowing binding of differently sized ligands. Interaction of a ligand within the ligand-binding cavity induces a structural transition which triggers a mechanism like a mouse trap: in case of unbound receptor, helix 12 is positioned outwards, in the opposite direction of the ligand-binding cavity. A ligand-induced reposition leads to a conformation where helix 12 seals the ligand pocket as a lid and thus further stabilizes ligand binding by contributing to the hydrophobic trap (Fig. 1.4). These conformational changes generate a new surface for the recruitment of coactivators [18] which include the p160 family (SRC-1/NCoR1; TIF2/GRIP-1/SRC-2; p/CIP/RAC3/ACTR/AIB-1/TRAM-1) and p300/CBP [19,20]. These coactivators, which have intrinsic acetyltransferase activity, recruit other large complexes with ATP-dependent histone remodeling, histone

acetyltransferase (PCAF) [21,22], histone methyltransferase (CARM1/PRMT1) [22,23] and histone kinase activities [24]. These complexes decondense chromatine through histone remodeling and covalent modifications in order to promote gene expression by binding to the receptor response elements embedded in the target gene promoter. For the most nuclear receptors recruitment of an additional complex is required (variously termed TRAP, DRIP or SMCC) to facilitate the entry of transcription machinery (RNA polymerase II and the general transcription factors) to the preinitiation complex [25,26].

1.1.2 Hormone Response Elements (HREs)

Nuclear receptors regulate gene transcription by binding to specific DNA sequences, known as hormone response elements or HREs, in the 5´-flanking regulatory region of a target gene. The analysis of a large number of natural occurring as well as synthetic HREs revealed a sequence of 6 base pairs as core recognition motif. The responsive elements consist in the nucleotide hexamer AG(G/T)TCA, and AGAACA for steroid receptors, respectively. These motifs represent idealized sequences, natural occurring HREs can show significant variation from that consensus. Although some monomeric receptors can bind to a single hexamer, most receptors bind as homo- or heterodimers to HREs composed of two core hexameric motifs. Steroid receptors almost exclusively bind as homodimers to the HREs. Two steroid hormone receptor monomers bind cooperatively to their response elements, dimerization interfaces have been identified both in the LBD and in the DBD. Other nuclear receptors use similar dimer interfaces because the corresponding residues are highly conserved in different receptors. Although several nonsteroidal nuclear receptors also bind DNA as homodimers, most nonsteroidal receptors bind preferentially as heterodimers. In this case, the Retinoid X Receptor (RXR) is the promiscuous partner for different receptors [27-29]. Typical heterodimeric receptors such as the TR, RAR or VDR can also bind as homodimers to their response elements, but heterodimerization with RXR strongly increases the efficiency of DNA binding and thus transcriptional activity. In addition, some receptors can bind as monomers, homodimers or heterodimers to different response elements. For dimeric HREs, the half-sites can be configured as palindromes, inverted palindromes or direct repeats (Fig. 1.5). Palindromic or inverted palindromic DNA repeats impose a symmetrical head-to-head arrangement of the DBDs making analogous contacts with one half-site. Direct repeats consist in two consensus motifs that head towards the same direction, connected by a linker of one to

six nucleotides (DR-1 to DR-6). In the case of binding as a monomer, a 5-6 bp long A/T-rich sequence precedes the hexamer [30].

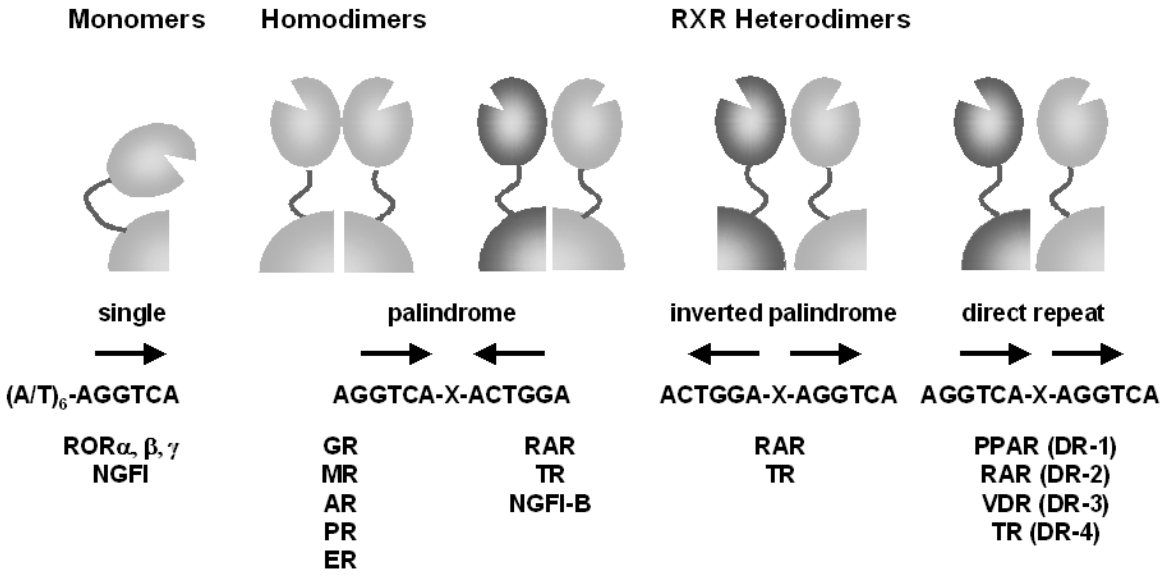

Fig. 1.5: Binding of receptors to the hormone response elements (HREs). *Receptors can bind as monomers, homodimers or RXR heterodimers to DNA. Nuclear receptor binding sites are composed of one or two half-core motifs, generally AGGTCA or a close variant that could be preceded by a 5′-flanking A/T-rich sequence. Half-core sequences in dimeric sites can be arranged as palindromes, inverted palindromes or direct repeats [3,12].*

1.1.3 Regulation of Nuclear Receptor Activity

The steroid hormone receptors, such as the estrogen (ER), androgen (AR), progesterone (PR) or glucocorticoid (GR) receptors, are associated to chaperone complexes and thus held in the cytoplasm. Binding of a ligand acts as an on-switch resulting in release from their chaperone complex, subsequent dimerization, entrance into the nucleus and the binding to their hormone response elements in the promoter region of the target genes. In contrast, the receptors for non-steroidal hormones such as the vitamin D (VDR), retinoic acid (RAR) and peroxisome proliferator-activated (PPAR) receptors are preliminary found in the nucleus and bound to their response elements as heterodimers with the Retinoid X Receptor (RXR). They are associated with histone deacetylase containing complexes and with corepressors, resulting in chromatin compaction and gene-silencing. Upon ligand binding, the nuclear receptor corepressor interface is destabilized leading to the dissociation of the corepressors and subsequent recruitment of coactivators [18]. The AF-2 domain within the LBD cooperates

with the second activation domain in the N-terminus, the AF-1 domain [31], to associate with multiple complexes to alter the chromatin structure surrounding of the target gene promoter [32,33]. At the end the transcription machinery is recruited, including RNA polymerase II and the general transcription factors (GTF) [34]. Simultaneously, the nuclear receptor and their coregulators are subjected to rapid modifications like phosphorylation, acetylation, methylation, ubiquitinylation and degradation by the proteasome, controlling transcriptional activation in a combinatorial, coordinated and sequential manner [35].

Recruitment of coregulators

Following the activation signal, nuclear receptors bound to their response elements, initiate an ordered and coordinated recruitment of a series of coactivator complexes. Five major classes of coactivators have been identified: (i) members of the p160 subfamily (SRC-1/N-CoR1, SRC-2/GRIP-2/TIF-2, SRC-3/ACTR/AIB1/p/CIP/RAC3/TRAM-1) [36] that serve as adapters recruiting other complexes, (ii) histone acetyltransferases (HATs), such as CBP/p300 [37], (iii) histone arginine methyltransferases (HMTs) [38], (iv) nucleosome remodeling complexes [21] and (v) the multisubunit mediator complex that acts as bridge between the nuclear receptor and the basal transcriptional machinery [39]. The temporal order of recruitment of these coactivators with different enzymatic activities is determined, but may differ from one target gene to another [40].

Ubiquitine proteasome pathway

Classically, the ubiquitine-proteasome pathway targets regulatory proteins for proteolysis. Recently it was demonstrated that nuclear receptors as well as coregulators and components of the GFT machinery are ubiquitinylated and degraded by the proteasome in response to a ligand. Degradation by the ubiquitine-proteasome pathway might provide an efficient mechanism for the termination of nuclear receptors interaction with the promoter [41-45].

Phosphorylation

Several extracellular signals such as growth factors, insulin, stress, cytokines, or other signals, activate cytosolic kinase cascade pathways, ending at different kinases, including MAPKs (ERKs, JNKs, p38), protein kinase C, or cyclic AMP-dependent protein kinase, which can subsequently enter the nucleus and phosphorylate nuclear receptors. Estradiol and retinoic acid signaling for example, leads to the rapid activation of MAPK (ERKs and p38 MAPK) which enter the nucleus and phosphorylate the AF-1 domains of ERα and RARγ [46-48].

PPARγ transcriptional activity is switched off in response to insulin, subsequent to phosphorylation by MAPKs. Several effects of nuclear receptor phosphorylation have been shown, such as reduction of the ligand-binding affinity through interdomain communication between the phosphorylated AF-1 domain and the ligand-binding pocket [6], or the degradation of the receptor by the ubiquitine proteasome pathway as it was shown for RARγ and PR [46,49,50]. In the case of RevErb, phosphorylation by GSK3β stabilizes against degradation by the proteasome. In addition, phosphorylation of several nuclear receptors in their DNA binding domain has been shown to switch off their activity by inducing them to dissociate from their promoter [47]. The activity of RARs is negatively modulated in response to stress upon phosphorylation of the LBD of their RXR heterodimerization partner [51]. It has been proposed that this phosphorylation sterically precludes the formation of the surface for coactivator recruitment. Thus, phosphorylation in response to extracellular signals seems rather to terminate the response to the ligand, ensuring the escape of nuclear receptors from the transcription inition complex.

However, phosphorylation of the N-terminal A/B region of ERα, ERβ, and PPARα by MAPKs or Akt helps the recruitment of coactivators, which increases the efficiency of target gene expression. RARs, ERα, PPARs and AR have been reported to be phosphorylated by the Cdk7/cyclin H/MAT1 (CAK) subcomplex of TFIIH, which is a general transcription factor mediating transcription activation and nucleotide excision repair. TFIIH is composed of 9 subunits, one of them, cdk7, has a cyclin dependent kinase activity. Binding to the promoter makes TFIIH able to dock the liganded nuclear receptor that is bound to its response element, thereby allowing the recognition of the cdk7 phosphorylation site in the proline-rich motif within the AF-1 domain by the cdk7 kinase subunit. Phosphorylation of the N-terminal A/B region of the nuclear receptor leads to an increase of ligand-dependent response.

As shown in Fig. 1.6, the majority of nuclear receptor phosphorylation sites lie within the N-terminal A/B region. For certain nuclear receptors such as PR, phosphorylation of this region is rather complex with at least 13 phosphorylation sites. For others such as RARs or PPARs, phosphorylation of this region concerns only one or two residues. VDR is an exception as this region is not phosphorylated at all, probably due to its very short length. Most of these sites are phosphorylated either “constitutively” or in response to the ligand. Table 1.7 shows an overview about the effects of nuclear receptor phosphorylation.

Moreover, corepressors and coactivators were also shown to be phosphorylated by MAPKs in response to steroidal and non-steroidal hormones. Recently it was suggested, that phosphorylation of the N-CoR/SMRT corepressors might represent a mark for their

ubiquitinylation and degradation to allow the recruitment of coactivators [52]. Finally, histones were found to be targets of the MAPKs. A combinatorial and coordinated model has been suggested whereby phosphorylation participates with acetylation, methylation, and ubiquitinylation to provide motifs for the recruitment of other chromatin modifying or remodeling complexes [53,54].

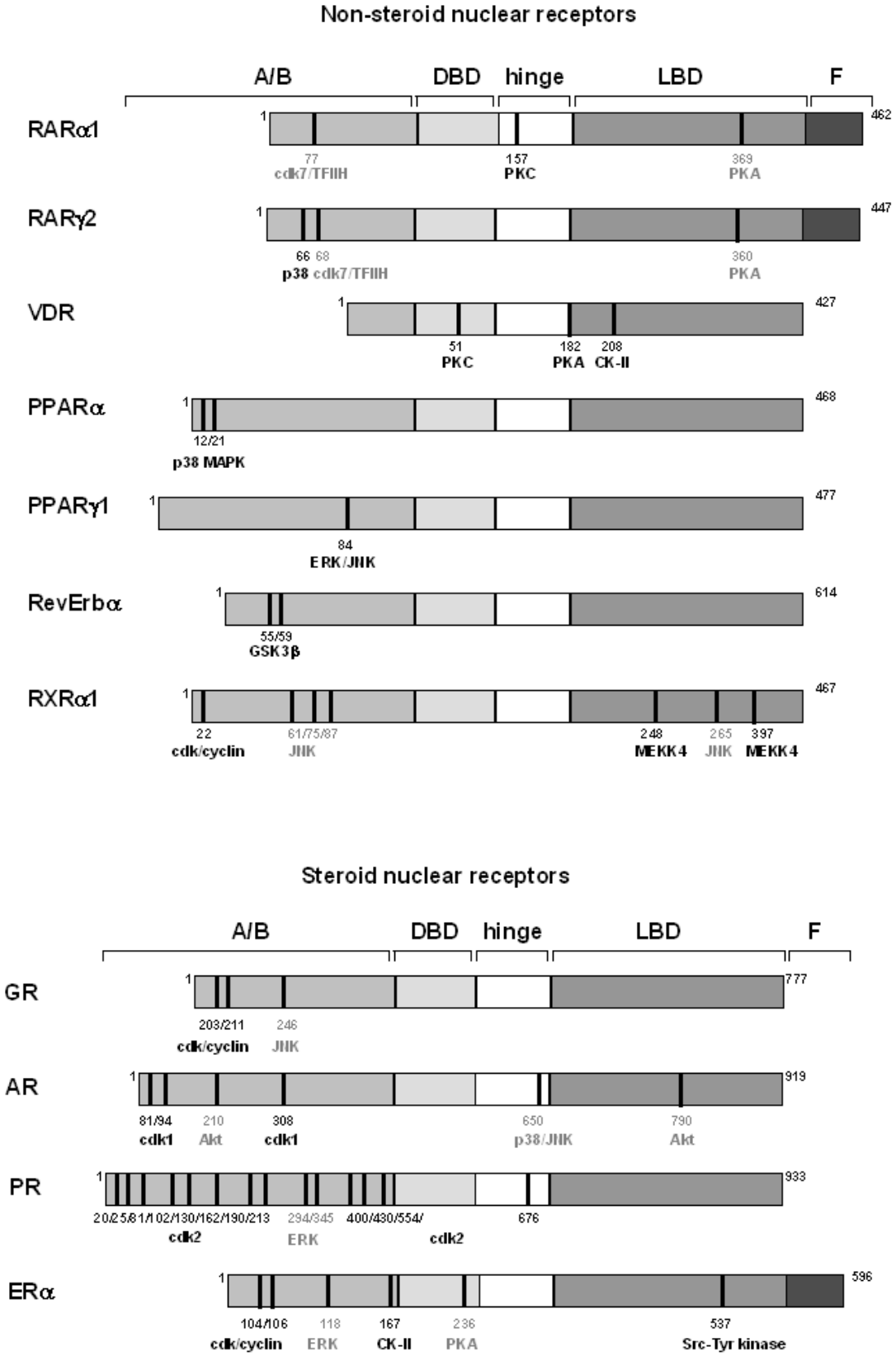

Fig. 1.6: Schematical constitution of non-steroid and steroid nuclear receptors with phosphorylation sites and corresponding kinases [47].

Class	Receptor	Kinase	Site	Effect
I	RARα1	cdk7/TFIIH	77	constitutive [55]
		PKC	157	heterodimerization, activation [56]
		PKA	369	enhancing activity? [57]
	RARγ2	p38 MAPK	66	ligand-dependent; degradation by proteasome [46]
		cdk7/TFIIH	68	constitutive [58]
		PKA	360	unknown function [59]
	VDR	PKC	51	decreased DNA binding affinity, decreased basal activity [60]
		PKA	182	suppression of activity [61]
		Casein kinase II	208	increased activity [62]
	PPARα	p38 MAPK	12/21	increased ligand-dependent activation [5,63]
		PKC	129/179	increased activity [64]
	PPARγ1	ERK-2, JNK	84	decreased ligand-dependent and basal activity [65,66]
	RevErbα	GSK3β	55/59	stabilization against degradation [67]
II	RXRα1	cdk1/cyclin	22	constitutive [68]
		JNK	61/75/87/265	no effect on activity [68]
		MEKK4	248/397	suppression of activity [69]
III	GR	cdk/cyclin	203/211	ligand-dependent activation [70]
		JNK	246	suppression of activity [71]
	AR	cdk1	81/94/308	stabilization? [72,73]
		Akt	210/790	decreased activity [74]
		p38, JNK	650	nuclear export [75]
	PR	cdk2	20/25/81/102/130/ 162/190/213/400/ 430/554/676	basal or ligand induced, activation [76,77]
		ERK	294/345	nuclear translocation [78]
	ERα	cdk/cyclin	104/106	ligand-dependent and independent activation [79]
		ERK	118	ligand-independent activation [80]
		Casein kinase II	167	ligand-dependent activation [81]
		PKA	236	suppression of dimerization [82]
		Src-Tyr kinase	537	constitutive; unknown function [83]

Table 1.7: Overview about phosphorylation sites of nuclear receptors with corresponding kinases and effect of phosphorylation on activity.

1.2 The Retinoic Acid Related Orphan Receptor (RORα)

The ROR (Retinoic Acid Related Orphan Receptor) subfamily of nuclear receptors is represented by the three subtypes RORα, RORβ and RORγ, which are encoded by three different genes. They are so-called "orphan" receptors, because up to now it was not possible to clearly identify their endogenous ligands.

1.2.1 RORα Isoforms

ROR receptors were identified as a result of different strategies to clone novel members of the nuclear receptor subfamily. By performing reverse transcription experiments on RNA isolated from human umbilical vein endothelial cells (HUVECs), using primers designed according to the conserved amino acid sequences of the zinc finger motifs of nuclear receptors, RORα4 was the first RORα isoform that was identified. Because of its high sequence homology to the Retinoic Acid Receptor it was first denoted as RZR (Retinoic Z Receptor). The denotation RORα was established by Giguere et al. who cloned three further isoforms RORα1-RORα3 from human retina and testis cDNA in 1994. The four isoforms share a common sequence of 356 amino acids, composed of the DNA binding domain, hinge and the ligand binding domain. RORα1-α4 only differ in their N-terminal A/B region because of alternative promoter usage and exon splicing. The isoforms display different DNA binding specificities and patterns of expression, and therefore regulate different physiological processes and target genes.

By performing Northern Blot analysis, RORα mRNA was detected in many tissues, including heart, brain, skin, muscle, lung, spleen, testis, ovary, thymus, and peripheral blood leukocytes [84]. Whereas RORα1 and α4 are expressed in most tissues, RORα2 and α3 are exclusively detected in testis after sexual maturation.

It was shown that the extent of RORα expression varies at a consequence of growth conditions. Chauvet et al. [85] demonstrated that hypoxia led to an enhanced RORα mRNA level in human hepatoma cells (HepG2). Stimulation with IL-1β, TNFα or lipopolysaccharids (LPS) increases RORα expression in human aortic smooth muscle cells (hASMC), whereas in atherosclerotic plaques, RORα expression is significantly decreased [86].

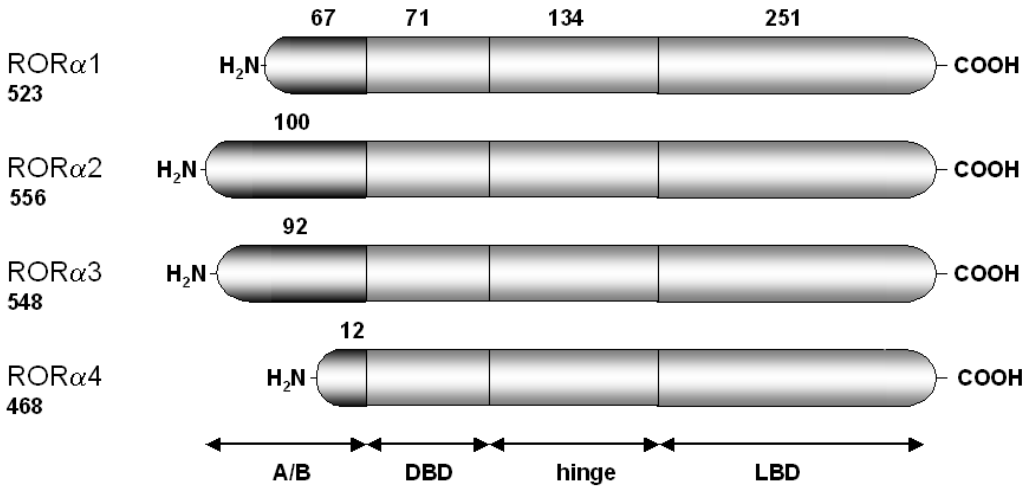

Fig. 1.8: Schematical constitution of the RORα isoforms. *The four isoforms differ in their N-terminal A/B region; the DNA binding domain (DBD), hinge and ligand binding domain (LBD) are conserved. Number of amino acids for each domain and for the complete proteins is indicated.*

1.2.2 ROR Response Element (RORE)

In contrast to most nuclear receptors that bind as dimers to the DNA, RORα binds as monomer to the half-core site motif (A/G)GGTCA preceded by a 6 bp long A/T–rich sequence. Both the DNA binding domain (DBD) and the carboxy-terminal extension (CTE) within the hinge domain are required for efficient DNA binding. Moreover, it was demonstrated that the A/B region influences binding of receptors in an isoform-specific manner. Whereas RORα1 binds to a large subset of response elements, RORα2 recognizes ROREs with strict specificity and shows weaker transcriptional activity [87].

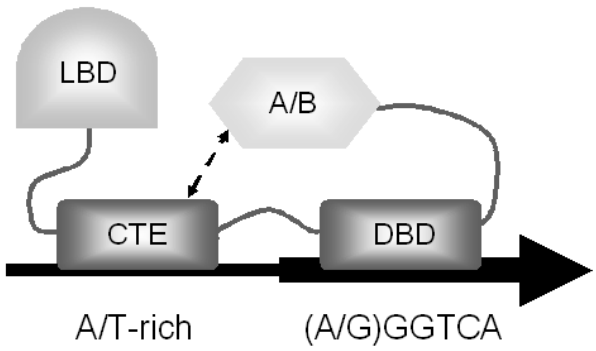

Fig. 1.9: Monomeric binding of a nuclear receptor to its response element. *Monomeric response elements are composed of a nucleotide hexamer (A/G)GGTCA that is recognized by the DBD and preceded by an A/T-rich sequence recognized by the carboxy-terminal extension (CTE). The modulatoric A/B domain interacts with the CTE to facilitate response element binding with isoform-dependent specificity [88].*

1.2.3 RORα Activity

Coactivators and corepressors

Glucocorticoid receptor-interacting protein (GRIP-1) and peroxisome proliferator-activated receptor (PPAR)-binding protein (PBP) were shown to associate with RORα [40]. However, in an *in vivo* system, only GRIP-1 was able to potentiate RORα activity, whereas PBP had little or no effect. By the use of a mammalian two-hybrid assay, Lau et al. [89] demonstrated a direct interaction of the RORα LBD with the coactivator p300. p300 either functions as bridge for the recruitment of other cofactors, or displays histone-acetylase activity. In addition, p300 is a coactivator of nuclear receptor- and MyoD-mediated transcriptional activation during muscle differentiation.

Harding et al. [90] demonstrated, that RORα interacts with both nuclear receptor corepressor (N-CoR) and silencing mediator of retinoid and thyroid receptors (SMRT) *in vitro*. However, when bound to its RORE, the RORα AF-2 seems to abolish binding affinity to these corepressors. DNA binding may alter the RORα protein conformation resulting in an constitutive active form that behaves like a ligand-bound receptor. The product of the gene *hairless* (hr) also was identified as a repressor protein of RORα. *Hairless* also mediates transcriptional repression by the unbound thyroid hormone receptor [91].

Passive repression by RevErbα

In contrast to RORα, the orphan nuclear receptors RevErbα and RevErbβ function as transcriptional repressors [92]. Both RevErbs miss helix 12 and the AF-2 domain which probably results in a lack of coactivator recruitment. Their amino acid sequence of the carboxy-terminal extension shows high homology to that of the RORα receptor, which leads to recognition of the same DNA consensus motifs [93]. RORα and RevErb receptors regulate the same target genes, but with opposite effect. A competition between the activator ROR and the repressor RevErb has been shown for the human Apo-CIII promoter [94], the enhancer of the rat α-fetoprotein gene [95], the IκBα promoter [96,97], the Bmal1 promoter [98], and the expression of genes that are necessary for muscle cell differentiation [89,99]. Interestingly, even the expression of RevErbα itself underlies the competitive interplay between RORα and RevErbα [100-102].

Ligands

In transient transfection assays, RORα activity depends on the addition of fetal calf serum (FCS) to the medium. Therefore, binding of an ubiquitous occurring ligand for RORα was postulated. In 1995, melatonin was discussed as the activating serum agent and thus as a ligand for RORα and RORβ [103,104]. Moreover, the thiazolidinedione derivative CGP 52608 was shown to increase RORα activity and for this reason postulated as synthetic RORα ligand [104,105]. However, melatonin enhancing activity on RORβ and *in vitro* binding experiments could not be reproduced, and up to now the question on ROR melatonin binding still remains to be clarified. Nevertheless, it could be demonstrated that the inhibiting effect of melatonin on the 5-lipoxygenase promoter is dependent on the presence of a functional ROR response element [106].

In contrast, it was suggested that RORα displays constitutive activity without binding of a ligand. A homology model of RORα using the closely related TRβ as template, highlighted a nonconserved amino acid in helix 11 of RORα (Phe-491) and a short-length helix at the N-terminus of AF-2. It was hypothesized that these circumstances ensure that AF-2 is locked permanently in the holo-conformation described for other ligand-bound receptors and thus enabled ligand-independent recruitment of coactivators. Interestingly, mutation of Phe-491 ablated transcriptional activation and recruitment of coactivators resulting in a decreased RORα activity [107].

1.2.4 Physiological Functions

The ubiquitous expression of RORα suggests that this protein is involved in many physiological procedures all over the organism. The physiological functions of RORα can be studied in detail with help of the staggerer (*sg/sg*) mutant mouse, which was first described by Sidman et al. in 1962 [108]. These animals suffer from severe neurological dysfunctions, they display a staggering gait, mild tremor and a disturbance of equilibrium. More than 50% die within the fourth weak after birth. Cerebellar Purkinje cells are reduced in number and size, they are generated in a normal number at the embryonic stage, but undergo cell death within 5 days after birth. At an age of two months, absence of functional RORα protein leads to an up to 80% decreased amount of Purkinje cells, and surviving cells demonstrate a progressive atrophy of the dendrites [109-113]. RORα has been shown to regulate the gene for Purkinje cell specific protein 2 (Pcp2), however, disruption of this gene in mice has not led to the

cerebellar phenotype of the staggerer mouse. Micro-array experiments with cerebellar RNA probes of staggerer and normal mice identified several genes that differ in their expression [114], but it is not yet clear, which genes under the transcriptional regulation of RORα are responsible for the phenotype displayed in the Purkinje cells of the staggerer mutant mouse.

In 1996 Hamilton et al. could show, that the staggerer phenotype bases on a 122 bp-deletion on chromosome 9 within the RORα gene [115]. This mutation shifts the reading frame and prevents translation of the RORα LBD due to the generation of a premature in-frame stop codon, the resulting truncated RORα protein is not functional. Steinmeyer et al. generated a null mutant mice RORα$^{-/-}$ by disrupting the RORα gene at the level of the second zinc finger. Thus, the emerging RORα truncation mutant is not able to bind to response elements on the DNA. RORα$^{-/-}$ mice exhibit very similar disorders to that of the *sg/sg* mice.

In addition to the cerebellar phenotype, further studies of the staggerer mutant mouse revealed a variety of age-related phenotypes beyond the cerebellum. The staggerer mouse has been shown to display abnormalities in the formation and maintenance of the bone tissue. In normal animals, RORα gene expression is increased during the osteogenic differentiation of mesenchymal stem cells derived from bone marrow. Two genes encoding important proteins for bone mineralization and for generation of the extracellular bone matrix, bone sialoglycoprotein and osteocalcin, have been shown to be under the transcriptional control of RORα [116]. The bones of homozygous staggerer animals are abnormally fine and long, mass and density of bones are decreased. Thus, RORα seems to play a pivotal role in modulation and maintenance of bone tissue and in osteoporosis.

Furthermore, the staggerer mutant mouse has been linked with heart disease. Animals fed with an atherogenic diet show a decreased HDL (high density lipoprotein) level and develop more severe atherosclerosis than wild-type mice [117]. In fact, RORα has been shown to bind to the RORE in the promoter of murine Apo-AI and Apo-CIII genes, and thus directly regulates their transcription [118]. Apo-AI is the major constituent of HDL, which is responsible for the cholesterol transportation. Controversially to the postulated anti-atherosclerotic effect of RORα, positive regulation of Apo-CIII causes an increased triglyceride plasma level by delaying the degradation of triglyceride-rich particles [94], and thus an elevated risk for atherosclerotic disease. In addition, cholesterol derivatives were found in the RORα ligand binding pocket, confirming the connection between RORα and the lipid metabolism [119-121].

Abnormalities in immune response of staggerer mutant mice were first discovered by Trenkner et al. [122], whose studies revealed a delayed thymic development and a defect in

terminating T-cell responses. Moreover, peripheral macrophages of staggerer mice produce an abnormally high amount of the pro-inflammatory cytokines IL-1, IL-6 and cyclooxygenase-2 (COX-2) on TNFα and LPS stimulation [123]. The expression of IL-1, IL-6 and COX-2 is controlled by NF-κB, a transcription factor that is inhibited by the binding to the protein IκBα, which masks the nuclear localization signals of NF-κB and abides its cytosolic habitation. An inflammatory stimulus caused e. g. by TNFα or LPS, evokes the dissociation of IκBα. NF-κB translocates into the nucleus and induces the expression of pro-inflammatory genes. Consistent to the elevated cytokine levels in staggerer mice, Delerive et al. [96] demonstrated that RORα inhibits the NF-κB pathway by the activation of IκBα gene expression which directly verified the anti-inflammatory effect of RORα.

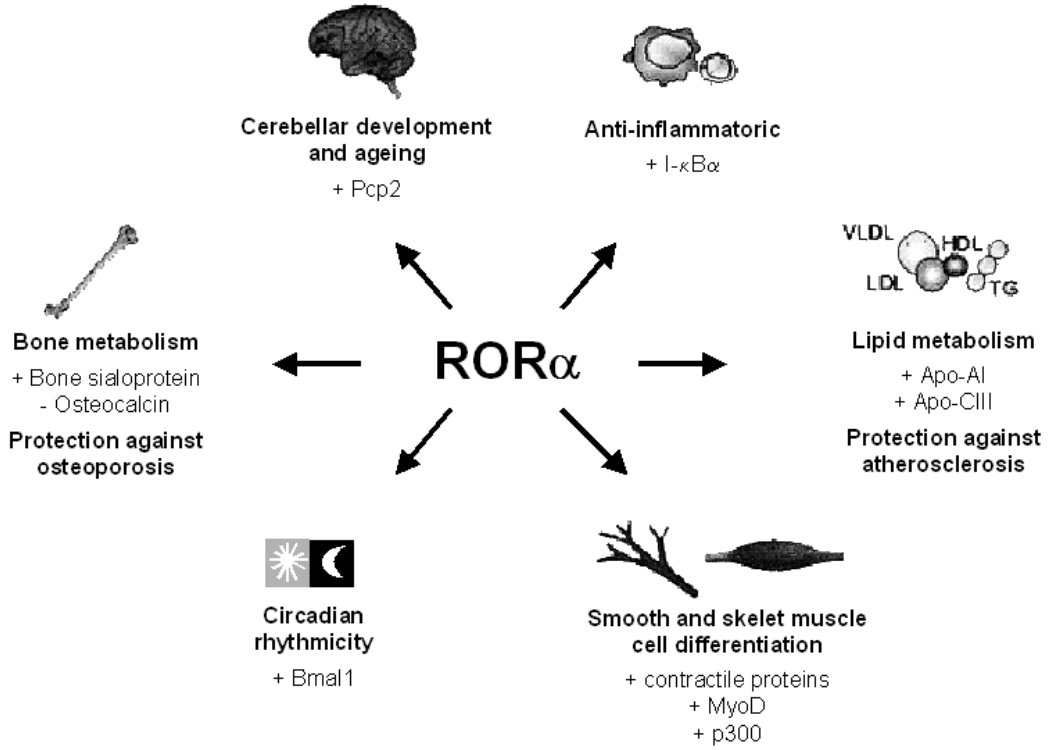

Fig. 1.10: Physiological functions of RORα. *Major tasks of the nuclear receptor are summarized with the yet identified positively or negatively regulated target genes, according to [88].*

RORα has a positive influence on development of skeletal and vascular muscles via up-regulation of MyoD and p300 expression, providing clue to the understanding of the muscular atrophy observed in the staggerer mutant. MyoD activates muscle specific gene expression and promotes cell-cycle exit after the induction of differentiation [89,124,125]. In staggerer mesenteric arteries, the expression of contractile proteins, such as smooth muscle myosin, calponin and heavy caldesmon, is significantly decreased. The response to vasodilators and

vasoconstrictors is significantly reduced, ascertaining that RORα is required for a normal contractile function of smooth muscle cells [126].

RORα also plays an important role in the regulation of circadian rhythmicity within the suprachiasmatic nuclei (SCN) (see chapter 1.3). Staggerer mice entrained in light-dark cycles show shorter free-running activity period lengths under constant darkness conditions [98]. Additionally, it was demonstrated that heterozygous staggerer mutants show a faster adaptation to altered light cycles compared to the nonmutant controls [127]. Fig. 1.10 summarizes the physiological functions of RORα.

1.3 Circadian Rhythmicity

1.3.1 Core-Clock

Circadian rhythms are daily cycles of physiology and behavior that are driven by an endogenous oscillator with a period of approximately (*circa*-) one day (*diem*). When subjects are temporally isolated, expression of these daily cycles continues (free-runs) with subjective day and night defined by the oscillator. The most obvious circadian rhythm is the cycle of sleep and wakefulness. In the phase of circadian day, the physiology is dominated by catabolic processes to facilitate adjustment to the environment, whereas at night anabolic functions of growth, repair and consolidation predominate. For example, in the evening the body temperature falls and melatonin is secreted to facilitate sleep. Sleep onset is accompanied by increased secretion of growth hormone and prolactin, whereas before dawn, circadian activation of the adenocorticotropic system prepares the organism for the physical and mental demands of awaking [128].

Circadian rhythmicity in mammals is governed substantially by the suprachiasmatic nuclei (SCN), paired cell clusters in the anteroventral hypothalamus. Because the periodicity of the circadian clock only approximates that of the environment, these clock must be adjusted to a precise 24 h-cycle. Circadian oscillators also exist in most peripheral cells and sometimes even in cultured cells [129,130]. The peripheral timekeepers are reset by signals from the SCN pacemaker [131]. In addition to light signals, which seem to be the predominant "Zeitgeber" (time-giver) for synchronization, other cyclic inputs such as temperature, noise or social cues may act as entraining agents. Feeding time also seems to influence the phase of oscillators in some peripheral tissues but, notably, is ineffective in resetting time in the SCN.

The molecular composition and function of circadian clocks have been subject of intense genetic and biochemical investigations. In mammals, *in vitro* studies have shown that the level of Bmal1 protein expression is the central pacemaker of mammalian circadian rhythms. Two RORE are located within the Bmal1 promoter. RevErbα, which acts as a transcriptional repressor [92,102,132], may be the major circadian regulator of Bmal1 expression. mRNA of transactivating ROR is constitutively expressed all over the day and has the potential ability to bind to the Bmal1 promoter at all times of the day. It was shown that ROR competes with RevErbα for binding to the RORE [132]. When the RevErbα protein level decreases during the circadian night, ROR effectively activates Bmal1 transcription, which consequently enhances the amplitude of Bmal1 oscillation and generates a robust and stable oscillation of the clock. It still is in discussion, whether an endogenous ligand, which remains unidentified so far, may modulate the core-clock by binding to the ROR protein. As shown in Fig. 1.11, expressed Bmal1 protein dimerizes with Clock and the Bma1-Clock complex activates the expression of Per1 and Per2 (period), Cry1 and Cry2 (cryptochrome) and other clock-controlled genes (CCGs). Per and Cry proteins in turn repress the Bmal1-Clock transactivation, which constitutes the major circadian feedback loop [133]. In addition to the feedback loop of Per and Cry which repress their own transcription, there are several forward and reverse feedback loops in the transcriptional circuits [134,135]. Bmal1 activates the expression of RORγ over E-boxes within the RORγ promoter, RORγ in turn activates Bmal1 expression via ROREs. Bmal1 activates RevErbα transactivation via E-boxes, RevErbα in turn represses Bmal1 and its own expression by binding to ROREs. E4bp4 expression also underlies the RORα/RevErbα interplay and E4bp4 protein represses Bmal1-Clock transactivation through D-boxes, whereas expressed Dbp protein activates through binding to D-boxes.

Gene expression analysis have shown that the mRNA levels of 16 clock and clock-related genes have high amplitude circadian oscillations in the central (SCN) and peripheral clock tissues. Nine of the analyzed genes participate in circadian regulation of gene expression through E-boxes (Per1/2/3, Cry1, Bmal1, Clock, Npas2, Bhlhb2, Bhlhb3) [136-143], two through D-boxes (E4bp4, Dbp) [144,145] and five through ROR/ RevErbα response elements (ROREs; RORα/β/γ, RevErbα/β) [98,146,147]. Fig. 1.12 shows the expression profiles of RORα, RevErbα, Bmal1, Per1, Cry1 and Clock mRNA in the SCN and liver. Wild-type mice were held under a schedule of 12 h light followed by 12 h dark (LD 12:12) for a couple of days and then set into constant darkness (DD), so-called free running conditions. In the SCN, mRNA of activating RORα peaked at Zeitgeber Time (ZT) 8 and was preceded by repressing

RevErbα mRNA that peaked at ZT 4. As a result of activator and repressor interplay, Bmal1 mRNA increased delayed to that of RORα mRNA. Bmal1 dimerizes with constitutively expressed Clock protein and thus activates the transcription of Per and Cry.

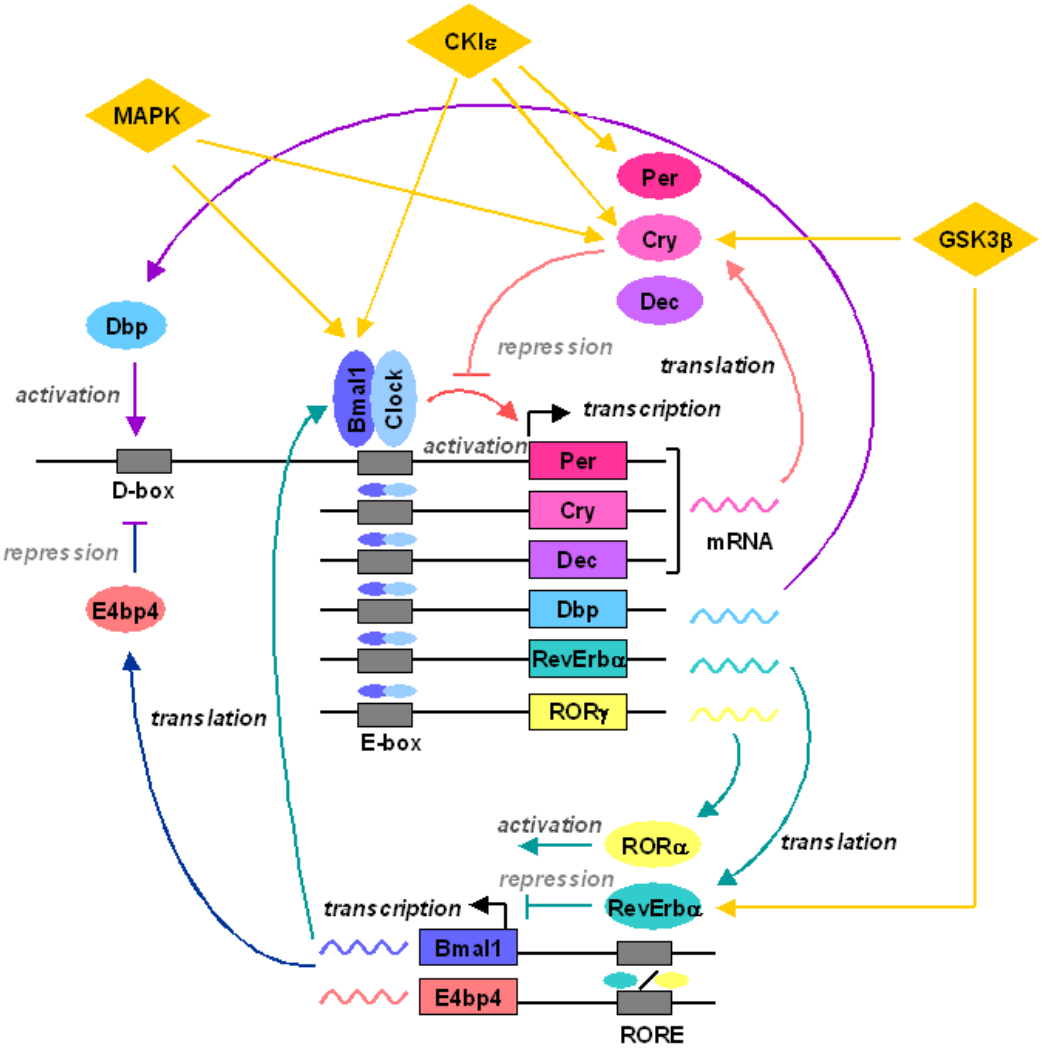

Fig. 1.11: Model of the core-clock, driven by Bmal1 oscillation. *MAPK: mitogen-activated protein kinase, CKIε: casein kinase Iε, GSK3β: glycogen synthase kinase-3β [148].*

While circadian expression of Per1 and Per2 is controlled preliminary through Clock/Bmal1 activation of E-boxes, it has been proposed that the Cry1 mRNA is determined by a combination of activities from both E-boxes and ROREs [149]. Indeed, Cry1 levels are higher in RevErbα mutant liver at the time of RevErbα expression peak and lower in staggerer SCN at the time of RORα expression peak [146]. In the liver of wild-type mice, expression profiles of these transcription factors are similar, however, RORα mRNA is expressed constitutively all over the day. Lack of RORα oscillation and an increased RevErbα expression results in a heightened amplitude of Bmal1, Per1 and Cry1 oscillation. In further peripheral tissues such

as heart, stomach, kidney and lung, also a slight oscillation of RORα mRNA was observed [127].

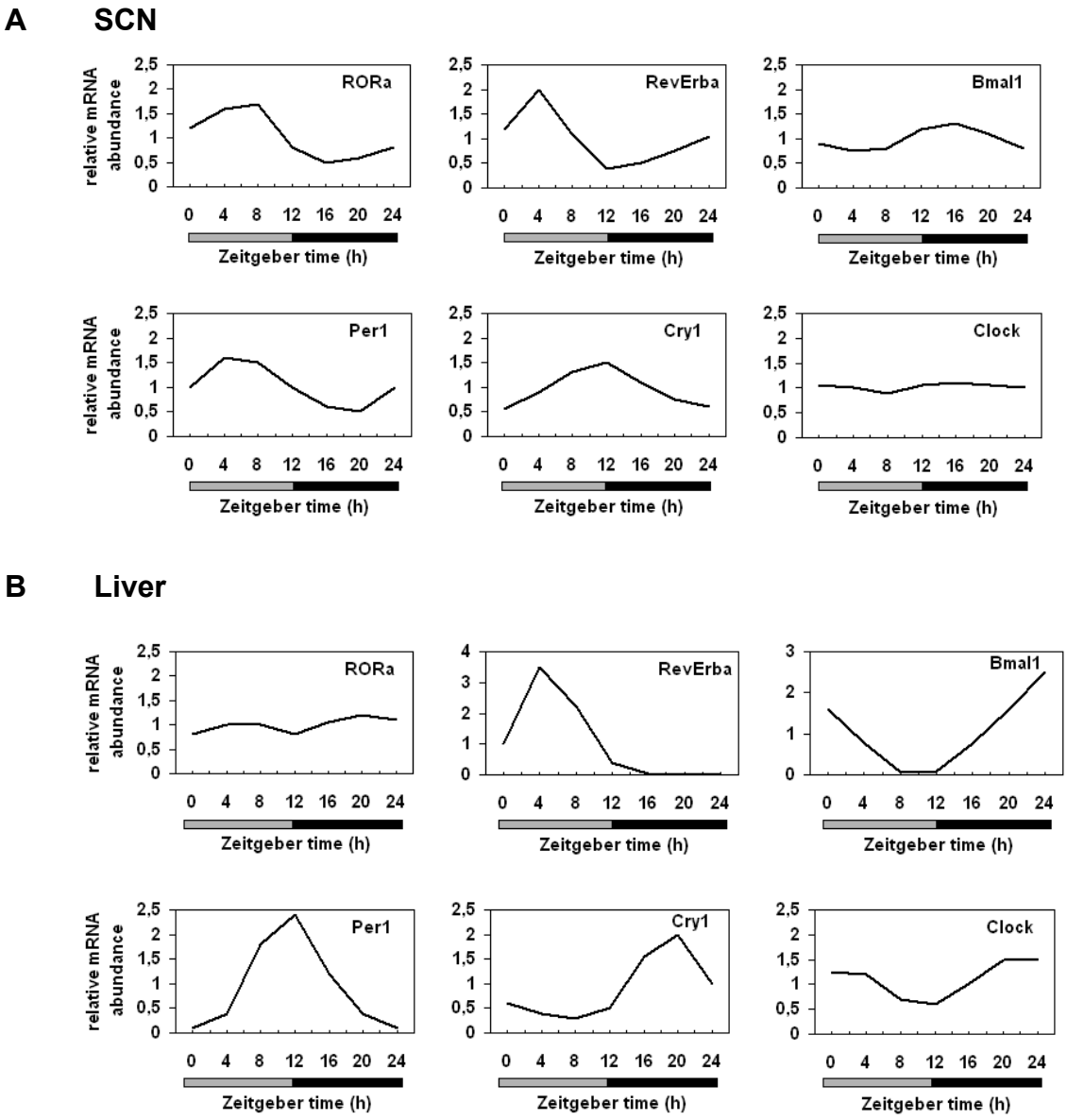

Fig. 1.12: Temporal expression profiles of transcription factor mRNA in mice (A) suprachiasmatic nuclei (SCN) and (B) liver under constant darkness (DD) conditions *according to Ueda et al. [135]. Relative mRNA levels under DD conditions of the indicated genes were measured in a quantitative PCR assay.*

Results from peripheral tissues suggest a model in which RORα would provide continual activation to counteract the rhythmic repression of Bmal1 expression by RevErbα. *In silico* studies revealed a simple hypothetic principle that governs the temporal relationships in the expression of these transcription factors. In E-box and RORE regulation, the repressor precedes the activator, which delays transcriptional activity. In D-box regulation, repressors

and activators are nearly antiphasic, generating transcriptional activities with high amplitude [135].

However, besides the regulation of protein expression level over feedback loops, regulation of circadian rhythmicity might be much more complex because additional events like chromatin modification, protein phosphorylation or stability probably influence the system. It was hypothesized that posttranscriptional as well as posttranslational modifications are needed to adjust the timing of the clock to produce a circadian oscillator that takes approximately 24 h [150].The importance of distinct core-clock members was investigated with the help of knockout mice. Loss of Bmal1 for example, results in an immediate and complete loss of circadian rhythmicity in constant darkness [137]. This demonstrates that Bmal1 is a non-redundant, essential component of the circadian pacemaker. In contrast, RevErbα deficient mice show a persistent circadian rhythm, but with a shorter period and impaired stability and precision. In these mice, Bmal1 transcript levels are expressed constitutively throughout the day. RevErbα deficient mice can perform unusually large phase-advances initiated during the second half of subjective night. The new steady-state phase is reached only a few days after exposure (Fig. 1.13) [146]. *In vitro* studies with a constitutively negative form of RORα that lacked the LBD and failed to bind coactivators but still could bind to the DNA, resulted in a severely dampened circadian rhythm of Bmal1 transcription. Similar results were obtained from transfection of RORα RNAi [127]. Homozygous staggerer mice (sg/sg) held under constant dark conditions, show a shortened period length of locomotor activity rhythm (sg/sg: 23.35 +/-0.066 h, wild-type: 23.84 +/- 0.021 h). When the lighting cycle was advanced for 4 h, heterozygous staggerer mice (+/sg) re-entrained almost completely at the first onset of darkness and entrainment was complete after 5 d. In contrast, wild-type mice re-entrained progressively over 10 d. When animals were maintained in a short light-dark cycle, LD 6:6, the activity of heterozygous (+/sg) was abruptly inhibited by light or became arrhythmic. Although RORα seems not to be required for generation of a circadian rhythm, it influences the period length and affects the stability of the clock. However, staggerer mice showed enhanced adaptability to a phase advance and were more sensitive to photic manipulation [127].

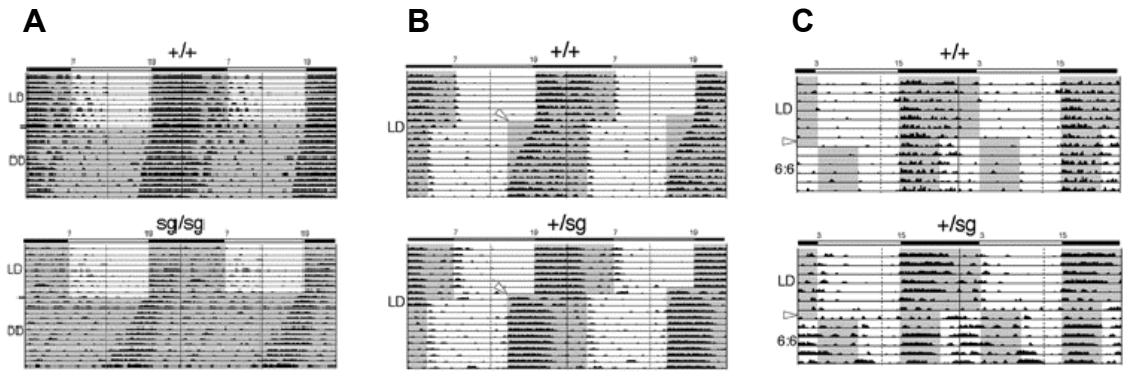

Fig. 1.13: Circadian phenotype of RORα-deficient staggerer mice. *(A) Activity records of a wild-type (+/+) and a homozygous mutant mice (sg/sg). Light regime: 10 d in LD followed by 13 d in DD. (B) Actograms of a wild-type (+/+) and a heterozygous staggerer mouse (+/sg) showing baseline activity and response to a 4 h phase advance. The arrow indicates the beginning of phase advance. (C) Actograms of a wild-type and a heterozygous staggerer mouse that were subjected to a 6 h light and 6 h dark (6:6) cycle [127].*

Melatonin

Ocular light plays a key role in human physiology by transmitting time of day information. Production of the pineal gland hormone melatonin is under control of the light-dark cycle, and its profile of secretion defines biological night. Receptors for melatonin are highly expressed within the SCN [151-153], but the physiological action of melatonin within maintenance of the core-clock is poorly understood. Indeed, daily melatonin injections in free-running rats resynchronize their locomotor activity to 24 h [154]. It was shown that expression of Per1, Cry1 and Bmal1 in the mouse hypophyseal pars tuberalis was dramatically reduced in melatonin receptor 1 knockout mice (MT1 ko). In MT2 ko mice, mRNA level of these transcription factors were unaffected [155]. Hyperphysiological injections of melatonin at the end of a subjective day did not affect RORα mRNA level, whereas RORβ mRNA level was slightly increased. Interestingly, the rhythm of RevErbα mRNA expression was phase-advanced by 1.3 +/- 0.8 h, but without effect on the amplitude [156].

1.3.2 Phosphorylation of Core-Clock Members

In addition to transcriptional positive and negative feedback loops, further levels of regulation operate to establish and maintain circadian rhythms. These include posttranscriptional regulation [157,158], posttranslational modifications [159], chromatin-remodeling [149,160,161], availability and stability of clock proteins [162,163], and regulation of intracellular localization [159,164]. The fine regulation of clock proteins by intracellular

signaling plays an essential role in the physiological control and resetting of circadian rhythmicity (Fig. 1.11).

Per proteins

Genetic studies have provided solid evidence for the crucial role played by phosphorylation of Period proteins. The gene effected by the *tau* mutation, which causes a short-period phenotype in the Syrian hamster, was identified to encode casein kinase I epsilon (CKIε) [165], which was demonstrated to phosphorylate Pers. The short-period phenotype observed in *tau* hamsters is directly linked to a lower rate of CKI-dependent phosphorylation. Intriguingly, a deficiency in Per phosphorylation by CKIε has also been implicated in human sleep disorders. Indeed, familiar advanced sleep-phase syndrome (FASPS) has been associated with a missense mutation in the human Per2 gene, which leads to a less effectively phosphorylated form [166]. CKIε has also been shown to control protein stability and subcellular localization of Per [167-169]. CKIε specifically interacts with and phosphorylates Per1, Per2 and Per3, and thus regulates each of them differently. CKIε binding domains are highly conserved in Per1 and Per2, whereas that of Per3 is divergent resulting in a much weaker CKIε binding affinity [163,170]. Interestingly, Per1 and Per2 seem to play a pivotal role in circadian rhythmicity, whereas Per3 is dispensable for a functional clock [138,140]. CKIε phosphorylation of Per2 and Per3 induces their degradation through the ubiquitine-proteasome pathway [163,166]. Phosphorylation of Per proteins by CKIε also influences the subcellular localization by masking or unmasking their localization sequences.

The intracellular distribution and posttranslational modifications of Per proteins are also influenced by the association of Pers with Crys. The two PAS domains and the C-terminal conserved regions of Per are required for Per-Per and Per-Cry dimerization. Per-Cry dimerization stabilizes both proteins by preventing their ubiquitinylation-proteasome mediated degradation [162].

Cry proteins

Mammals have two Cry proteins, Cry1 and Cry2 that seem to exert opposite functions within the circadian oscillator, because mice lacking Cry1 or Cry2 genes exhibit accelerated or delayed free-running periodicity of locomotor activity [171]. Nevertheless, both Cry1 and Cry2 are strong repressors of Clock-Bmal1 mediated transcription by direct interaction with the Clock-Bmal1 heterodimer in the nucleus [172,173]. In mouse liver, Crys are detected mainly in the cytoplasm, where they dimerize with Per proteins and subsequently translocate

to the nucleus. Besides controlling the subcellular distribution of Cry proteins, Pers appear to be essential for Cry phosphorylation by CKI. CKIε and Cry do not interact directly, but both can bind simultaneously to Per proteins. Thus, Pers seem to act as a bridge, bringing both proteins into the same ternary complex, in which CKIε can phosphorylate Crys [174].
A recent study reported that MAPK phosphorylates mouse Cry1 (Ser-247) and Cry2 (Ser-265) and thus reduces Cry repressor activity [175]. MAPK also phosphorylates Ser-557 in mouse Cry2, preparing the protein for a further phosphorylation by glycogen synthase kinase-3 beta (GSK-3β). After phosphorylation by GSK-3β, Cry gets degradated by the ubiquitine-proteasome pathway. The Ser-557 phosphorylated form accumulates in the liver during the night and peaks in parallel with Cry2 protein [176]. Interestingly, GSK-3β exhibits a circadian rhythm in its activity with a peak from late night to early morning [177], at the same time when Ser-557 of Cry2 is highly phosphorylated.

Clock and Bmal1 proteins

Bmal1 protein shows circadian oscillation in its phosphorylation status and subcellular distribution in mouse liver as well as in the suprachiasmatic nuclei. The phosphorylated form of Bmal1 protein is mostly nuclear [159,164,178]. Additionally, Clock-Bmal1 dimerization induces Bmal1 phosphorylation and facilitates nuclear localization. Crys are directly involved in these posttranslational modification and subcellular distribution, but so far the mechanism is poorly understood [179]. Two kinases, CKIε and MAPK have been shown to phosphorylate Bmal1 *in vitro*. MAPK phosphorylates three residues, Ser-527, Thr-534 and Ser-599 [180], but the CKIε consensus motif has not yet been identified. A well conserved consensus site for CKIε is located within the C-terminal domain of Bmal1 protein. Interestingly, this putative motif overlaps in part with a MAPK consensus, suggesting that these two kinases could compete to regulate Bmal1 function. Consistent with this idea, MAPK phosphorylation results in a decreased Clock-Bmal1 transcription activation, whereas CKIε-mediated phosphorylation increases transactivation [174]. In addition, Bmal1 is sumoylated at Lys-259, which is induced by Clock protein; the circadian pattern of Bmal1 sumoylation is parallel to its activation in the mouse liver [181].
Clock protein also contains a well conserved CKI phosphorylation site in its center. However, CKIε does not seem to phosphorylate Clock *in vitro*. In mouse liver, CKIε forms a trimeric complex with Per-Cry, which translocates to the nucleus and associates with Clock-Bmal1. CKIε might phosphorylate Clock in addition to Bmal1 in this multimeric complex.

1.4 Mitogen-Activated Protein Kinases (MAPKs)

Cells respond to extracellular signals by generating intracellular signals and instructions to coordinate appropriate responses. Among the pathways often used to transduce extracellular signals, are the highly conserved mitogen-activated protein kinase (MAPK) or extracellular signal-regulated protein kinase (ERK) cascades. These cascades are found in all eukaryotic organisms and consist of a three-kinase module that includes a MAPK, which is activated by a MAPK/ERK kinase (MEK), which is in turn activated by a MEK kinase (MEKK) [182-185]. This cascade is activated by diverse extracellular stimuli and by pro-oncogenic products that induce proliferation or enhance differentiation. MAP kinase phosphorylations influence processes in the cytoplasm, the nucleus, the cytoskeleton, and the membrane.

ERK1 and 2 are widely expressed and are involved in the regulation of meiosis, mitosis, and postmitotic functions in differentiated cells. Many different stimuli, such as growth factors, cytokines, virus infection, ligands for G-protein coupled receptors, transforming agents, and carcinogens, activate the ERK1/2 pathways. Most stimuli that activate ERKs convert plasma membrane anchored Ras from its GDP-bound state into its GTP bound state. Ras-GTP binds directly to the seryl/threonyl kinase Raf, forming a transient membrane-anchoring signal [186]. Active Raf phosphorylates the kinase MEK on Ser-218 and Ser-222 [187,188], allowing MEK to phosphorylate its only known substrates ERK1 and 2. MEK mutants which mimic the effect of phosphorylation of residues 218 and 222 (by substitution of serines with either aspartic acids or glutamic acids) have constitutive activity *in vitro* and are oncogenic *in vivo* [189,190]. Once phosphorylated on Thr-183 and Tyr-185 [191,192], ERK1 and 2 phosphorylate numerous cytoplasmatic proteins (pp90 ribosomal S6 kinase [RSK], cytosolic phospholipase A2, and the EGF receptor [193-195]). In addition, ERKs translocate to the nucleus, where they can phosphorylate nuclear receptors like Elk-1, ERα [80], PPARγ [65,66] and other transcription factors.

MAPKs are grouped into subfamilies on the basis of sequence similarity, mechanisms of upstream regulation and sensitivity to activation by different MEKs. Ten years ago, only three subfamilies were known, ERKs, c-Jun N-terminal kinase/stress activated protein kinase (JNK/SAPK) and p38. ERK3 lacks the dual phosphorylation motif and thus probably lies in a fourth, uncharacterized pathway [196]. Many MAPKs have been discovered recently, including ERK5 [197] and four p38-like kinases namely Mxi2 [198], a truncation form of kinase subdomain XI, ERK6 [199], which is 63% identical to p38, SAPK3 [200] and

p38β [201]. Eight additional splice variants of JNK/SAPK were identified within the brain [201].

As mentioned above, the activation of GSK-3β underlies a circadian rhythmicity which contributes to the rhythmic degradation of Cry2 protein. Moreover, RevErbα is also phosphorylated by GSK-3β followed by protein degradation, suggesting that the circadian oscillation of kinase activity may contribute to the maintenance of the biological clock [202].

Obrietan et al. [203] were the first who found that in mice maintained in constant darkness, levels of the active, phosphorylated form of ERK in the SCN showed significant variation across the circadian cycle, with levels being high during the subjective day and low during subjective night. When mice are exposed to light pulses during the subjective night, p-ERK is rapidly up-regulated in the SCN. Light impulses during the subjective day fails to induce any changes in ERK phosphorylation. The levels of p-ERK caused by light pulses during subjective night quickly decline on termination of the pulse with levels back at baseline 1 h after initiation of the pulse. If the photic stimulation is not terminated and lights are left on, elevated levels of p-ERK decline after 90-120 min [204-208]. This finding might suggest that the ERK cascade in the SCN is under autoregulatory feedback regulation. It was reported that in addition to a circadian rhythm in the total expression of p-ERK, the distribution of intra-SCN p-ERK is time-dependent regulated. During subjective day, p-ERK is spontaneously expressed in the 'shell' area of the SCN and during subjective night solely in the mid-caudal level of the SCN. Expression by the mid-caudal neurons is dependent on the presence of a retinal innervation, as optic enucleation (blinding) ablates this 'core' p-ERK formation [209]. These findings support the idea of a functional compartmentalization within the SCN clock [210]: the 'core' area of the SCN is primarily responsible for processing incoming photic information, and the 'shell' region represents the subpopulation of spontaneously rhythmic neurons that, in turn, receive photic information from the 'core' neurons.

The upstream regulation of ERK within the SCN remains to be determined. NMDA receptor activation seems to be necessary for photic induction of p-ERK [205]. However, the intracellular events linking NMDA receptor activation and ERK phosphorylation are not clear. Inhibitors of calcium/calmodulin kinase II (CAMKII) block both light-induced behavioral phase shifts [211] and Per1 and Per2 expression [212,213], and suppress photic induction of p-ERK [204]. Calcium influx via the NMDA receptor channel therefore may activate CAMKII which, in turn, may lead to phosphorylation of ERK [214]. This mechanism, however, does not explain the spontaneous rhythm in ERK activation. The upstream regulators of ERK, Raf-1 and Ras, oscillate in-phase with p-ERK and p-MEK in the

chick pineal gland, a tissue known to contain an endogenous circadian clock [215]. A recently described novel protein inhibitor of Ras activation, the SCN circadian oscillatory protein (SCOP), oscillates in the SCN in anti-phase to p-ERK [216]. Overexpression of SCOP attenuates up-regulation of p-ERK. Spontaneous expression of SCOP therefore may regulate the cyclic expression of p-ERK in the SCN (Fig. 1.14).

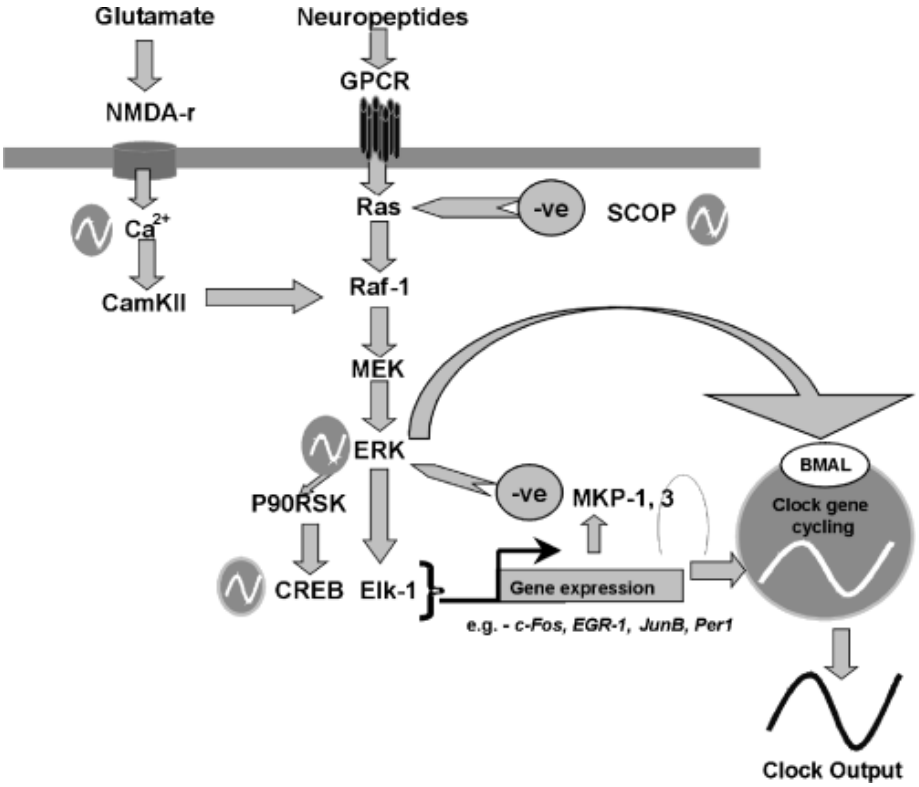

Fig. 1.14: Putative signaling of ERK activation within the SCN. *Factors displaying a waveform beside them have shown circadian rhythmicity in their expression/activity. The circadian rhythm in p-ERK at constant conditions may be due to a fluctuating, calcium-dependent positive drive and an oscillating, SCOP-mediated negative drive [206].*

2 AIM OF THE PRESENT INVESTIGATION

RORα4 was first identified in 1993 [84], and up to now few is known about the RORα signaling pathways and methods of activation or inactivation. In order to perform a detailed functional analysis of the nuclear receptor regulation, this investigation starts with the establishment of a method for production of pure RORα4 protein in *E. coli*. The overexpression and purification method should be optimized to obtain large amounts of very pure RORα4, whose functionality should be confirmed in a DNA binding affinity test. In addition to that, an antibody for ROR should be developed that features high sensitivity and specificity. Moreover, a method for isolation a pure antibody that could be stored for long-term usage should be found.

Subsequently, on the basis of this method and material equipment, studies on RORα4 phosphorylation came into the focus of interest. Effects of phosphorylation on protein function, localization and interaction with the RORα opponent RevErbα were tested. Further posttranslational modifications should be examined, including protein cleavage and sumoylation.

3 MATERIALS AND METHODS

All used chemicals and reagents were purchased from Applichem (Darmstadt), Sigma-Aldrich (Steinheim), Merck (Darmstadt) or Fluka (Buchs, Switzerland). Kits for DNA and plasmid preparation were from Machery-Nagel. Constitution of buffers that is not described here, can be found in Sambrook et al. [217].

3.1 Western Blot

For immunochemical detection and identification of proteins, samples were separated electrophoretically on a 10% SDS-polyacrylamide gel (electrophoresis buffer: 0.25 M Tris-HCl, 0.8 M glycine, 0.04 M SDS) and afterwards transferred on a polyvinylidendifluoride membrane (PVDF, Millipore) by electroblotting (transfer buffer: 25 mM Tris-HCl, 190 mM glycine, 20% methanol). After blocking the membrane surface by gently shaking in 5% low-fat-milk powder/TBS for 60 min, the blot was incubated with the particular first antibody (e. g. mouse anti-ROR) for 90 min. Unbound antibody was washed off from the membrane by shaking 3x 10 min in TBS/1% Tween. Subsequently, the blot was incubated with alkaline phosphatase conjugated second antibody (e. g. anti-mouse, Sigma) for 90 min, washed 2x 10 min with TBS and prepared for detection by washing 10 min with TBS/0.1 % NP-40 and detection buffer (0.1 M Tris-HCl pH 9.5, 0.1 M NaCl, 0.05 M $MgCl_2$). In a last step, the blot was incubated with detection buffer containing nitroblue-tetrazolium chloride (NBT, 330µg/ml) and 5-bromo-4-chloro-3-indolylphosphate (BCIP, 170 µg/ml) until clear bands appeared. The reaction was stopped with TBS/2 mM EDTA. Blots were stored in Milli-Q at 4°C. Blots were scanned with an AGFA Arcus II Scanner.

3.2 Coomassie Staining

For the detection of total proteins in a probe separated by SDS-PAGE, staining was performed with Coomassie brilliant blue R-250 or G-250 (Biorad). The SDS-polyacrylamide gel was incubated in 20% trichloro-acetic acid for 30 min immediately after electrophoresis, then washed with Milli-Q and subsequently incubated in Coomassie staining solution (0.1% Coomassie R-250/G-250, 50% methanol, 10% acetic acid) for 60 min with gentle shaking.

Destaining of the background was performed by washing with 20% methanol/10% acetic acid until clear bands appeared (2-3 h). Gels were scanned with an AGFA Arcus II Scanner.

3.3 Bradford Protein Determination

For Bradford [218] protein concentration determination, a standard concentration series was prepared. As standard protein for concentration determination of RORα or RevErbα solutions bovine serum albumin (BSA, Sigma) was used, γ-globulin (Sigma) was chosen for antibody solutions. 100 µl of the standard concentration series solutions and protein solution were applied onto a 96-well plate. 25 µl Bradford-reagent (Sigma) was added to each well, and after plate vortexing and incubation for 10 min at room temperature, absorbance at 600 nm was determined by a Dynatech MR5000 ELISA Reader. Concentration of protein solutions was calculated from linear equation of calibration curve.

3.4 Electrophoretic Mobility Shift Assay (EMSA)

5´-IRDye700 labeled oligonucleotides were purchased from Metabion. The following complementary oligonucleotides were annealed to generate double-stranded DNA fragments encompassing the ROR response element (RORE, underlined):

RORE-sense 5´-TCGAGTCGTATAAC<u>TAGGTCA</u>AGCGCTGGAC-3´;
RORE-antisense 5´-GTCCAGCGCT<u>TGACCTA</u>GTTATACGACTCGA3´.

The standard 20 µl binding reaction mixture contained 1 mg of purified recombinant RORα4, 3 µg poly-dA-dT (Amersham), 5 mM DTT, 5% Tween 20, 4 mM EGTA and 1.8 mM Na_3VO_4 in Binding Buffer (20 mM HEPES pH 7.5, 1 mM DTT, 150 mM KCl, 1 mM $MgCl_2$, 0.5mM EDTA, 0.05g/l BSA, 5% Glycerol). After pre-incubation on ice for 15 min, 0.6 fmol IRDye700-RORE was added and preparation was incubated for another 15 min on ice. The reaction mixture was loaded on a 4% polyacrylamide gel and the complexes were separated in 0.5x Tris-borate-EDTA at 4°C. Gels were scanned with an Odyssey infrared imaging system (Licor). Specificity of RORα4-DNA and RevErbα-DNA complexes was demonstrated by the addition of 2.2 µg anti-RORα antibody or 6 µg anti-RevErbα (US Biological) antibody to the binding reaction mixture which caused a complete loss of shifted bands.

3.5 In-Gel Kinase Assay (IGKA)

Preparation of cell lysates. Human polymorphonuclear leucocytes (PMNL) were isolated immediately from fresh leukocyte concentrates obtained from healthy donors at St. Markus Hospital (Frankfurt, Germany) as described [219]. For incubations, cells were resuspended in isotonic PBS containing 1 mg/ml glucose and 1 mM $CaCl_2$ (PGC buffer) and incubated with different stimuli such as N-formyl-Met-Leu-Phe (fMLP, 1.5 min; Calbiochem), platelet activating factor (PAF, 1.5 min; Calbiochem), O-acetyl 11-keto boswellic acid (AKBA, 1.5 min), arachidonic acid (AA, 1.5 min; Sigma), ionophore A23187 (Iono, 2 min; Sigma), phorbol 12-myristate 13-acetate (PMA, 3 min; Calbiochem), sodium arsenite (SA, 3 min; Sigma) and sucrose (3 min; Sigma) at 37°C. Incubations were stopped by addition of ice-cold 2xSDS-PAGE sample loading buffer and heating at 95°C for 6 minutes.

Electrophoresis. A Mini-Protean system (Bio-Rad) was used. Aliquots of total cell lysates were loaded on a 10% SDS-PAGE gel containing 2-3 mg/ml purified recombinant human RORα4 or RevErbα protein, respectively. As positive control a gel polymerized with 500 µg/ml myelin basic protein was used, a gel without any added protein served as negative control.

In-gel renaturation. After electrophoresis, SDS was removed by washing the gels 5x 10 min with buffer A (20% isopropyl alcohol, 50 mM Tris-HCl pH 8.0) and 5x 10 min with buffer B (50 mM Tris-HCl pH 8.0, 1 mM DTT). In-gel proteins were denatured by incubation for 60 min in buffer C (50 mM Tris-HCl pH 8.0, 20 mM DTT, 2 mM EDTA, 6 M guanidine-HCl (Sigma)). To renature proteins, gels were washed once for 10 min in buffer D (50 mM Tris-HCl pH 8.0, 1 mM DTT, 2 mM EDTA, 0.04% Tween 20) followed by overnight incubation in 300 ml of the same buffer at 4°C with shaking.

In-gel phosphorylation. Gels were incubated in kinase buffer (20 mM HEPES pH 7.6, 20 mM $MgCl_2$, 25 mM β-glycerolphosphate, 10 mM 4-nitrophenylphosphate, 2 mM DTT, 0.2 mM Na_3VO_4) for 60 min at room temperature and finally incubated in 10 ml kinase buffer containing 10 µCi/ml γ-[^{32}P]-ATP (Amersham) for 60 min at 30°C with shaking. To remove unbound γ-[^{32}P]-ATP, gels were washed in washing buffer (1% sodium pyrophosphate, 5% trichloro-acetic acid) for two days with several buffer exchanges, followed by *in vacuo*-drying and incubation on imaging plates for three days. For visualization, imaging plates were scanned with a FLA-3000 Scanner (Fuji).

3.6 *In Vitro* Kinase Assay (IVKA)

Purified recombinant RORα4 (3-7µg) or RevErbα (1 µg) was incubated with activated ERK-2 MAPK (rat, recombinant; Biomol), PKA (catalytic subunit from bovine heart; Sigma) or p38-MAPK (GST-fusion, mouse, recombinant; Calbiochem) in kinase buffer (25 mM HEPES, pH 7.5, 25 mM $MgCl_2$, 25 mM β-glycerolphosphate, 2 mM DTT, 0.1 mM Na_3VO_4) containing ATP (100 µM, Sigma) and γ-[^{32}P]-ATP (2 µCi/ml; Amersham). The samples were incubated at 30°C for 30 min. The reaction was determined by addition of 2x SDS-PAGE loading buffer, probes were heated at 95°C for 6 min and separated by SDS-PAGE. Phosphorylated RORα4 was visualized by incubation of the dried gel for 24 h on an imaging plate followed by scanning with a FLA-3000 Scanner (Fuji).

3.7 Cell Culture

HeLa, HEK293 and MCF-7 cells were grown at 37°C in a humified atmosphere with 6% CO_2 in Dulbecco´s modified Eagle medium (D-MEM, Gibco) supplemented with 10% (vol/vol) fetal calf serum (FCS, Sigma-Aldrich), 100 µg/ml streptomycin and 100 U/ml penicillin (PAA Laboratories). For transient transfection, cells were seeded in D-MEM without phenol red (Gibco).
Stripped FCS was prepared by stirring 100 ml heat-inactivated FCS with 2 g charcoal (Sigma-Aldrich) for 2 h at 4 °C. The suspension was centrifuged at 51,500 g and the clear supernatant was frozen at –20°C. Immediately prior use, treated FCS was added to the cell culture medium and solution was sterile filtrated (0.45 µM, Roth).

3.8 Transient Transfection

Transient transfections were performed using the calcium phosphate precipitation method as described [217]. 24 h before transfection, cells were seeded in 24-well plates (Greiner bio-one): HeLa: $4x10^4$/well, HEK-293: $10x10^4$/well, MCF-7 $8x10^4$/well in 1 ml D-MEM cell culture medium without phenol red (Gibco). 10 µg or 20 µg reporter gene plasmid (400 ng/well viral promoters or 800 ng/well human promoters, respectively) along with 0.5 µg of the internal standard plasmid pCMV-SEAP were diluted with Milli-Q water to 450 µl. After addition of 50 µl 2.5 M $CaCl_2$, the solution was dropped slowly into 500 µl 2xHeBS buffer

(50 mM HEPES, 28 mM NaCl, 1.5 mM Na_2PO_4, pH 7.05) during continuous influx of sterile air. After a precipitation time of 1 min, 40 µl suspension was pipetted into each well. Cell culture medium was changed after 16 h of incubation and stimulating substances were added if necessary. Cells were grown for another 24 or 48 h; immediately before reporter gene analysis was performed, 33.3 µl cell supernatant was collected for standard determination.

3.9 Reportergene Assay

3.9.1 Luciferase Assay

For determination of luciferase activity, cell culture medium was replaced by 100 µl fresh phenol red-free D-MEM (Gibco), and 100 µl Steady-Glo reagent (Promega) was added to each well. Cell suspensions were transferred from 24 well plate into a 96 well microtiter plate (Greiner bio-one) and 15 min after addition of Steady-Glo reagent to the first well, measurement of luciferase activity was started by monitoring the light emission in a Mikrolumat Plus LB96V EG&G Berthold Luminometer. Luminescence was integrated from 5 sec for each well. All transfection experiments were performed as triplicates and as mean of three independent experiments.

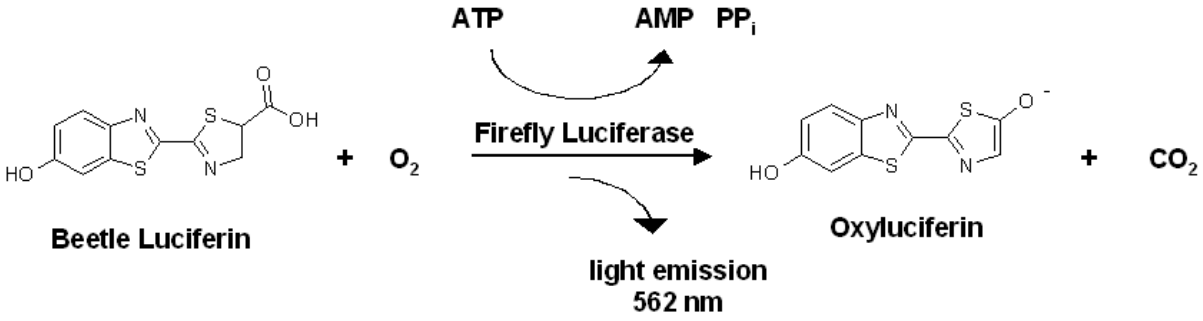

Fig. 3.1: Chemiluminescent conversion of luciferin to oxyluciferin, catalyzed by the firefly luciferase enzyme. *Emitted light was quantified by luminescence measurement.*

3.9.2 SEAP Assay

In order to equalize the varying transfection efficiencies, activity of the secreted alkaline phosphatase (SEAP) was assayed with the Phospha-Light kit (Tropix) according to the manufacturers instructions. For this purpose, 33.3 µl cell supernatant were heated for 30 min at 65°C along with 100 µl dilution buffer. 2x 50 µl of this solutions were transferred into a 96 well microtiter plate (Greiner bio-one), incubated with 50 µl assay buffer for 5 min and afterwards 20 min with 50 µl reaction buffer. Signals were detected with a Mikrolumat Plus LB96V EG&G Berthold Luminometer which was programmed to integrate light emission for 1 second. Relative light units (RLU) were calculated as follows: **RLU= $(LU_{luciferase}/LU_{SEAP})$x1000** [$LU_{luciferase}$: light units of luciferase activity; LU_{SEAP}: light units of alkaline phosphatase activity].

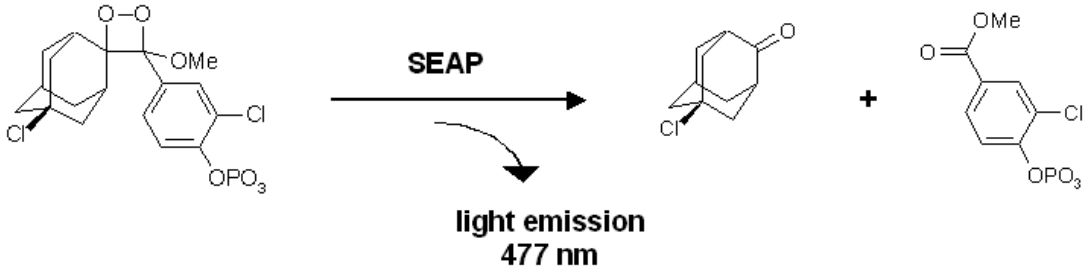

Fig. 3.2: Chemiluminescent conversion of CSPD dioxetane catalyzed by the secreted alkaline phosphatase enzyme (SEAP). *Emitted light was quantified by luminescence measurement.*

3.10 Analysis of EGFP-RORα4 Subcellular Distribution

For analysis of the intracellular distribution of EGFP-tagged RORα4-WT and mutants, HeLa or HEK293 cells were grown on glass cover slips. Cells were transiently transfected by calcium phosphate method [217]. 16 h after transfection the medium was changed, and after another 24 h cells were fixed with 4% paraformaldehyde in PBS for 10 min. For co-staining of the nucleus, cells were permeabilized with 0.1% Triton X-100 in PBS for 5 min and stained for 20 min with 1 mM TO-PRO-3 iodide (Molecular Probes) in PBS with 1% BSA. Images were taken by confocal laser scan microscopy (Zeiss LSM 510 Meta).

3.11 Genetic Engineering and Plasmid Construction

Sequences of all used primers (Sigma-Genosys) are given in Tables 10.3-10.9 (see Appendix).

3.11.1 RORα4 Protein Overexpression in *E. coli*: pET28a-RORα4-6xHisN

For cloning the coding sequence (cds) of human RORα4 into the empty vector pET28a, the pSG5-RORα4 vector (as a kind gift from C. Carlberg, Kuopio, Finland) was used. Two new restriction sites for NdeI and HindIII flanking the coding region were generated during amplification of the cds by PCR. The PCR product and the empty pET28a vector were digested with the restriction enzymes NdeI and HindIII and the insert was ligated into the vector subsequently. By performing this cloning strategy, hRORα4 was fused to a cleavable N-terminal hexahistidyl tag linked over a thrombin restriction site (LVPRGS), both provided in frame by the vector pET28a. The resultant construct was denoted as pET28a-RORα4-6xHisN and the entire nucleotide sequence of the RORα4-6xHisN gene was verified by sequencing.

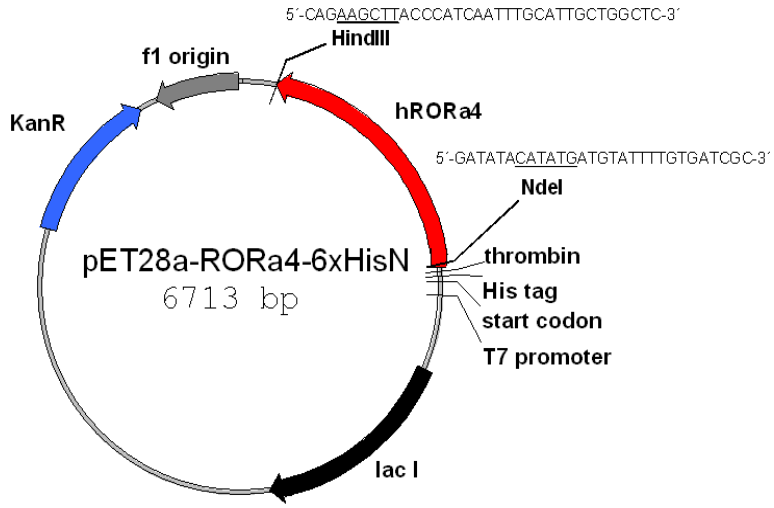

***Fig. 3.3: Plasmid map of pET28a-RORα4-6xHisN**, containing a T7 polymerase promoter, the gene that encodes for the resistance to the antibiotic kanamycin and the coding sequence for hRORα4 flanked by a N-terminal His-tag linked over a thrombin cleavage site. Primers for generating the new HindIII and NdeI restriction sites (underlined) are indicated.*

RORα4 mutants (T128A, T128D, T128E and others) were generated from wild-type by site directed mutagenesis. To introduce point mutations into the RORα4 coding sequence, a pair of two oligonucleotides was designed that were complementary to the respective opposite strand of the vector, but contained the desired mutations as mismatches. PCR cycle

parameters were chosen as given in Table 3. 4. The template was digested with DpnI for 2-24 h at 37°C and amplification product transformed into *E. coli* (sure). Successful mutagenesis was verified by sequencing.

Segment	Cycles	Temperature	Time
1	1	95°C	30 sec
2	20	95°C	30 sec
		55°C	1 min
		72°C	1 min / 550 bp of plasmid length
3	1	4°C	hold

Table 3.4: PCR cycling parameters for site directed mutagenesis.

3.11.2 hBmal1 Promoter: pGL3-Bmal1

The human Bmal1 promoter sequence was amplified from genomic DNA obtained from Mono Mac 6 cells. Two oligonucleotides flanking the promoter sequence encompassing a MluI and a XhoI restriction site, respectively (as can be seen from Fig. 3.5), were designed and used for PCR. The amplification product and the pGL3 empty vector were digested with MluI and XhoI for 2 h at 37°C and restriction products were separated on an agarose gel. After DNA elution out of the gel, backbone and insert were ligated at 16°C for 4 h. By performing this cloning strategy, the Bmal1 promoter sequence was set in front of the luciferase coding sequence, activation of the Bmal1 promoter would result in luciferase protein expression. A schematical constitution of the resulting construct is given in Fig. 3.6 A.

MluI

5´ACGCGTCCCAGAGAAGAGGGACATCCCGGGCGACCCCGAGGAGCGCGGCTTGG
GCACCGCAGTGGCCGCGGCTAGTGGGAGACCTGAGGGGAAAGGGAGAGGGCAG
GGGCGAGGAACCCAGGGAGCGCGCGCGGATTGGTCCTCTCCTCGGGGCGTGCGC
TCCTGTGCGCCAAATGATTGGTGGCAGGAAAGTAGCAGGTAAACCGGCTCCCGCC
GCCTCGCCATTGGTCAGCGGCCTCTCTAGCCGCCACACAACTGGCCAGCGGGCTG
CCGAGCCGCGCGCGGATTGGCTGGGGGCGGCCGCCGGGACCGGCTCCCTTCGGG
CGTTCGGATTGGCTGGCGGGAAGAGGCAGGTATCCGGGCGCTGCGGCTCCTCCAT
TGGTGGGCGGGGAAGGGGGGTTGGGCACAGCGATTGGTGGGCGGGGGGCCGGG
CCTGGGCCGGCGGGGAGCGGATTGGTCGGAAAGTAGGTTAGTGGTGCGACATTTA
GGGAAGGCAGAAAGTAGGTCAGGGACGGAGGTGCCTGTTTACCCGCGCCGGACT
CACCGCCGCCGCCGCCGCGGGATCCGAGTGCGGGCGCGCTCGAG-3´

XhoI

Fig. 3.5: Sequence of hBaml1 promoter embedded in the pGL3 plasmid. *Sequence is flanked by a MluI and a XhoI restriction site, by which it was cloned into the vector. Underlined sequences were used as primers for PCR (preceded by GATA). ROR response elements (ROREs) are marked in dark gray.*

3.11.3 hBmal1 Isoform A and B Protein Expression: pSG5-Bmal1-A, B

The coding sequences of human Bmal1 isoform A and B were cloned from Mono Mac 6 cDNA. PCR primers are shown in Fig. 3.6 B, two different forward primers were needed to generate the two isoforms A and B. Both forward primers embedded an EcoRI, the reverse primer a BglII restriction site, over which the amplified PCR product was ligated in the multiple cloning site of the pSG5 empty vector.

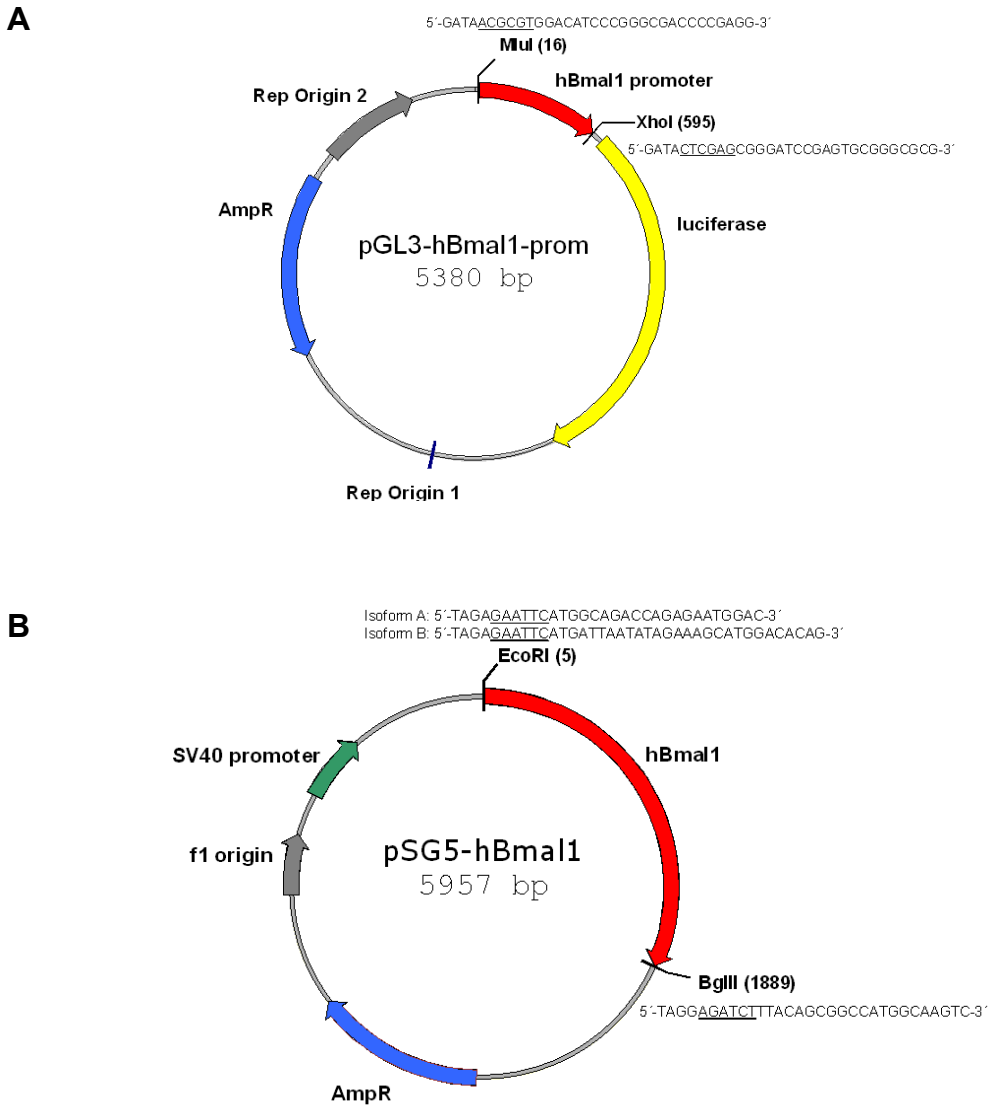

***Fig. 3.6 (A) Plasmid map of pGL3-hBmal1-prom**, containing the human Bmal1 promoter in front of the luciferase coding sequence and a gene that encodes for the resistance to the antibiotic ampicillin. Primers for generating the MluI and XhoI restriction sites (underlined) are indicated. **(B) Representative plasmid map of pSG5-hBmal1-A/B,** that contains the coding sequence of hBmal1 protein isoform A or isoform B, respectively. Protein expression is regulated by a SV40 promoter. The gene encoding for the resistance to the antibiotic ampicillin and primers for generating the EcoRI and BglII restriction sites (underlined) are indicated.*

3.11.4 Determination of Anti-RORα Antibody Epitope: pEGFP-C2-HI-LBD-1-6

For determination of anti-RORα antibody epitope, expression plasmids for six different RORα truncation mutants fused to EGFP were cloned. Each of them contained the coding sequence of the RORα ligand binding domain, a part of the hinge domain varying in length, and the EGFP coding sequence. Six different PCRs with pSG5-RORα4 as template were arranged. The six forward primers (as indicated in Fig. 3.7) annealed at six different positions within the hinge domain coding sequence, the reverse primer annealed at the end of the cds of the ligand binding domain. The varying length of resulting amplification products was controlled by agarose gel electrophoresis. After digestion of PCR products and the pEGFP-C2 empty vector (Clontech) with HindIII and Acc65l, the hinge-LBD fragments 1-6 were set behind the EGFP cds. A plasmid map is given in Fig. 3.8.

Fig. 3.7: Cloning of pEGFP-HI-LBD1-6. *Coding sequence of hinge and LBD embedded in pSG5-RORα4, hinge domain is marked in light gray. Six forward (f1-f6) and one reverse (rev) primers were designed for PCR. The resulting truncation mutants differ in the length of their hinge domain.*

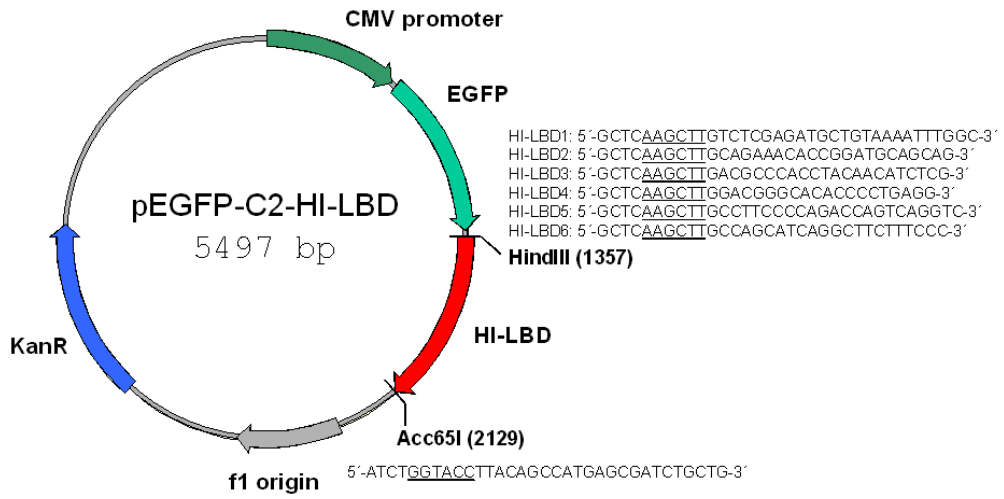

Fig. 3.8: Representative plasmid map of pEGFP-C2-HI-LBD-1-6. *Expression of the EGFP-HI-LBD mutants 1-6 is controlled by a CMV promoter. The gene that encodes for the resistance to the antibiotic kanamycin and primers for generating the HindIII and Acc65l restriction sites (underlined) are indicated.*

3.11.5 Ca/Dn-MEK1 Expression Plasmid: pcDNA3.1(+)-ca/dn-MEK1

The coding sequence of MEK1 was cloned from cDNA of Mono Mac 6 cells in two fragments encompassing 481 and 701 bp, respectively. Primers for amplification of the 481 bp-fragment contained a HindIII (for) and an EcoRI (rev) restriction site, primers for the 701 bp fragment embedded an EcoRI (for) and a XhoI restriction site (see Fig. 3.9, restriction sites are underlined). After double-digestion of the purified PCR fragments and the empty pcDNA3.1(+) vector with the respective enzymes, fragments and backbone were ligated. The resulting construct was controlled by sequencing.

In order to generate a constitutive active (ca) form of MEK1, two mutations were introduced into the MEK1 cds by site directed mutagenesis. MEK1 Ser-218 was replaced by glutamic acid and Ser-222 by aspartic acid subsequently. The dominant negative (dn) MEK1 was obtained by mutation of Lys-97 to methionine. Primers for generation of MEK1-S218E-S222D (ca) and MEK1-K97A (dn) are described in Table 10.9 (Appendix). A representative plasmid map is given in Fig. 3.9. Functionality of the two constructs and MEK1 protein expression were tested by transfection of HeLa cells and immunoblotting with anti-MEK1 antibody.

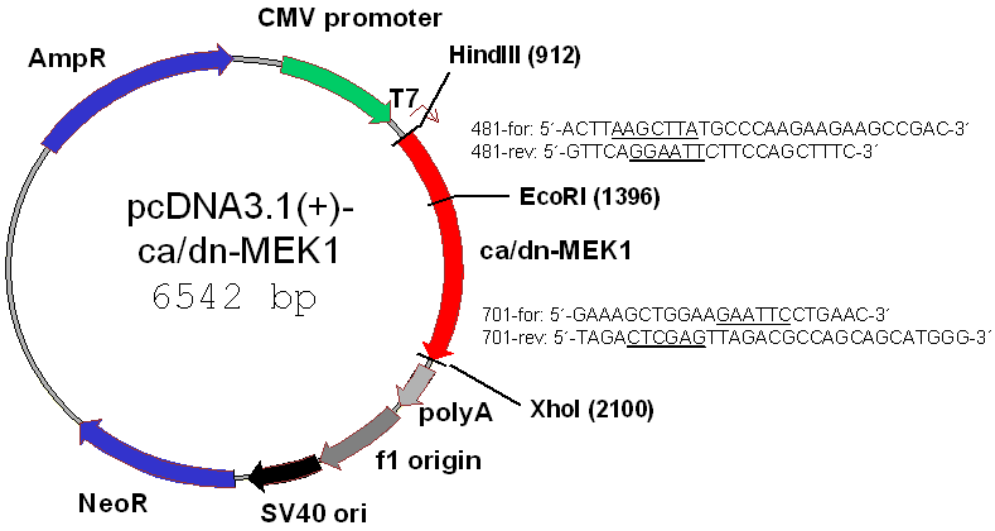

Fig. 3.9: Representative plasmid map of pcDNA3.1(+)-ca/dn-MEK1. *Expression of ca/dn-MEK1 is controlled by a CMV promoter. The genes that encode for the resistances to the antibiotics ampicillin and neomycin and primers used for cloning are indicated.*

3.11.6 SUMO1 Expression Plasmid: pSG5-SUMO1

The coding sequence of SUMO1 was cloned from Mono Mac 6 cDNA using the following primers (restriction sites underlined):

SUMO1-SpeI-for: GCCACCACTAGTATGTCTGACCAGGAGGCAAAACCTTC
SUMO1-HindIII-rev: GCCACCAAGCTTAACTGTTGAATGACCCCCCGTTTG

The resulting 327 base pairs amplification fragment was restricted with SpeI and HindIII and analyzed by agarose gel electrophoresis. After DNA elution out of the gel, the PCR product and pSG5 empty vector were double-digested with SpeI/HindIII and the SUMO1 coding sequence was inserted in the opened pSG5 empty vector.

4 RESULTS

4.1 Overexpression and Purification of Human RORα4 in *E. coli*

4.1.1 RORα4 Overexpression

Overexpression of eukaryotic, especially human proteins in bacterial strains like *Escherichia coli* is a very effective method to obtain large amounts of pure protein. By transformation of a vector that contains the protein coding sequence into one of the common bacterial strains for overexpression, almost every human protein can be produced in full-length, or as truncation mutant for investigation on functional domains. Fusion of an additional N- or C-terminal polyhistidine tag to the target protein facilitates an easy purification, by the fusion of GFP (green fluorescent protein), the transfected recombinant protein can be visualized and observed inside intact cells. A variety of further useful tags had been developed that influence protein solubility, localization, the affinity to diverse reagents or protein recognition, showing that this kind of genetic engineering provides a lot of possibilities.

In order to obtain pure and native RORα4 protein for biochemical investigations, a method for overexpression in *E. coli* and subsequent purification was established. For this purpose, pET28a-RORα4, a constructed plasmid containing the RORα4 coding sequence fused to a N-terminal polyhistidine tag, was transformed into *E. coli* and the rate of RORα4 protein production during cell cultivation optimized. Different parameters concerning the overexpression host, culture and induction conditions were varied. As overexpression host, three kinds of *E. coli* strains were tested, BL21 (DE3), BL21 pLysS and Rosetta, however, the use of different strains did not influence the expression efficiency significantly. Finally, *E. coli* BL21(DE3) was chosen because of its rapid growth rate. As culture medium Luria Broth (LB) standard nutrient was used, and the impairment of culture conditions by addition of 3% ethanol or the use of M9 minimal salt medium plus casein hydrolysate diminished protein yield (Fig. 4.1 B). RORα4 expression yield was sensitive to the modification of induction conditions. Start of protein expression with 1 mM Isopropyl-β-D-thiogalactopyranoside (IPTG) at an optical density (measured at 660 nm, OD660) lying between 0.4 and 0.6, and 22°C as incubation temperature after the point of induction were found to be important parameters to enhance RORα4 protein expression (Fig. 4.1). Variation of IPTG concentration had no influence on expression efficiency. Cells were harvested and

lysed by sonication, supernatant and insoluble residues were separated by centrifugation and analyzed by SDS-PAGE. In all cases RORα4 protein appeared to be nearly exclusively expressed as inclusion bodies and therefore found in an insoluble form in the centrifugation pellet.

Based on the yield optimizing studies, the following conditions were set as standard protocol for overexpression of RORα4: *E. coli* BL21 (DE3) cells harboring the plasmid pET28a-RORα4 were grown at 37°C with shaking overnight in 20 ml of LB medium containing kanamycin (50 µg/ml). A 6 ml aliquot of this culture was diluted into 500 ml of the same medium and grown at 37°C with shaking. When cells reached an OD660 of 0.4-0.6, addition of IPTG to a final concentration of 1 mM induced expression from the T7 promoter. After growth was continued for another 4 h at 22°C, cells were harvested by centrifugation at 12,000 rpm in a Sorvall GSA rotor for 15 min at 4°C. The cell pellet was frozen and kept at -20°C.

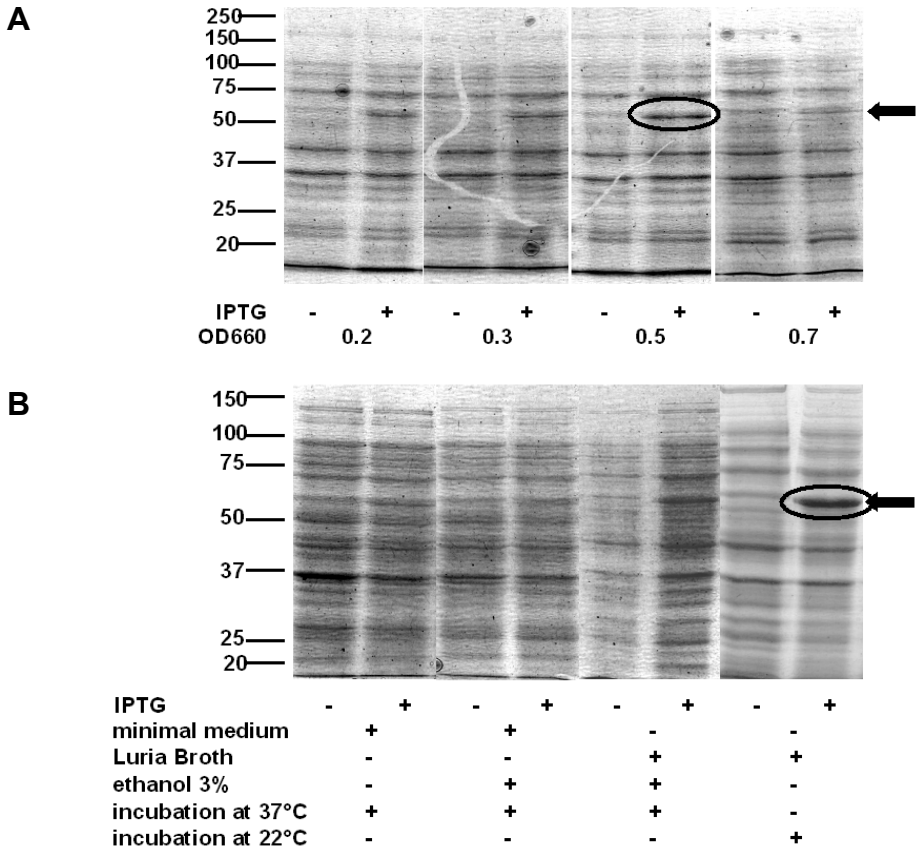

Fig. 4.1: Optimizing RORα4 overexpression conditions. *Cell aliquots were harvested immediately before and 4 h after induction with IPTG. Bacteria were lysed with loading buffer and analyzed by SDS-PAGE with subsequent Coomassie brilliant blue staining of the gel. Equal cell amounts were loaded onto each lane. (A) Variation of optical density at induction point. Cells were grown at 37°C with shaking, optical density was determined with a Hitachi U-2000 spectrometer at 660 nm (OD660). IPTG was added to a final concentration of 1 mM. The arrow points at the RORα4 migration height, RORα4 yield at induction of the optimal optical density is indicated. (B) Variation of culture medium and incubation temperature. The arrow points at RORα4 protein at optimized culture conditions.*

4.1.2 Separation of Inclusion Bodies and Refolding

As mentioned above, RORα4 was expressed in an insoluble, denatured and therefore inactive form, as it is often observed when eukaryotic proteins get overexpressed in prokaryotes. The attribute of insolubility was used for purification, by washing the pellet with 1% Triton X-100 about 70% protein purity could be achieved . Subsequently, the protein was solubilized in 6 M guanidine and refolded into the native structure.

The cell pellet from 1.5 l *E. coli* culture (approx. 5-6 g wet weight) was thawed and lysed by suspending in 20 ml lysis buffer (25 mM Tris-HCl pH 8, 0.5 mM EDTA, 1 mg/ml lysozyme, 5 µg/ml DNaseI and 10 µg/ml RNaseA) and sonication on ice for 20 min with 50% cycles using a Bandelin Sonoplus HD 200 sonicator. The homogenous suspension was centrifuged at 4,000 rpm in a Heraeus Sepatech 8080E rotor for 10 min and the supernatant representing the soluble cell fraction was discarded. The insoluble cell fraction was washed three times with 50 ml 1% Triton X-100 each. SDS-PAGE analysis was used to check the effectiveness of the purification procedure (Fig. 4.2).

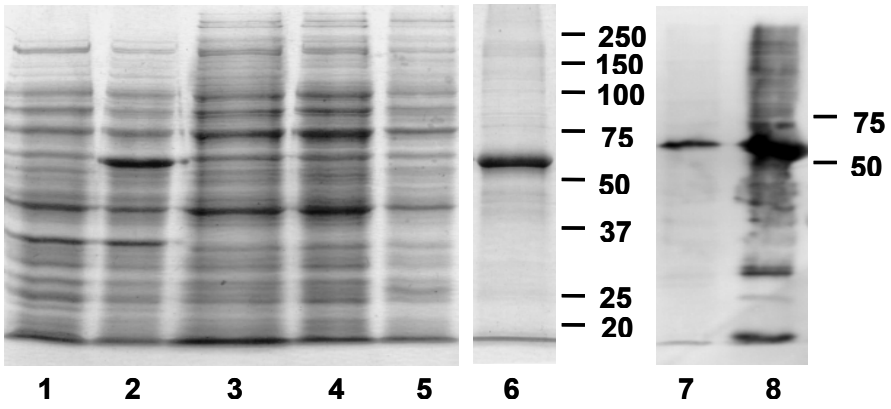

Fig. 4.2: SDS-PAGE analysis of RORα4 overexpression in E. coli. *Lanes 1-6 stained with Coomassie brilliant blue: 1-2: total cell proteins from E. coli immediately before and 4 hours after induction with 1 mM IPTG, 3: soluble supernatant of lysed cells, 4-5: supernatant of inclusion bodies washed with 1% Triton X-100, 6: insoluble inclusion body fraction. Lanes 7-8 immunoblot using anti-RORα antibody (Santa Cruz), followed by staining with NBT (330 µg/ml) and BCIP (170 µg/ml): total cell proteins from E. coli before and after induction with 1 mM IPTG, respectively. Equal cell amounts were loaded onto each lane.*

The RORα4 inclusion body pellet (about 70% purity) was dissolved in refolding buffer A (6 M guanidine-HCl (Sigma), 20 mM NaH_2PO_4 pH 9.3, 0.1 M KCl, 6 mM DTT, 25 µM $Zn(OAc)_2$) to a final concentration of approx. 25 µg/ml protein and heated at 100°C for 10 min. Insoluble residues that might act as seed crystals were separated by another centrifugation at 4,000 rpm for 5 min. 4 ml of denatured RORα4 solution were renatured by

dialysis against a 100-fold volume of refolding buffer A with stepwise descending guanidine content (4 M, 2 M) for 3 h at 4°C each, followed by dialysis against a 100-fold volume of refolding buffer B (0.5 M L-arginine (Fluka), 20 mM NaH_2PO_4 pH 9.3, 0.1 M KCl, 6 mM DTT, 25 µM $Zn(OAc)_2$) overnight. Dialysis was continued by using refolding buffer B with stepwise descending L-arginine content (0.3 M, 0.15 M, 0 M) for 3 h at 4°C each. To concentrate the protein solution 50% glycerol was added to the last dialysis step that was performed overnight at 4°C. Then the refolded protein was stored at -70°C. Protein concentration was determined by Bradford standard method, 200-300 µg/ml were achieved (overall yield 16-20 mg RORα4 per 1 liter *E. coli* culture). Fig. 4.3 shows an overview about the refolding procedure.

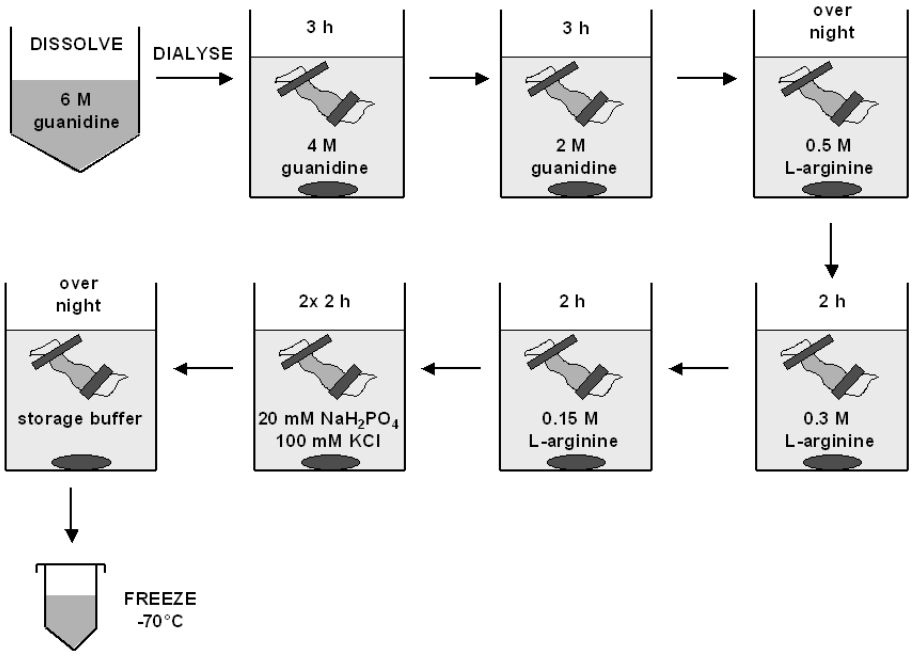

Fig. 4.3: Schematical flowchart of RORα4 refolding procedure. *Denatured RORα4 was dissolved in 6 M guanidine and refolded by dialysis against seven different buffers within three days.*

4.1.3 Nickel Affinity Chromatography

For the purpose of applications requiring a further increased protein purity, a method utilizing Nickel affinity chromatography was developed. Therefore, the Nickel-ion affinity of the N-terminal polyhistidine tag was utilized. For optimal protein recovery it was necessary to vary the buffer conditions during the refolding procedure. Addition of DTT was avoided since the presence of DTT impairs the resin by reduction of Ni^{2+} ions. No Zn^{2+} ions were added to the solutions because they might occupy the polyhistidine tag and prevent RORα4 from binding

to the resin. Nevertheless, Zn^{2+} ions are essential for RORα4 activity and had to be added to the elution buffer. In the last refolding step the sample was dialyzed into purification buffer providing optimal column binding conditions (50 mM NaH_2PO_4 pH 8.0, 0.3 M NaCl, 50% glycerol). For batch purification, 2 ml of the refolded sample (approx. 500 µg RORα4) were applied onto 1.5 ml Ni-NTA agarose (Qiagen) equilibrated with equilibration buffer (50 mM NaH_2PO_4 pH 8.0, 0.3 M NaCl). After the protein-Ni-NTA mix was shaken very gently for 90 min at 4°C, the slurry was poured into an empty column and the flowthrough was collected. Unbound proteins were washed off with a cascaded imidazole gradient (50 mM NaH_2PO_4 pH 8.0, 0.3 M NaCl, with 20, 30, 40, 50 and 60 mM imidazole) and RORα4 finally eluted with elution buffer (50 mM NaH_2PO_4 pH 8.0, 0.3 M NaCl, 25 µM $Zn(OAc)_2$, 250 mM imidazole). SDS-PAGE was used to analyze the purity of protein (Fig. 4.5). To determine RORα4 purity, gels were stained with Coomassie brilliant blue and gels were evaluated with Odyssey quantification software (Licor). RORα4 identity was controlled by Western Blotting on a PVDF membrane and incubation of the blot with anti-RORα antibody (Santa Cruz), followed by detection with nitro blue tetrazolium chloride (NBT, 330 µg/ml) and 5-bromo-4-chloro-3-indolylphosphate (BCIP, 170 µg/ml).

By performing a batch purification procedure, approx. 90% of the applied RORα4 protein bound to the resin. The protein was washed and eluted with an imidazole gradient, elution of RORα4 appeared between 50 and 100 mM imidazole, therefore the imidazole gradient in this interval is cascaded in a very fine way. While the color of the loaded sample was slightly

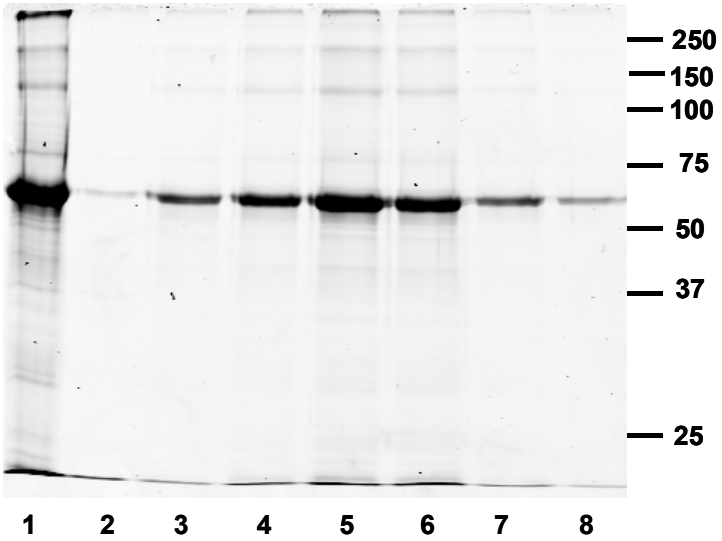

Fig. 4.4: SDS-PAGE analysis of RORα4 purification by nickel affinity chromatography. *Proteins were stained with Coomassie brilliant blue. 1: refolded RORα4, 2: flow-through from Ni-NTA column; lane 3-9 elution fractions, elution with 250 mM imidazole. Equal proportions (20 µl solution) were loaded onto the various lanes.*

brown, which was probable caused by insoluble non-protein *E. coli* residues, the eluted fractions were colorless and concentrations of 400 µg/ml were achieved. However, RORα4 protein dimers, trimers and small fragments, bearing the N-terminal His-tag, possibly formed during sonication, could not be separated by Nickel affinity chromatography.

4.1.4 DNA Binding Activity of Refolded RORα4

The DNA binding activity of purified RORα4 was tested in an electrophoretic mobility shift assay (EMSA). The following complementary 5`-IRDye700 labeled oligonucleotides were annealed to generate double-stranded DNA fragments encompassing the ROR response element (RORE, underlined):

RORE-sense 5` TCGAGTCGTATAACTAGGTCAAGCGCTGGAC 3`;
RORE-antisense 5` GTCCAGCGCTTGACCTAGTTATACGACTCGA 3`.

The EMSA standard 20 µl binding reaction mixture contained 1-2 µg of purified recombinant RORα4 protein, poly-dA-dT as competitor for unspecific DNA binding of proteins, and EGTA and Na_3VO_4 as inhibitors for remaining DNaseI residues from purification. Addition of bovine serum albumin (BSA) was needed to stabilize the labeled oligonucleotides. The reaction mixture was loaded on a 4% polyacrylamide gel and complexes were separated in 0.5x Tris-borate-EDTA at 4°C. Gels were scanned with an Odyssey infrared imaging system (Licor). As can be seen from Fig. 4.5, refolded RORα4 was able to bind the ROR response element of the oligonucleotide, leading to a shifted band. The specificity of RORα4-DNA complexes was demonstrated by the addition of 2.2 µg anti-RORα-antibody to the binding reaction mixture which caused a complete loss of RORα4-DNA binding affinity.

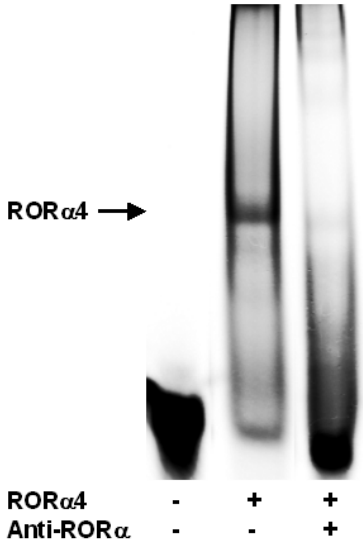

Fig. 4.5: DNA binding activity of refolded RORα4 was analyzed by electrophoretic mobility shift assay (EMSA) *with 5`-IRDye700 labeled, double-stranded oligonucleotides and recombinant RORα4 protein. Specificity of protein-DNA complexes was demonstrated by the addition of anti-RORα antibody. The RORα4-DNA complex is indicated.*

4.1.5 Protein Recovery

At the point of cell harvest, RORα4 represents approx. 10% of the total bacterial proteins in transformed *E. coli* BL21(DE3). After sonication and washing of 5-6 g *E. coli* pellet wet weight (from 1 Liter culture), 18-22 mg denatured and inactive inclusion body protein could be recovered. Subsequent Ni-affinity chromatography facilitated an overall yield of 16-20 mg per 1 liter *E. coli* culture. Quantification was performed from Coomassie gels using Odyssey Application Software (Licor).

Purification step	Estimated amount of protein [mg]	Purity of RORα4 protein [%]
E. coli	~ 400	10
↓ sonication, wash		
inclusion bodies	18-22	70
↓ refolding, Ni affinity chromatography		
native, purified RORα4	16-20	85

Fig. 4.6: Purification table of recombinant RORα4 from 1 liter E. coli

4.1.6 Overexpression of Human RORα4 in HeLa

For protein overexpression in eukaryotic HeLa cells, transient transfection was performed. Cell count as well as DNA amount were optimized (Fig. 4.7) as follows: 0.5-2.5×10^6 HeLa cells were seeded in plates with 9 cm diameter using Dulbecco´s Modified Eagle Medium (D-MEM). Cells were transfected the following day with 20-70 µg expression vector pSG5-RORα4 by the standard calcium phosphate method as described [217]. Cells were incubated with the precipitate for 16 h before medium was replaced. 24 h after transfection, cells were harvested and nuclear and cytosolic fractions were separated by incubation with 0.1% NP-40 (in 10 mM Tris pH 7.4, 10 mM NaCl, 3 mM $MgCl_2$, 1 mM EDTA, phenylmethanesulfonyl fluoride (PMSF), soybean trypsin inhibitor (STI), leupeptin) and centrifugation at 2700 rpm in a Heraeus Sorvall 3329 rotor for 10 min at 4°C. The supernatant represents the cytosolic fraction, the pellet nucleus and membranes. As shown in Fig. 4.7, 0.5×10^6 cells and 25 µg DNA were found as optimized conditions for RORα4 overexpression in HeLa cells.
The resulting cell preparations were important tools to analyze antibody specificity or to perform localization experiments by Western Blotting described in the following chapters.

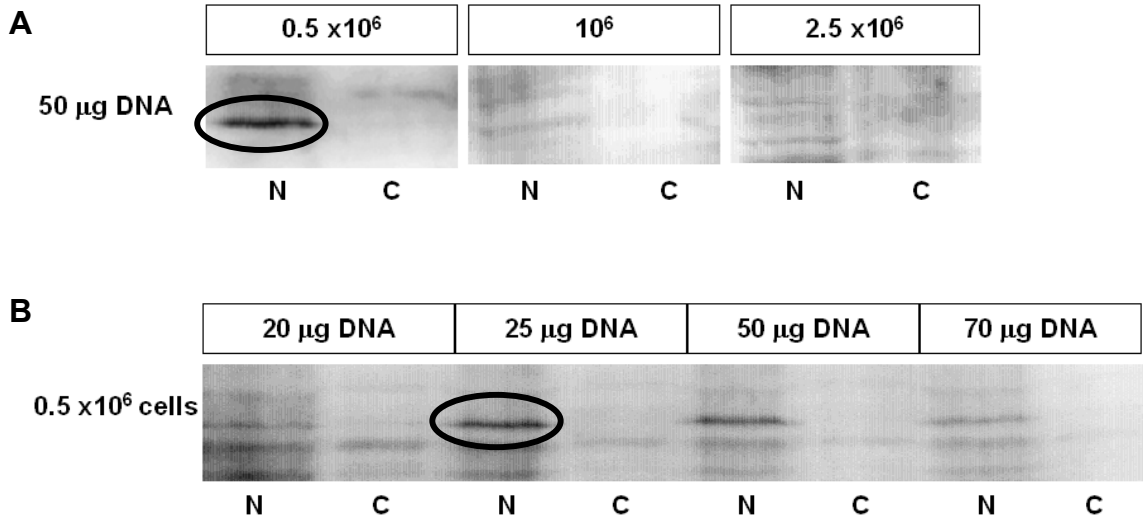

Fig. 4.7: Optimizing RORα4 overexpression in HeLa. *(A) Variation of cell count seeded one day before transfection of 50 µg pSG5-RORα4. (B) Variation of DNA amount used for preparation of precipitates applied onto 0.5x10^6 cells. N: nuclear, C: cytosolic fraction.*

4.2 Generation of an Anti-RORα Antibody

Antibodies are important tools for qualitative and quantitative detection of proteins in biochemical experiments. For a doubtless identification, these antibodies must feature high sensitivity and specificity, furthermore, the antibody itself should be characterized for a reasonable usage. In order to generate an antibody targeted against RORα, mice were immunized with recombinant human RORα4 protein.

4.2.1 Preparation of Protein and Immunization

Purified RORα4 inclusion bodies were used as basis for the recovery of the immunization serum. To avoid generation of an antibody targeted against the polyhistidine tag, this tag was cut off from RORα4 protein by taking advantage of the thrombin cleavage site. The inclusion body pellet from 1.5 l cell culture was dissolved by heating at 100°C for 7 min in cleavage buffer (200 mM Tris-HCl pH 8.4, 1.5 M NaCl, 25 mM $CaCl_2$) containing 0.5% SDS. For the cleavage reaction, 10 units thrombin were added and the preparation was incubated at room temperature overnight.

To obtain very pure RORα4 protein, the sample was loaded on a 10% polyacrylamide gel and bands corresponding to RORα4 were cut out of the gel. The protein was eluted out of the polyacrylamide gel by stirring the fragments in running buffer (0.2 M glycine, 25 mM Tris-HCl, 3.5 mM SDS) overnight at 4°C. The solution was concentrated 10-fold by dialysis against 10% polyvinylpyrrolidone for 24 h at 4°C. Denatured RORα4 was renatured by dialysis against PBS containing 0.5 M L-arginine, 25 mM $ZnSO_4$ and 26 nM cholesterol for 8 h in a first step and against PBS overnight at 4°C in a second step.

According to Brand et al. [220], about 50 µg RORα4 protein (determined by Bradford protein assay) in a final volume of 200 µl were injected i.p. into two female Balb/C mice. Eight immunizations were given with intervals of 15-21 days between the injections, a final i.p. boost was given three days before cell preparation. Each mouse was sacrificed under anesthesia and the spleen was dissected under sterile conditions. After fusing lymphocytes with NS-1 cells by adding PEG 4000, cells were separated into 96-well micro plates and supernatants of the growing clones were screened for antibody production by ELISA.

4.2.2 Control of Specificity

Antibody specificity of a couple of clones was tested by Western Blotting. Probes from prokaryotic as well as eukaryotic cells were prepared, separated by SDS-PAGE and blotted on a PVDF membrane. After blocking the membrane surface with 5% milk (in TBS), the blot was incubated with clone cell culture supernatant, washed with TBS/Tween and incubated with anti-mouse antibody (alkaline phosphatase conjugated) subsequently. As can be seen from Fig. 4.8, the antibody producing clone 6E8 featured especially high sensitivity and specificity and was therefore chosen for further purification.

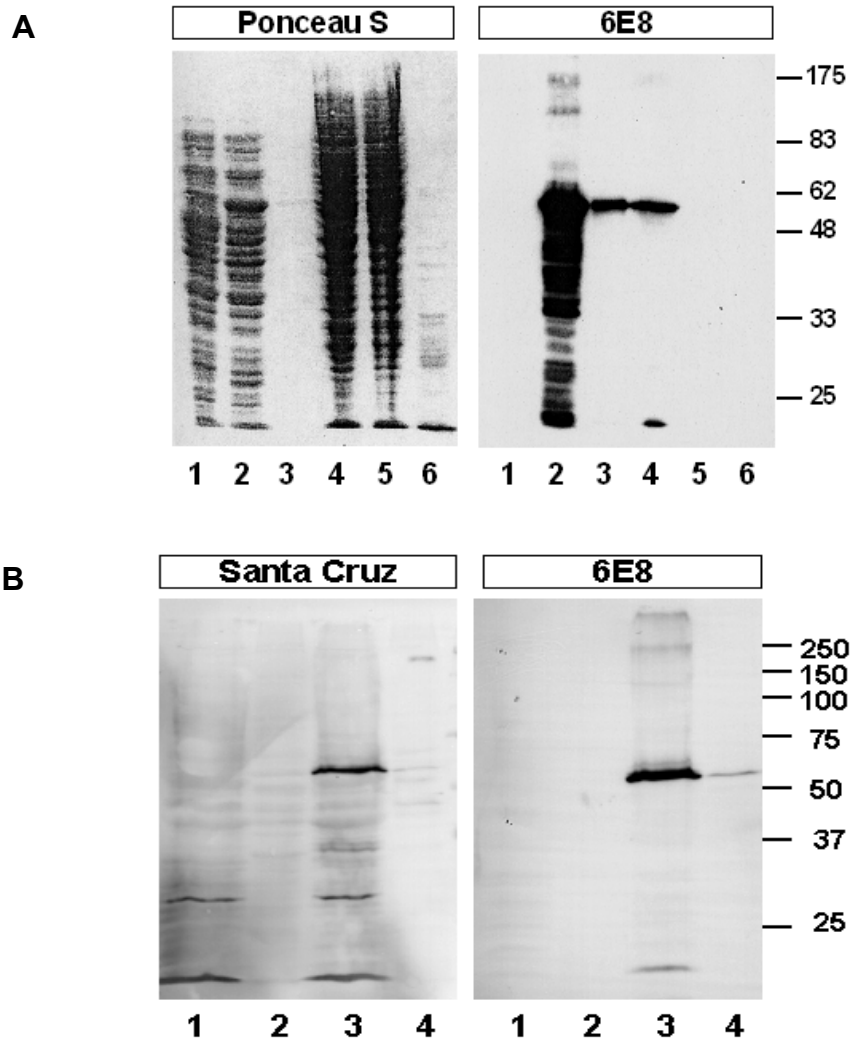

Fig. 4.8: Control of clone 6E8 antibody specificity by Western Blotting on a PVDF membrane. *(A) General proteins versus proteins detected with clone 6E8. Left: Blot stained with Ponceau S, right: detection with clone 6E8 followed by incubation with ECL. 1: untransformed E. coli, 2: E. coli transformed with pET28a-RORα4,induced with 1 mM IPTG, 3: purified RORα4, 4: U266 nuclear extract + purified RORα4, 5: U266 nuclear extract, 6: E. coli transformed with PKA-His. (B) Comparison of anti-ROR antibody purchased from Santa Cruz versus clone 6E8; Blots stained with NBT and BCIP. Left: detection with polyclonal anti-RORα antibody developed in goat (Santa Cruz); right: detection with monoclonal anti-RORα antibody clone 6E8 developed in mouse. Lanes 1, 2: nuclear and cytosolic fraction of HeLa cells; 3, 4: nuclear and cytosolic fractions from HeLa cells transfected with pSG5-RORα4.*

4.2.3 Purification of Anti-RORα Antibody Clone 6E8

Purification of the IgG_1 antibody from cell line 6E8 was performed using protein G Sepharose. Serum-free cell culture supernatant was adjusted to 20 mM NaH_2PO_4 pH 7.0 and applied to a column filled with protein G Sepharose resin equilibrated with binding buffer (20 mM NaH_2PO_4 pH 7.0). After the resin was washed with binding buffer, the bound antibody was eluted with 100 mM glycine pH 2.5 and immediately neutralized by addition of 1/10 volume of 1 M Tris-HCl pH 9. Antibody purity was controlled by SDS-PAGE and Coomassie brilliant blue staining. After dialysis against PBS, protein concentration was examined by Bradford protein assay using γ-globulin (from bovine plasma) as standard. Antibody solutions were stored at 4°C.

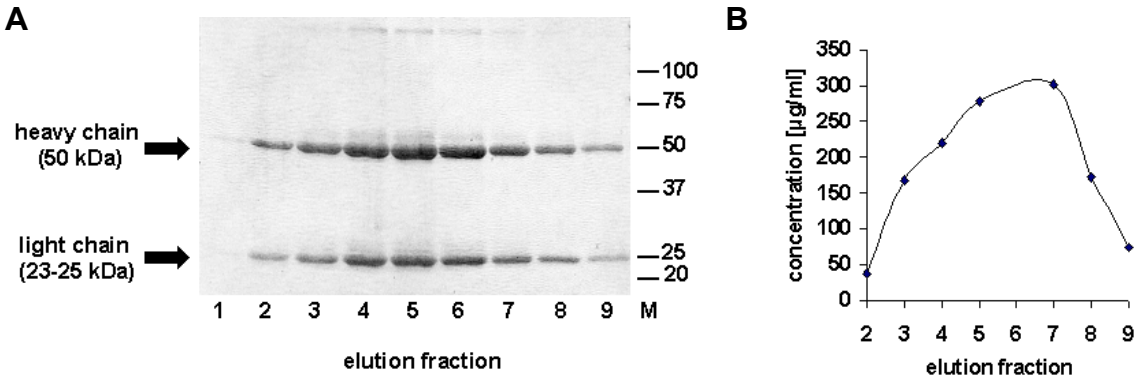

Fig. 4.9: Purification of antibody from 200 ml cell supernatant. *(A) Elution fractions were analyzed by SDS-PAGE and Coomassie brilliant blue staining. Antibody was eluted from the column in fractions by addition of 500 µl elution buffer each. (B) Concentration of elution fractions was determined by Bradford standard method.*

4.2.4 Determination of Epitope

Since monoclonal antibodies bind to only one definite epitope, truncation mutants lacking different protein domains were cloned. The truncation mutants were transfected into HeLa cells, nucleic and cytosolic fractions blotted on a PVDF membrane and after blocking the surface with 5% milk, the membrane was incubated with antibody clone 6E8.

In a first experiment two constructs were tested, pEGFP-A/B-DBD providing the A/B and the DNA binding domain, and pEGFP-HI-LBD that codes for the hinge and the ligand binding domain. Both truncated forms are fused to EGFP to facilitate the control of protein expression with help of an anti-EGFP antibody. As can be seen from Fig. 4.9, monoclonal antibody clone

6E8 detected the protein mutant composed of the hinge and ligand binding domain. The A/B-DBD mutant was not detected, promising that the epitope was provided by RORα4 amino acids 83-468.

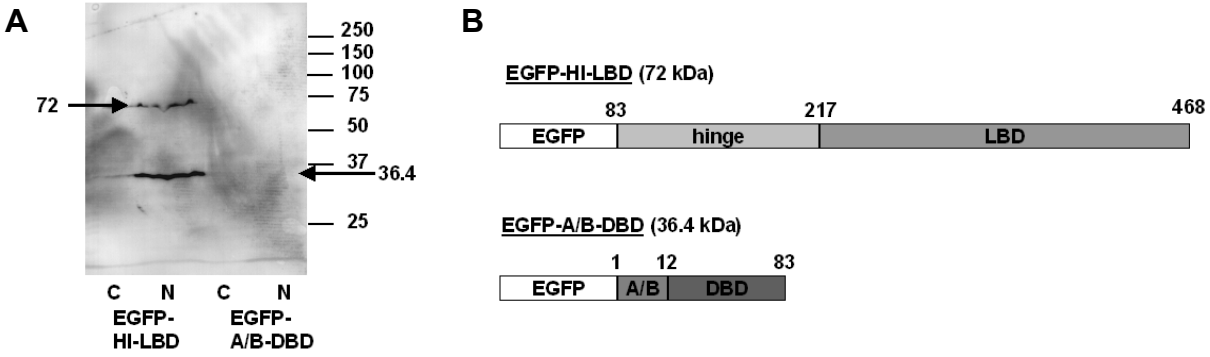

Fig. 4.10: Determination of antibody epitope. *(A) pEGFP-HI-LBD and pEGFP-A/B-DBD were transfected into HeLa cells, nuclear (N) and cytosolic (C) fractions were blotted on a PVDF membrane which was incubated with antibody clone 6E8 subsequently. (Occurrence of a putative cleavage fragment of 36.4 kDa is discussed in chapter 4.4.2.) (B) Schematical constitution of truncation mutants.*

For further specification of the antibody epitope, the hinge domain was divided into six segments. As can be seen from Fig. 4.11, six constructs were cloned, HI-LBD 1-6 contained one to six of these hinge segments, fused to the ligand binding domain on the 3´-side and the EGFP coding sequence on the 5´-side.

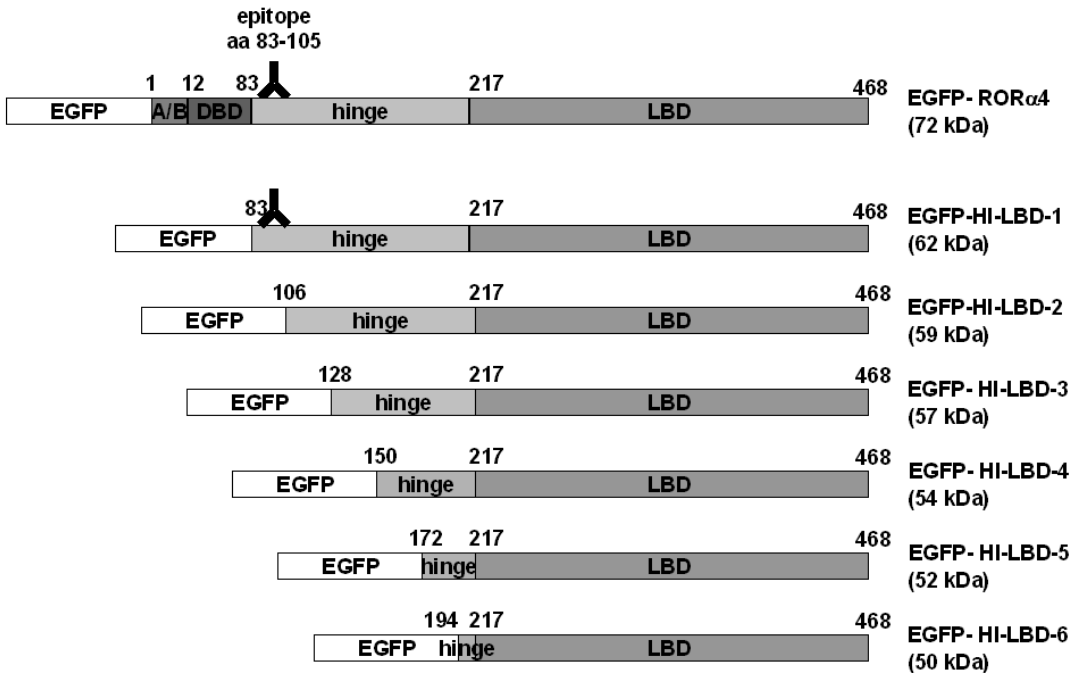

Fig. 4.11: Schematical constitution of RORα4 protein and truncation mutants. *HI-LBD 1-6 differ in the length of the hinge domain. Length of protein mutants and antibody epitope are indicated.*

Truncated mutants were cloned by PCR using six forward primers that each bound to different locations on the hinge coding sequence and that were attached to a SacII restriction site. The reverse primer annealed at the end of the LBD and embedded a HindIII restriction site. The resulting fragments varying in length were ligated into the pEGFP vector over the SacII and HindIII restriction sites. pEGFP-HI-LBD-1 to -6 were transfected into HeLa cells and protein expression was demonstrated by incubation of Western Blot membrane with anti-GFP antibody. As can be seen from Fig. 4.12, all mutants appeared at the predicted molecular weight. In contrast, incubation with clone 6E8 detected full-length EGFP-RORα4 and only one of the six constructs, HI-LBD-1, suggesting that the epitope lies between amino acids 83 and 105.

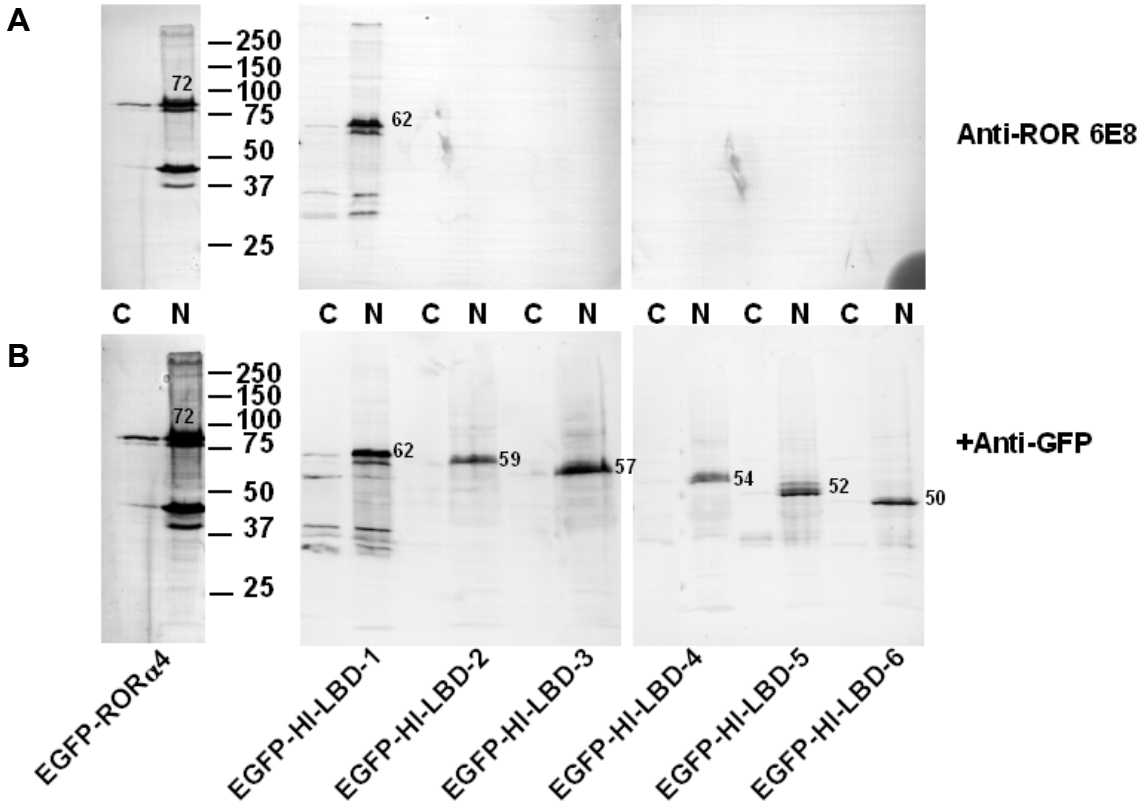

Fig. 4.12: Western Blot of HeLa lysates transfected with EGFP-RORα4 or truncation mutants*. HeLa cells were transfected in 9 cm Petri-dishes by calcium phosphate method, separation of nuclear (N) and cytosolic (C) fractions as described. Blots were incubated with (A) anti-ROR antibody or (B) anti-GFP antibody. Proteins were visualized by subsequent incubation with anti-mouse antibody (alkaline phosphatase conjugated) and NBT/BCIP. C: cellular, N: nuclear fraction. Predicted molecular weight of truncation mutants are indicated.*

4.3 Phosphorylation of RORα4

Phosphorylation is a key process for the regulation of nuclear receptor activity. Affected parameters are protein interaction with DNA or receptor coactivators/-repressors, subcellular localization, protein stability and degradation by the proteasome [47]. Against this background, a RORα phosphorylation as activity regulating event was taken into account.

4.3.1 In-Gel Kinase Assay

In order to screen for protein kinases that phosphorylate RORα4, in-gel kinase assays using purified recombinant RORα4 as substrate were performed. Isolated human polymorphonuclear leucocytes (PMNL) from healthy donors were incubated with different stimuli such as N-formyl-Met-Leu-Phe (fMLP), platelet activating factor (PAF), O-acetyl 11-keto boswellic acid (AKBA), arachidonic acid, ionophore (Iono), phorbol 12-myristate 13-acetate (PMA), sodium arsenite (SA) and sucrose for 1.5-3 min at 37°C. PMNL were immediately lysed by addition of 2x SDS-PAGE loading buffer and heated for 5 min at 100°C. After sonication for 3 sec, aliquots of whole cell lysates were loaded on a 10% SDS/polyacrylamide gel that has been polymerized with purified and dissolved RORα4 inclusion bodies (2.3 mg/ml) or myelin basic protein (0.5 mg/ml, MBP, positive control) or without addition of any protein (negative control). After electrophoresis, gels were incubated in 6 M guanidine. By washing out the guanidine, proteins were refolded within the gel matrix. Then gels were incubated in [γ-^{32}P]-ATP for 30 min at 30°C. Unbound [γ-^{32}P]-ATP was washed off, and the dried gel was incubated on imaging plates (IP) for 3 days. Phosphorylated proteins were visualized by a FLA-3000 IP Scanner (Fuji). As shown in Fig. 4.13 A, lysates from PMNL cells that have been stimulated with 40 µM arachidonic acid, 5 µM ionophore, 100 nM PMA, 100 µM sodium arsenite or 570 mM sucrose gave phosphorylated bands at approximately 40 kDa in the RORα4 as well as in the MBP containing gels. In contrast, lysates of unstimulated cells or cells incubated with fMLP, PAF or AKBA lead to no phosphorylation signal.

A database request at SwissProt (http://www.expasy.org/sprot/) registrated over 70 kinases with an approximate molecular weight of 40 kDa (+/- 6 kDa), including protein kinase A (PKA) and the mitogen activated protein kinases (MAPKs) p38 and ERK. In search for the

identity of the phosphorylating kinase, PMNL cells were pre-treated with different inhibitors of kinase activation and afterwards incubated with the stimuli described above.

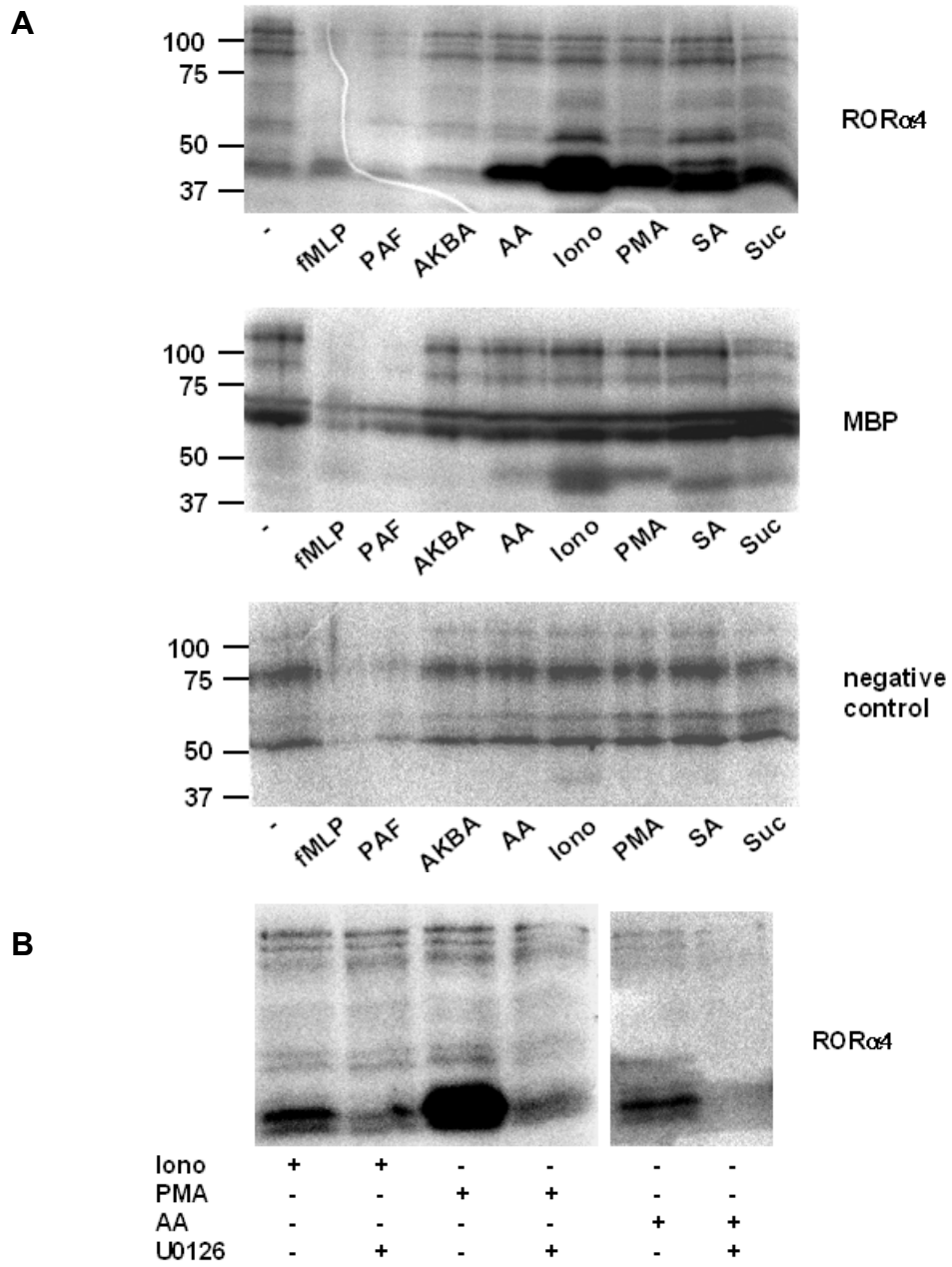

***Fig. 4.13: In-gel kinase assays**. (A) Cell extracts of human PMNL (10^6) in PBS containing 1 mg/ml glucose and 1 mM $CaCl_2$ were incubated for 1.5-3 min at 37°C in the absence or presence of diverse stimuli as indicated. Samples were separated over a 10% SDS-polyacrylamide gel which had been polymerized in the presence of either purified recombinant RORα4, myelin basic protein (MBP, positive control) or without addition of any protein (negative control). Gels were analyzed for protein phosphorylation by in-gel kinase assay as described [219]. fMLP: N-formyl-Met-Leu-Phe, 1 µM; PAF: platelet activating factor, 1 µM; AKBA: O-acetyl 11-keto boswellic acid, 100 µM; AA: arachidonic acid, 40 µM; Iono: Ca^{2+}-ionophore A23187, 5 µM; PMA: phorbol 12-myristate 13-acetate, 100 nM; SA: sodium arsenite, 100 µM, Suc: sucrose, 570 mM. Positions of the standard proteins are indicated. (B) RORα4 phosphorylation is prevented by U0126. PMNL (10^6) were pre-incubated with 3 µM U0126 for 10 min at 37°C and subsequently stimulated with ionophore (Iono), phorbol 12-myristate 13-acetate (PMA) or arachidonic acid (AA) for 3 min. Aliquots were electrophoresed over a 10% SDS/polyacrylamide gel, which had been polymerized with 2.3 mg/ml purified recombinant RORα4.*

10^6 PMNL cells were pre-treated with the ERK activation inhibitor U0126 (3 µM) [221,222] for 10 min at 37°C and subsequently stimulated with 5 µM ionophore, 100 nM PMA or 40 µM arachidonic acid for 1.5-3 min, respectively. Cell lysates were prepared and subjected to in-gel kinase assay using RORα4 (2.3 mg/ml) as substrate. As shown in Fig. 4.13 B, pre-incubation with 3 µM U0126 completely suppressed phosphorylation of RORα4 by the kinase appearing at 40 kDa, irrespective of the stimulus that was used.

4.3.2 *In Vitro* Phosphorylation by ERK-2

1-3 µg of purified and refolded RORα4 protein were incubated with commercially available ERK-2 (rat, recombinant) in an *in vitro* kinase assay. Clear bands corresponding to phosphorylated RORα4 were obtained after incubation with increasing concentrations of activated ERK. In absence of ERK no such bands appeared ruling out autophosphorylation or unspecific [γ-^{32}P]-ATP-binding (Fig. 4.14 A).

The optimal consensus sequence for ERK1/2 is Pro-X-Ser/Thr-Pro (X can be any amino acid), whereas the last two amino acids Ser/Thr-Pro play the substantial role for recognition [185]. As shown in Fig. 4.14 B, the protein sequence of RORα4 contains six putative consensus motifs (PLTP at amino acids 126-129, TP at 153-154, SP at 173-174, TP at 193-194, SP at 210-211 and SP at 332-333).

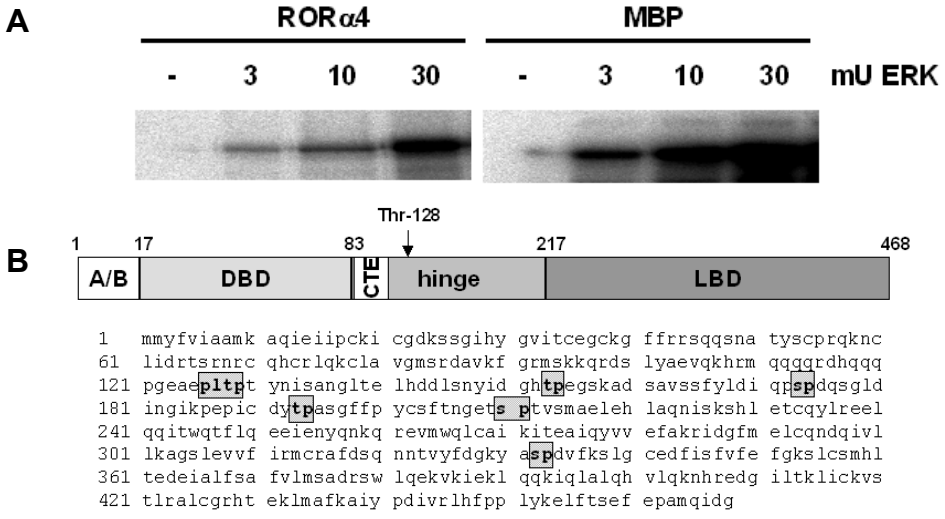

Fig. 4.14 In vitro phosphorylation of RORα4. *(A) Recombinant RORα4 protein was purified and refolded as described. 3 µg RORα4 were incubated with activated ERK at 30°C for 30 min. Samples were loaded onto a 10% SDS-polyacrylamide gel, phosphorylation of protein was detected by autoradiography. Myelin basic protein (MBP) was used as positive control. (B) Schematical representation of the RORα4 nuclear receptor, potential ERK phosphorylation sites are in bold. Thr-128 is located in the hinge region which connects the DNA binding (DBD) and the ligand binding domain (LBD).*

In order to identify an ERK phosphorylation site, Thr-128, Thr-153, Ser-173, Thr-193, Ser-210 and Ser-332 were mutated to alanine and the resulting mutants T128A, T153A, S173A, T193A, S210A and S332A were subjected to *in vitro* phosphorylation with ERK-2 as described. As shown in Fig. 4.15, only mutation of Thr-128 could anticipate phosphorylation, mutation of the other putative sites did not lead to a significant decrease in the phosphorylation signal. However, mutation of Thr-128 to alanine caused a complete loss of the phosphorylation signal and revealed Thr-128 as unique ERK-2 phosphorylation site.

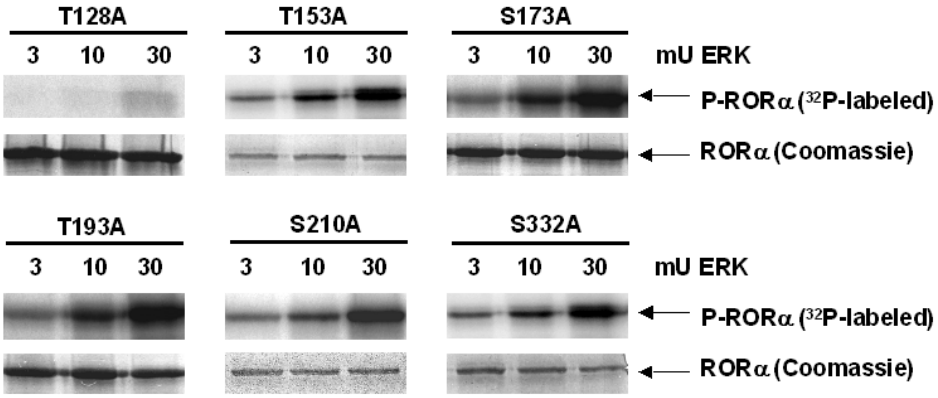

Fig. 4.15: RORα4 is phosphorylated by ERK-2 on Thr-128. *pET28a-RORα4 mutants were obtained from WT by site directed mutagenesis. After production of insoluble proteins in E. coli BL21(DE3), inclusion bodies were isolated and refolded into the active form as described. Proteins were subjected to in vitro phosphorylation by ERK, gels were stained with Coomassie brilliant blue simultaneously to facilitate a comparison of protein amount.*

4.3.3 p38 and PKA

Moreover, refolded RORα4 protein was incubated with recombinant protein kinase A (PKA, catalytic subunit from bovine heart) and p38 kinase (mouse, GST-fusion) for 30 min at 30°C, bovine MBP was used as positive control in both cases. In these *in vitro* kinase experiments PKA gave only moderately phosphorylated bands, and p38 failed to phosphorylate RORα4.

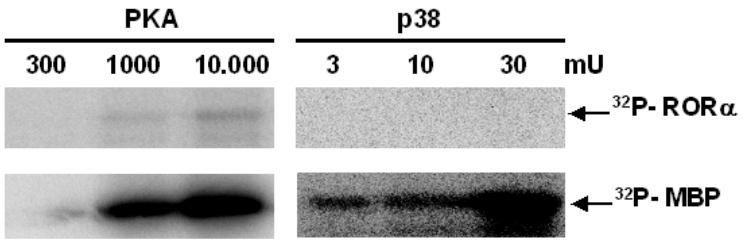

Fig. 4.16: In vitro kinase assay with PKA and p38. *Purified and refolded RORα4 protein was incubated with each kinase at 30°C for 30 min. Probes were loaded on a 10% SDS/ polyacrylamide gel. After drying, the gels were incubated on imaging plates for 24 h.*

4.3.4 Receptor-RORE Complex Formation

In order to compare the DNA binding properties of the RORα4-T128A mutant with RORα4 wild-type, we subjected both proteins to an electrophoretic mobility shift assay (EMSA). RORα4 wild-type and -T128A were phosphorylated by incubation with ERK. For EMSA analysis, double-stranded, 5´-IRDye700 labeled oligonucleotides containing one copy of the ROR consensus motif AGGTCA were incubated with 1 µg of the pre-treated RORα4 wild-type or RORα4-T128A, respectively. After 15 min on ice, samples were separated on a 4% non-denaturing polyacrylamide gel for 2 h, and shifted bands were visualized by scanning the gels with an Odyssey infrared imaging system (Licor). Interestingly, we observed that RORα4-T128A reveals a stronger binding affinity to the RORE compared to the wild-type protein (Fig. 4.17, first lane). For further comparison of the binding strength, we directly assessed the competition between RevErbα and RORα4-WT or -T128A for binding to the RORE. This was achieved by addition of increasing amounts of a nuclear extract containing RevErbα to a fixed amount of RORα4 (1 µg). The addition of increasing amounts of RevErbα promoted formation of the RevErbα-DNA complex in a concentration-dependent manner. In the case of RORα4-T128A, a stronger formation of the receptor-DNA complex was detected compared to RORα4-WT, suggesting that RevErbα shows a reduced binding when competing with the T128A mutant (Fig. 4.17).

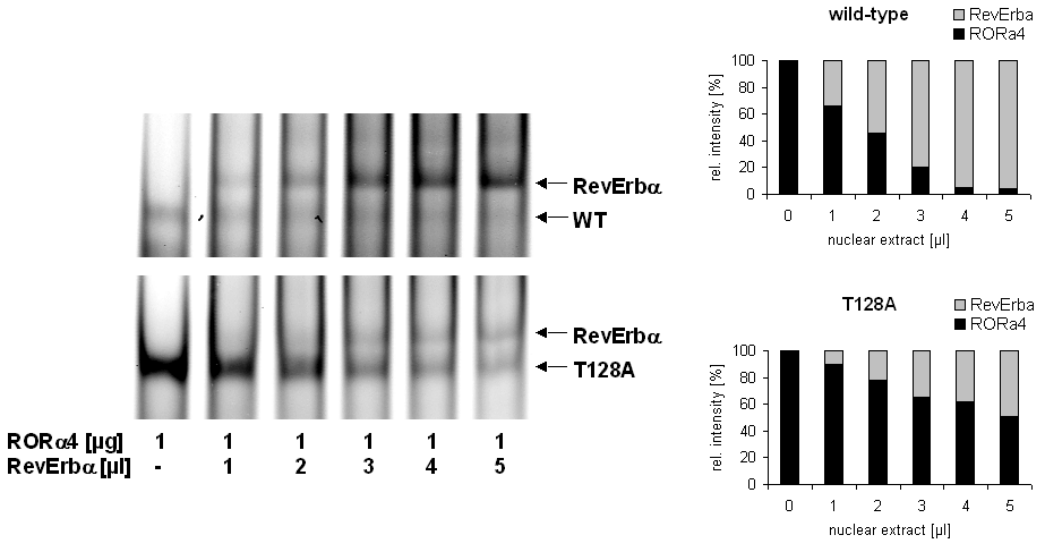

Fig. 4.17: Mutation of Thr-128 to alanine promotes receptor-RORE complex formation in an electrophoretic mobility shift assay. *Left: a double-stranded 5´-labeled oligonucleotide embedding the ROR response element AGGTCA was used for testing the DNA binding affinity of RORα4 wild-type and -T128A. For competition experiment increasing amounts of RevErbα containing nuclear extracts were added to the DNA binding reaction mixture. Right: quantification of DNA complex formation was performed with Licor Odyssey software (Licor). The sum of ROR and RevErb shift intensities was set as 100%.*

The influence of RORα4 phosphorylation status on DNA binding properties was tested by incubation of phosphorylated and unphosphorylated protein with the 5´-IRDye labeled RORE. Purified RORα4-WT and -T128A protein were incubated with ERK-2 or kinase buffer, respectively, for 30 min at 30°C. As shown in Fig. 4.18 A, phosphorylated and unphosphorylated wild-type protein displayed similar DNA binding properties. As expected, incubation with ERK did not affect T128A DNA binding affinity.

Specificity of RORα4 and RevErbα shifts was verified by the addition of the respective antibody to the binding reaction mixture that caused a complete loss of detected shift bands (Fig. 4.18 B).

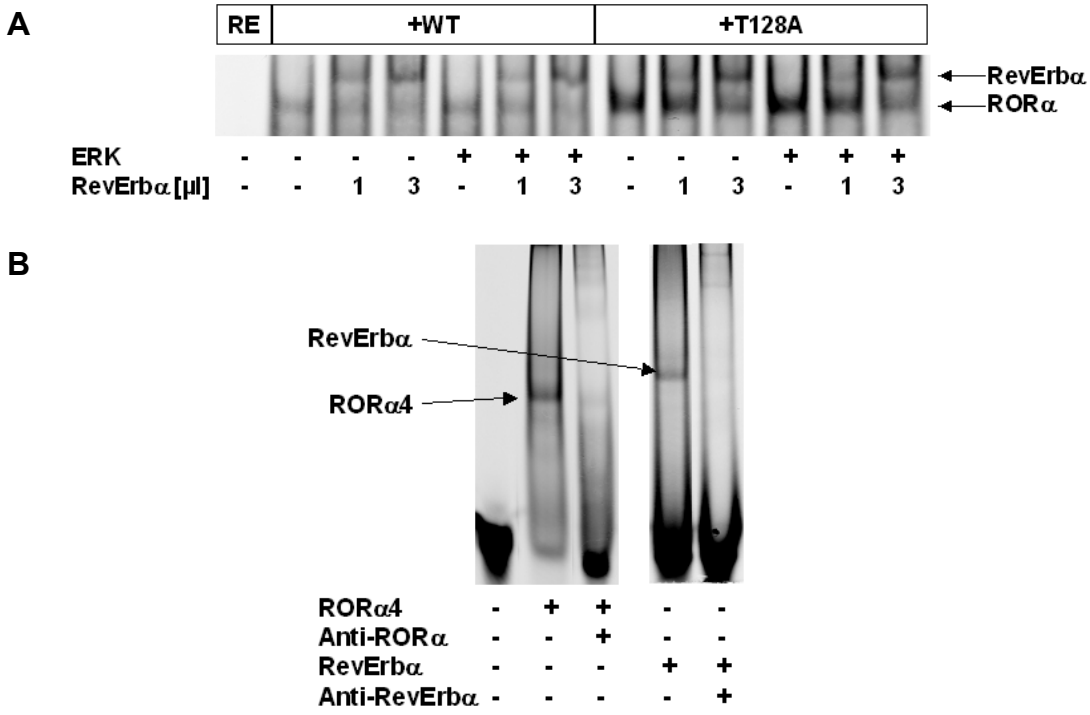

Fig. 4.18: (A) Influence of RORα4 phosphorylation on DNA binding affinity. *Phosphorylated (30°C, 30 min, ERK-2) and unphosphorylated (30°C, 30 min, buffer) WT and T128A were incubated with 5´-IRDye labeled RORE as described.* ***(B) Verification of shift specificity****. Anti-RORα (6E8) and anti-RevErbα antibodies were added to the protein mixture prior to incubation with the RORE.*

4.3.5 Transcriptional Activation

The transcriptional activities of RORα4-WT and -T128A were compared in a reporter gene assay system. For this purpose two different promoter constructs were cloned: (i) the artificial REa23 promoter which is composed of three copies of the ROR response element AGGTCA,

was set in front of the TK-promoter and the luciferase coding sequence, and (ii) the physiological human Bmal1 promoter, embedding two ROR response elements AGGTCA and AGGTTA, which was cloned from Mono Mac 6 genomic DNA and set in front of the luciferase coding sequence. Both RORα4 wild-type and the T128A mutant were cotransfected in HeLa cells with each of these constructs, and relative luciferase activities were determined after 24 h (REa23) and 48 h (Bmal1), respectively. As can be seen from Fig. 4.19 A, the T128A mutant showed 1.6-2.4-fold higher inductions of the luciferase transcription than the wild-type receptor, for both the REa23 and the Bmal1-promoter. In addition, two phosphomimetic mutants RORα4-T128D and -T128E revealed transcriptional activities ranging between that of RORα4-WT and RORα4-T128A. Mutation of Thr-128 to Val or Ile also increased RORα4 transcriptional activity, whereas mutation of Thr-128 to Arg led to an attenuation. These observations suggest that RORα4 residue 128 represents a sensitive position within the functional RORα4 molecule, whose modification influences protein activity. Experiments performed with HEK293 cells led to similar activities for RORα4-WT and the mutants on both promoter constructs (Fig. 4.19 B).

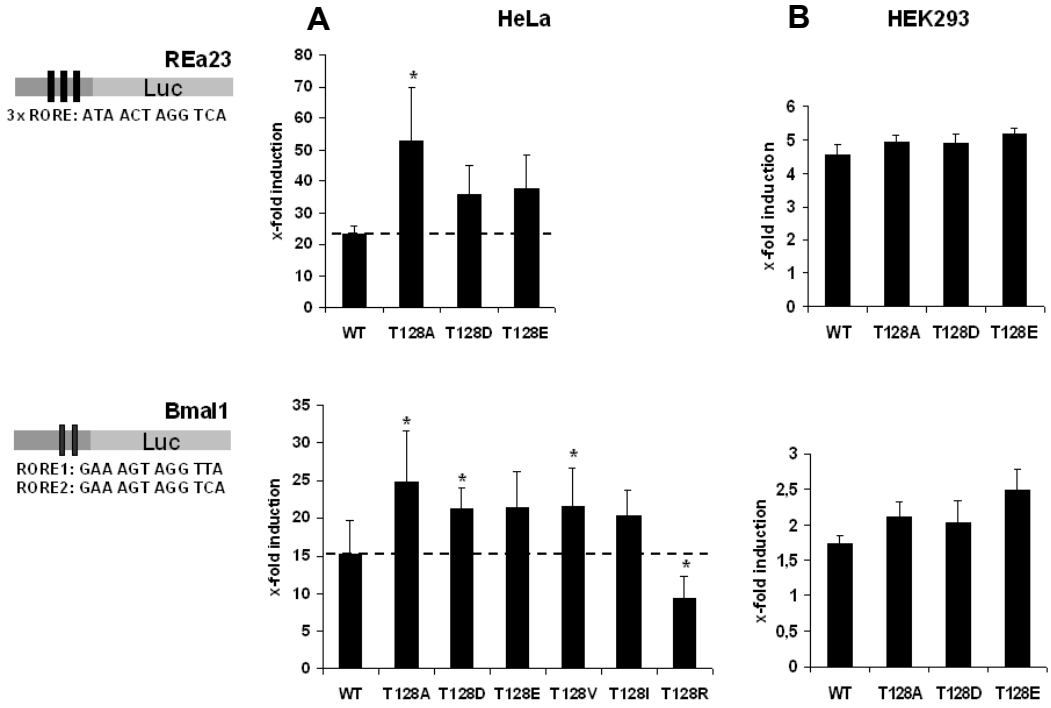

Fig. 4.19: Mutation of Thr-128 influences transcriptional activation. *HeLa (40,000/well) or HEK293 (100,000/well) cells distributed in 24-well-plates were cotransfected with 80 ng pSG-RORα4-WT, -T128A, -T128D, -T128E or empty expression plasmid and 400 ng pTKluc-REa23 or 800 ng pGL3-Bmal1 along with pCMV-SEAP using the calcium phosphate method. 16 h after transfection medium was changed and another 24 h (REa23) or 48 h (Bmal1) later luciferase activities were determined. Luciferase values were normalized by secreted alkaline phosphatase activity values. For formation of x-fold inductions, relative luciferase activity of the empty vector plasmid was taken into account. Results are given as means of three independent experiments.* $p<0.05$, significant different from WT (Student´s t-test, one-sided).*

4.3.6 Replacement by RevErbα

It was previously shown that RORα and RevErbα have opposing effects on a RORE. Whereas binding of RORα to its RORE activates gene transcription, RevErbα represents a constitutive repressor which functionally antagonizes RORα. Hence, the molecular ratio of RORα and RevErbα is the determinant for transcriptional activation [223]. Therefore, we assessed the possibility of RevErbα to antagonize the activities of RORα4 wild-type and RORα4-T128A in a reporter gene assay system. For this purpose varying ratios of RORα and RevErbα were cotransfected in HeLa cells and transcriptional activities were determined with REa23-luc as well as with the Bmal1-luc reporter construct. As can be seen from Fig. 4.20, substantially higher amounts of RevErbα were required to attenuate transcriptional activity induced by the RORα4-T128A mutant compared to the wild-type protein. Stability of the phosphomimetic mutants T128D and T128E against replacement by RevErbα was similar to that of the wild-type RORα4 (data not shown).

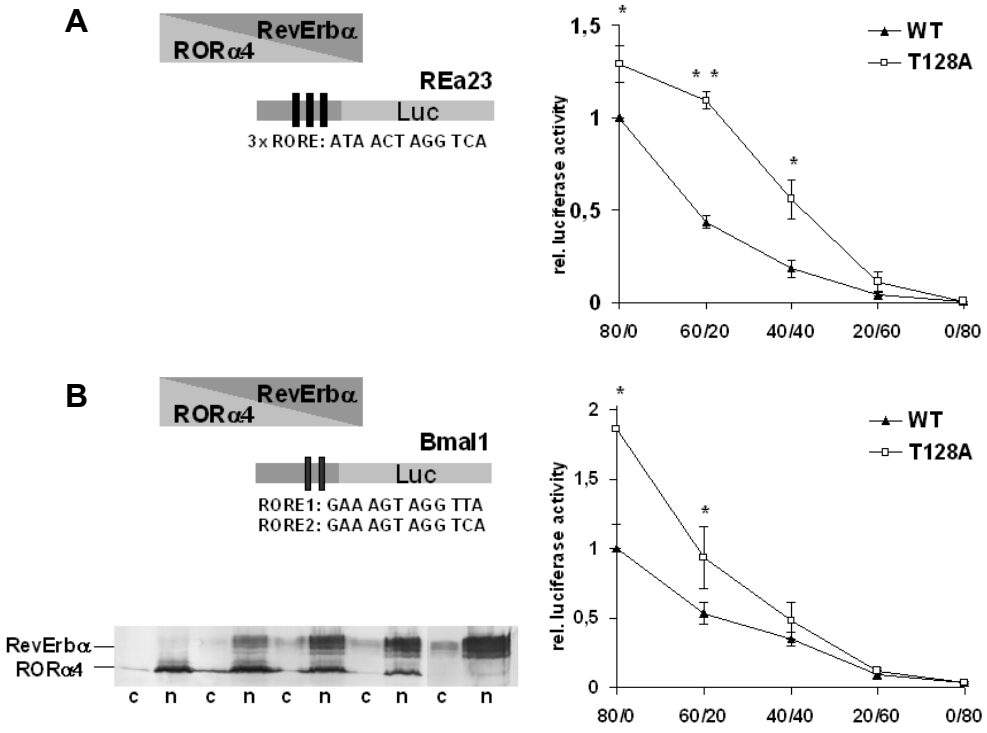

Fig. 4.20: Mutation of Thr-128 to alanine prevents RevErbα to gain influence on the RORE. *HeLa cells were cotransfected with 400 ng REa23 (A) or 800 ng Bmal1 (B) reporter construct along with varying ratios of the RORα4 (80-0 ng) and RevErbα (0-80 ng) expression plasmids. Luciferase values were normalized by secreted alkaline phosphatase activity values. Results are given as means of three independent experiments. * p<0.05,** p<0.01, significant different from WT (Student's t-test, one-sided). Transfected cells were analyzed by Western Blotting to control expression of proteins (n: nuclear, c: cytosolic fraction), RORα4-WT and -T128A gave similar results.*

4.3.7 PMA and U0126

In order to investigate if direct activation or inhibition of cellular ERK effects RORα4 transcriptional activity, transfected HeLa cells were incubated with 160 nM PMA, 20 µM U0126 or both compounds in combination. After 24 h relative luciferase activities were determined. Whereas incubation with PMA reduced RORα4 transcriptional activity by 75%, the ERK inhibitor U0126 was able to increase the activity up to 150%. Interestingly, a combination of both PMA and U0126 resulted in an unaltered induction when compared to incubation with the solvent DMSO. However, the T128A mutant was influenced by PMA and U0126 in a similar manner (Fig. 4.21 A). To further investigate whether the PMA/U0126 effect is based on a second ERK phosphorylation site, five RORα4 double-mutants were cloned. Additive to the substitution of threonine in position 128, one of the five further potential phosphorylation sites was mutated, and the resulting double-mutants T128A-T153A, T128A-S173A, T128A-T193A, T128A-S210A and T128A-S332A were subjected to the PMA/U0126 incubation as described above. The activities of each double-mutant was decreased by PMA and increased by U0126, and all double-mutants acted similar to the T128A mutant. Western Blot experiments suggest that incubation of transfected HeLa cells with PMA reduces RORα4 protein expression (Fig. 4.21 B).

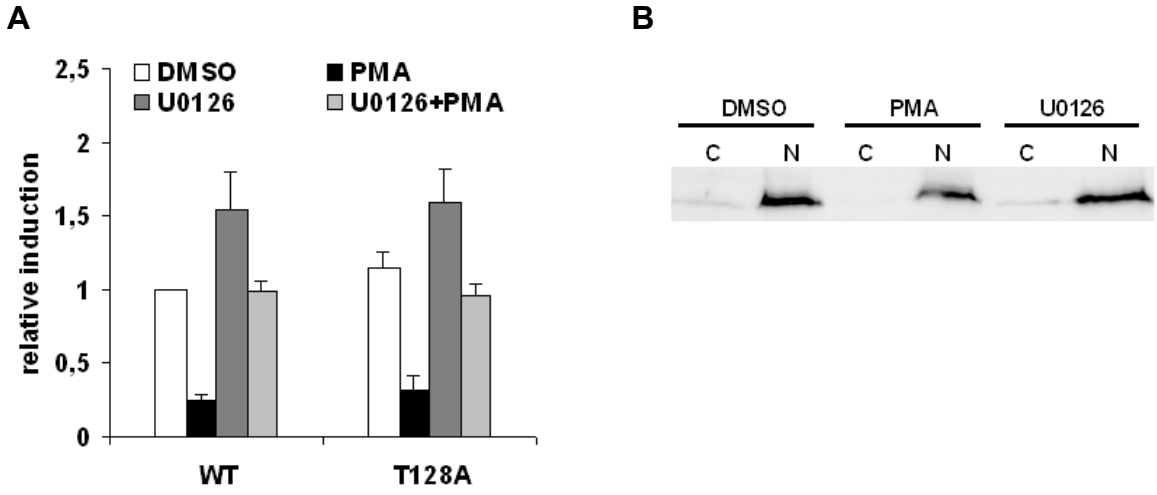

Fig. 4. 21: Effects of PMA and U0126 incubation on RORα4 transcriptional activity. *(A) Expression plasmids for RORα4-WT and -T128A were cotransfected with pTKluc-REa23 in HeLa cells. 16 h after transfection medium was changed and cells were incubated with 20 µM U0126 30 min prior to the optional addition of 160 nM PMA. Cells were harvested 24 h later and relative inductions were evaluated. Results are given as means of three independent experiments. (B) Transfected HeLa cells were blotted on a PVDF membrane and incubated with anti-RORα4 antibody clone 6E8. C: cytosolic, N: nuclear fraction.*

4.3.8 Ca/Dn-MEK1

In the signal transduction pathway, MEK (MAPK/ERK kinase) phosphorylates and thus activates ERK. Transfection of a constitutive active (ca) form of MEK leads to a permanent activation of cellular ERK [189,224], a dominant negative (dn) form inhibits the activation of cellular ERK [225,226]. In order to construct ca-MEK1, MEK1-S218D/S222D was cloned and inserted into the pcDNA3.1 empty expression vector, the dn-MEK was constructed by mutation of K97 to methionine. The resulting plasmids pcDNA3.1-MEK1-S218D/S222D and pcDNA3.1- MEK1-K97M were cotransfected with each the pSG5-RORα4 wild-type and the -T128A mutant. Two different (ca/dn)-MEK1: RORα4 ratios were tested, 1:50 and 1:10, and the inductions were compared to cotransfection of the empty vector pcDNA3.1 as negative control. Neither the presence of constitutive active nor dominant negative MEK1 did alter RORα4 transcriptional activity significantly (Fig. 4.23). Expression of both MEK mutants was demonstrated by Western Blotting.

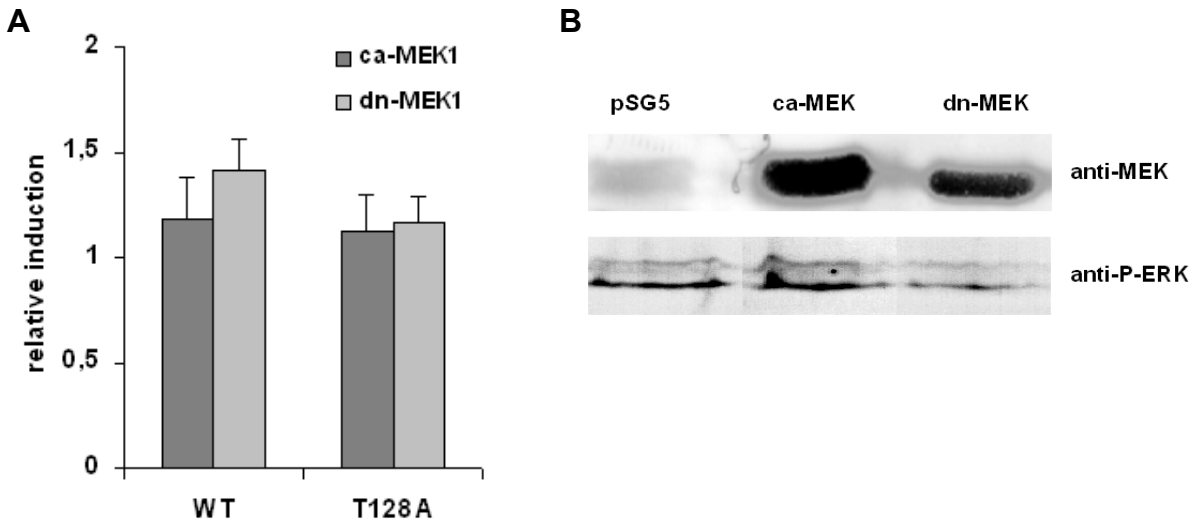

Fig. 4.23: Cotransfection of constitutive active (ca) and dominant negative (dn) MEK1 with RORα4-WT and T128A in HeLa cells. *(A) 72 ng pSG5-RORα4-WT or -T128A, were cotransfected with 8 ng pcDNA3.1-ca-MEK1, pcDNA3.1-dn-MEK1 or pcDNA3.1 empty vector (1:10) on the REa23 promoter construct. Luciferase activities were determined 24 h after changing the medium and values were normalized with secreted alkaline phosphatase activity values. Relative inductions were obtained by comparison with the luciferase activities of the empty pcDNA3.1 vector. Results are given as means of three independent experiments. (B) Western Blot of nuclear fractions of transfected HeLa cells. Equal cell counts were loaded onto the various lanes.*

4.3.9 Interaction with Bmal1

Since phosphorylation of nuclear receptors can influence the interaction with other proteins [51,82], a direct interaction between RORα and Bmal1 protein was taken into account.

Two expression vectors for the Bmal1 protein isoforms A and B, that only differ in their N-terminal domains, were cloned and cotransfected in HeLa cells with RORα4-WT and -T128A mutant. As can be seen from Fig. 4.22, cotransfection of Bmal1A or B induced RORα4 transcriptional activity 1.2 to 1.7 fold on the REa23 promoter construct, for both the WT and T128A mutant. In case of the human Bmal1 promoter, only Bmal1 isoform B induced RORα4 transcriptional activity 1.5 fold. However, influence of the RORα4 phosphorylation status on the interaction with Bmal1A/B protein is not immediately apparent. PMA (160 nM)-incubation of RORα4-WT or -T128A combined with Bmal1A/B reduced transcriptional activity in all cases, and had no influence on RORα activity inducing abilities of Bmal1 (data not shown).

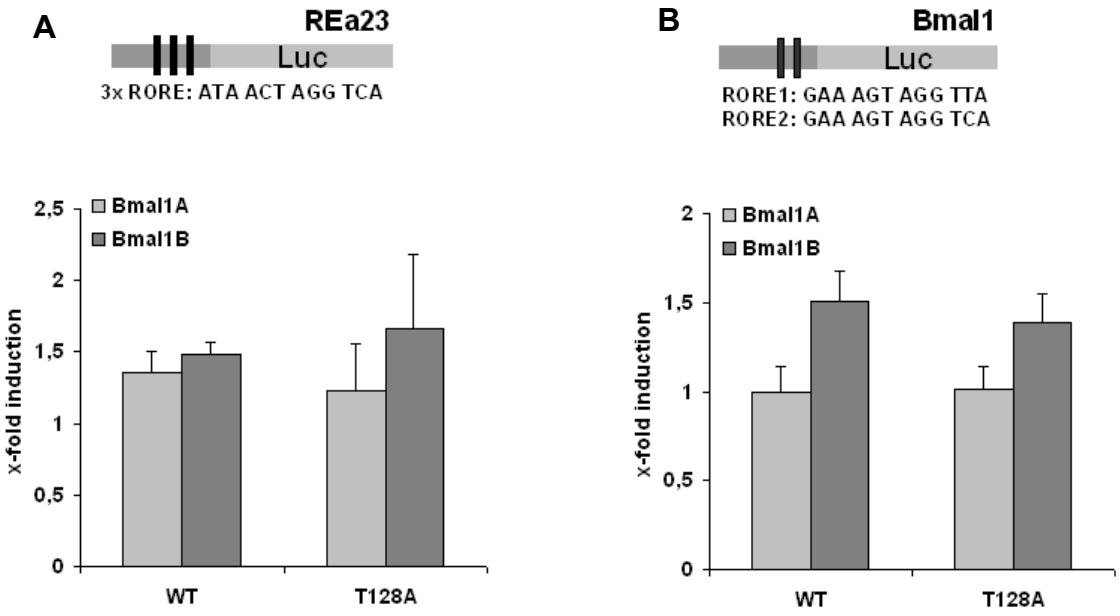

Fig. 4.22: Cotransfection of RORα4-WT or -T128A with Bmal1A/B on (A) pTKluc-REa23 and (B) pGL3-Bmal1. *HeLa cells (40,000/well) distributed in 24-well-plates were cotransfected with 40 ng pSG-RORα4-WT, -T128A or empty expression plasmid and 40 ng pSG5-Bmal1A or B, together with 400 ng pTKluc-REa23 or 800 ng pGL3-Bmal1 using the calcium phosphate method. 24 h (REa23) or 48 h (Bmal1) after the medium was changed, luciferase activities were determined. Luciferase values were normalized by secreted alkaline phosphatase activity values. Results are given as means of three independent experiments. For formation of x-fold inductions, relative luciferase activity of the empty vector was taken into account.*

4.3.10 Cellular Distribution

Cellular localization of RORα4 wild-type and the three mutants T128A, T128D and T128E was analyzed by Western Blot after separating the cytosol of transfected HeLa cells from the nuclei and membranes. As described previously [227], RORα4 is predominantly found in the nucleic fraction, only a small amount appears in the cytosol. Interestingly, both the unphosphorylatable as well as the phosphomimetic mutants revealed the same cellular distribution pattern (Fig. 4.24 A). Furthermore, Western Blot analysis showed that the wild-type and all mutants are expressed at a similar level. The results of cellular distribution could be further confirmed by cloning of EGFP fusion proteins followed by the observation of transfected HeLa cells in a confocal laser scan microscope. These experiments confirmed the predominant localization of RORα-WT and all mutants in the nucleus. Even after cotransfection of increasing amounts of RevErbα, RORα4 was predominantly found in the nucleic fraction, neither the wild-type protein nor the T128A mutant showed an altered subcellular distribution.

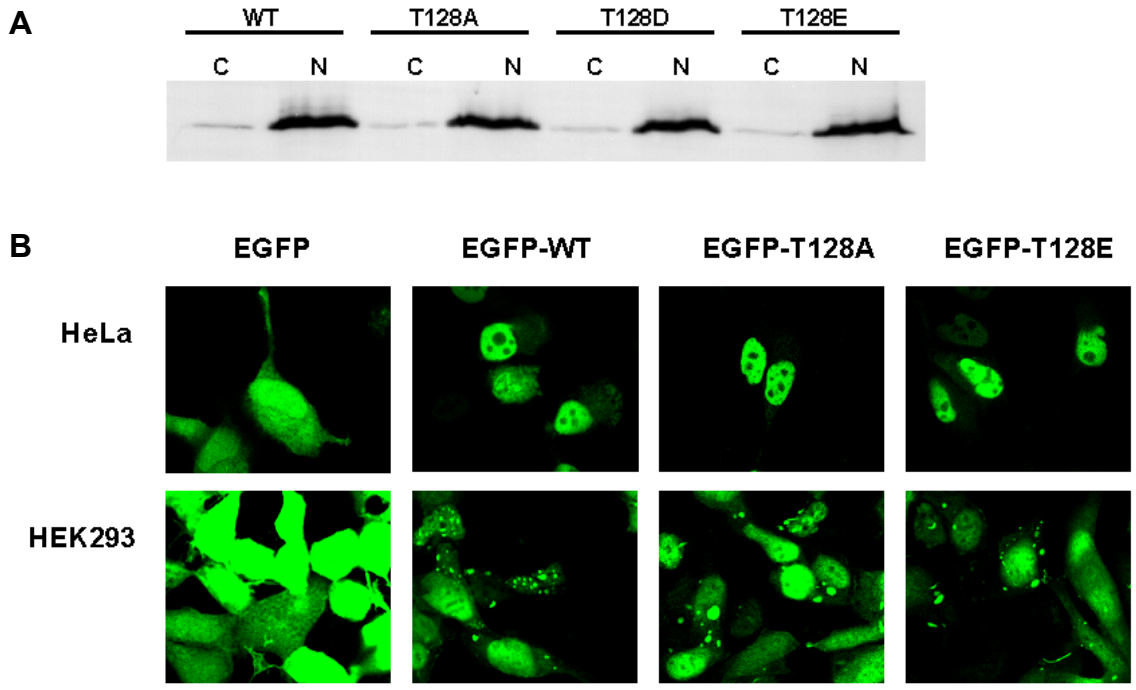

Fig. 4.24: Cellular localization of transfected RORα4-WT and -T128 mutants in HeLa cells. *(A) 30 µg pSG5-RORα4 and mutants were transfected into HeLa cells seeded in Petri-dishes with 9 cm diameter by calcium phosphate method. Medium was changed 16 h after transfection and another 24 h later cells were harvested. Cytosolic and nucleic/membrane fraction were separated and aliquots were subjected to SDS-PAGE and Western Blot. RORα was detected by antibody clone 6E8. C: cytosolic, N: nucleic/membrane fraction. (B) Transfected cells growing on glass cover slips were fixed with 4% paraformaldehyde in PBS after 24 h for 10 min, permeabilized with 0.1 % Triton X-100 for 5 min and stained for 20 min with 1 mM TO-PRO-3 iodide in PBS with 1% BSA. Images were taken by confocal laser scan microscopy (CLSM).*

Besides a predominantly nuclear and little cytosolic distribution, EGFP-tagged RORα4 was additionally detected at cellular membranes in HEK293 cells [227]. Therefore, we investigated whether phosphorylation status influences receptor membrane association. Neither mutation of Thr-128 nor incubation with 160 nM PMA did alter subcellular distribution of EGFP-RORα4 in HEK293 cells significantly. After cotransfection of increasing amounts of its opponent RevErbα, RORα4 was predominantly found in the nucleic fraction, neither the wild-type protein nor T128A changed the cellular compartment (data not shown).

4.3.11 Degradation by the Proteasome

It was postulated by Moraitis et al. [228] that RORα is ubiquitinylated and that subsequent degradation by the proteasome is needed to start transcriptional activation. This was demonstrated by the addition of the proteasome inhibitor MG-132 to a reporter gene assay system that led to decreased RORα activities. In order to investigate a connection between RORα4 phosphorylation status and degradation by the proteasome, the influence of MG-132 on transcriptional activation of wild-type and T128A was determined on the REa23 promoter construct. Fig. 4.25 shows that the WT and T128A mutant are effected by MG-132 in a similar manner suggesting that the phosphorylation status has no influence on the degradation by proteasome.

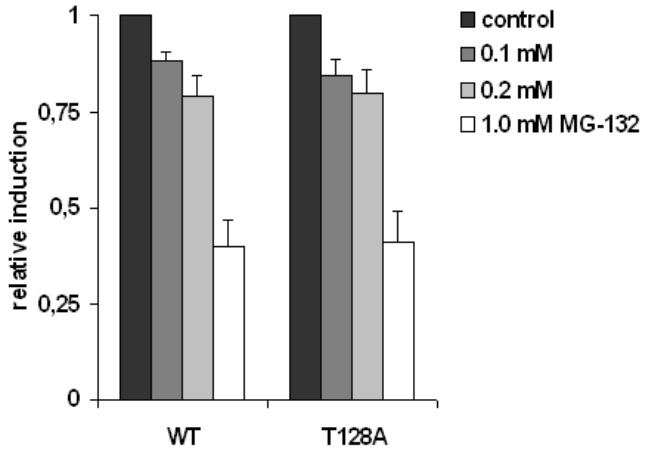

Fig. 4.25: Influence of MG-132 on transcriptional activity of RORα4-WT and –T128A. *40 ng pSG5-RORα4-WT or -T128A were transient transfected along with pTKluc-REa23 in HeLa cells. 16 h after transfection medium was changed and incubated with 0.1, 0.2, 1.0 mM MG-132 or DMSO as control. After 24 h cells were harvested and relative inductions were evaluated. Results are given as means of three independent experiments.*

4.4 Further Posttranslational Modifications

4.4.1 Sumoylation

When transfected into HeLa cells and detected by immunoblotting, RORα4 protein appears as a group of three bands that differ in approx. 5-10 kDa molecular weight, a case that might suggest a posttranslational modification like a sumoylation. A potential sumoylation site is composed of four amino acids: ψ-K-X-D/E/G, whereas ψ represents a hydrophobic and X any amino acid, within this recognition site, SUMO is covalently linked over the lysine (K).

As can be seen from Fig. 4.26, the RORα4 amino acid sequence contains four consensus motifs, potential lysine sumoylation sites are located at K89, K185, K302 and K386. Site directed mutagenesis was performed to replace the potential sumoylatable lysines by alanine. The resulting mutants were denoted as K89A, K185A, K302A and K386A. Disappearance of one of the three observed bands would give evidence for a destructed sumoylation site. However, after transfection into HeLa cells and analysis by immunoblotting, all four mutants appeared as the typical pattern consisting of three bands, as it was observed for the wild-type protein. Moreover, SUMO1 protein was cloned from Mono Mac 6 cDNA and ligated into the pSG5 expression vector. Cotransfection of this SUMO1 overexpressing construct in ascending concentrations led to no additively detected bands.

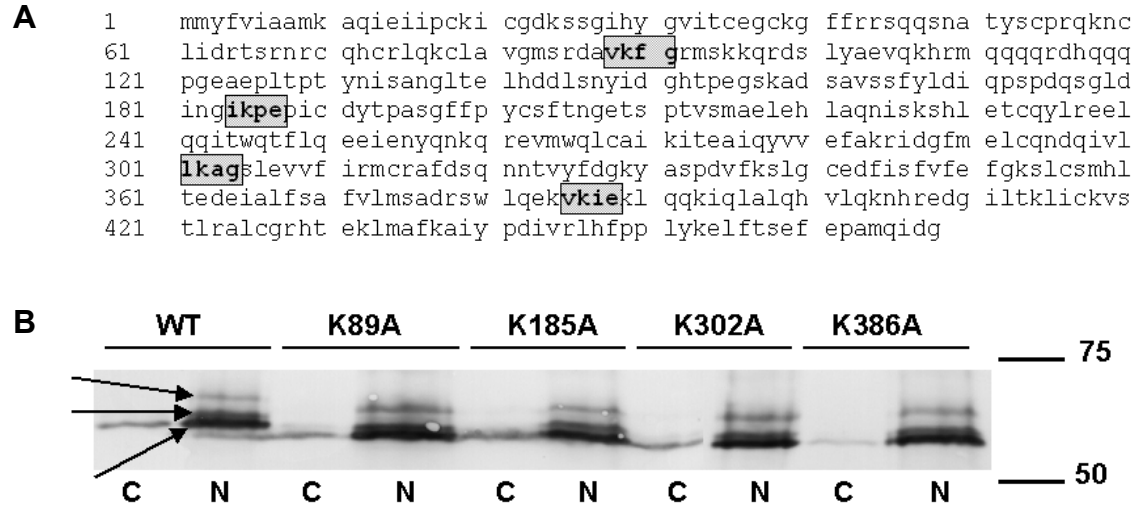

Fig. 4.26: Test on RORα4 sumoylation. *(A) Amino acid sequence of RORα4. Potential sumoylation consensus motifs are in bold. (B) 30 µg pSG5-RORα4 and mutants were transfected into 0.5x10^{6}HeLa cells seeded in 9 cm Petri-dishes, cellular and nucleic fractions were separated and blot was analyzed with anti-ROR antibody 6E8 (C: cytosolic, N: nucleic fraction).*

4.4.2 Protein Cleavage

pSG5-RORα4, pEGFP-RORα4 and pEGFP-HI-LBD1 were transiently transfected into HeLa cells seeded in 9 cm Petri-dishes; after 24 h nucleic fractions were prepared and blotted on a PVDF membrane.

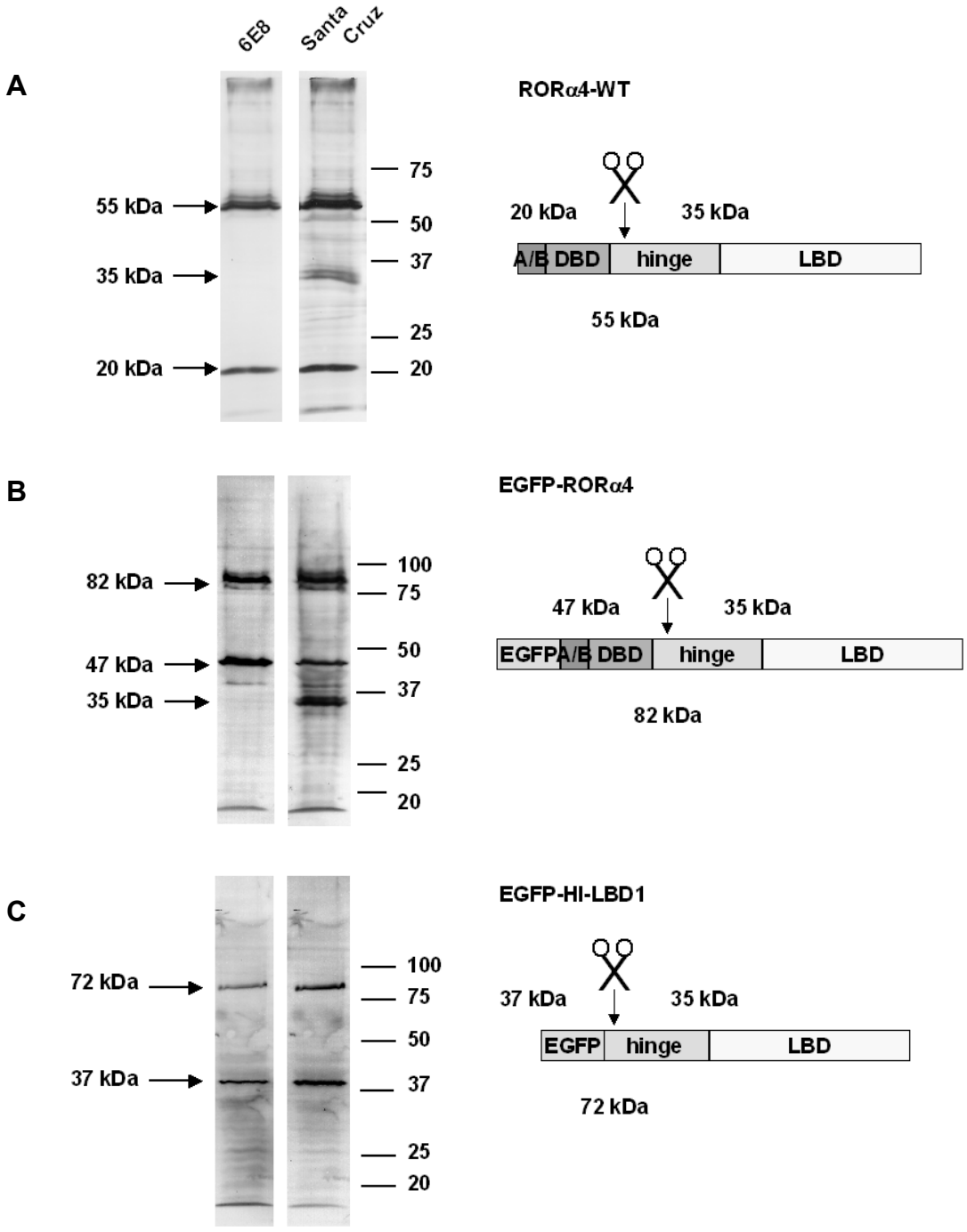

Fig. 4.27: Cleavage of RORα4 protein in transfected HeLa cells. *Left: 0.5x10^6 HeLa cells seeded in Petri-dishes were transfected with 30 µg expression plasmid encoding RORα4-WT (A), EGFP-RORα4 (B) and EGFP-HI-LBD1 (C). Nucleic fractions were isolated and blotted on a PVDF membrane. After blocking the membrane with 5% milk in TBS, blots were incubated with anti-RORα antibody clone 6E8 (left panel) and subsequent with Santa Cruz antibody (right panel). Right: Schematical structures and molecular weights of overexpressed proteins. Proposed cleavage sites and resulting fragment weights are indicated.*

As can be seen from Fig. 4.27 A, incubation of wild-type protein with monoclonal anti-ROR antibody clone 6E8 visualized two clear bands: one band at 55 kDa as expected for the intact protein and additively a fragment at 20 kDa probably caused by protein cleavage. Subsequent incubation with the polyclonal anti-RORα antibody purchased from Santa Cruz visualized a third clear band at 35 kDa, probably the second cleavage fragment. All three bands were not detected after transfection of the pSG5 empty vector into HeLa cells. Western Blot of transfected HeLa cells expressing the 82 kDa-sized EGFP-RORα4 (Fig. 4.27 B) showed additively to the expected band at 82 kDa a clear band at 47 kDa. Santa Cruz polyclonal anti-ROR antibody revealed a second fragment at 35 kDa. Overexpression of EGFP-HI-LBD1 in HeLa revealed a similar pattern, the 72 kDa-sized protein showed an additive band at 37 kDa (Fig. 4.27 C). These three experiments clearly suggest a cleavage of RORα4 protein in transfected HeLa cells. Addition of the fragment molecular weight values always resulted in the molecular weight value of the protein in full-length, irrespective of which mutant was analyzed. Detailed theoretical considerations of the putative antibody epitopes and the respectively detected fragments indicated that the cleavage site is located within the hinge region. Further studies will be necessary to clearly identify the cleavage motif and to investigate the mechanism of RORα4 cleavage. So far, there is no evidence that phosphorylation on T128 by ERK influences RORα4 protein cleavage.

4.5 RevErbα

4.5.1 Overexpression and Purification

The coding sequence of RevErbα was cloned into the pET28a vector and the resulting N-terminal His-tagged protein was overexpressed in BL21(DE3) in analogy to the protocol for RORα4 overexpression and purification. RevErbα inclusion bodies were washed with 1% Triton-X100, and purification procedure was analyzed by SDS-PAGE and Coomassie brilliant blue staining of the gel (see Fig. 4.28). The identity of RevErbα protein was verified by Western Blot and subsequent immunodetection with anti-RevErbα antibody. Per 1 l *E. coli* culture, approx. 2 mg RevErbα inclusion bodies of 50% purity could be recovered.

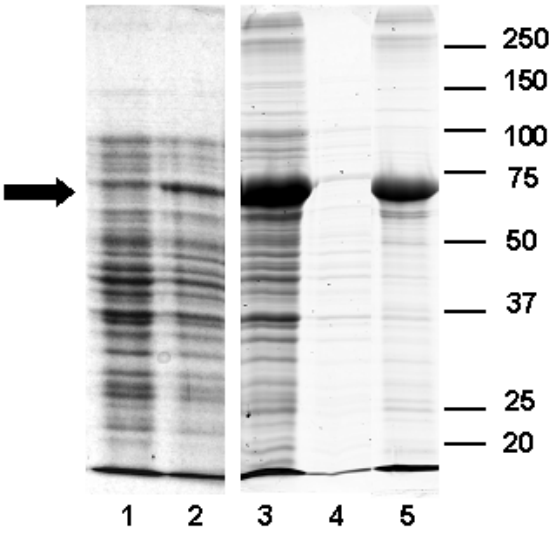

Fig. 4.28: Analysis of RevErbα overexpression and purification (1.5 l E. coli culture). *Probes (20 µl each) were separated on a 10% SDS/polyacrylamide gel and stained with Coomassie brilliant blue. Lanes 1, 2: uninduced and with 1 mM IPTG induced BL21(DE3)-pET28a-RevErbα (equal cell amounts), 3: insoluble fraction of sonicated E. coli (dispersed in 15 ml), 4: soluble supernatant from inclusion body washing with 50 ml 1% Triton X-100, 5: purified inclusion body fraction (dispersed in 15 ml). The arrow indicates the migration height of RevErbα.*

4.5.2 Phosphorylation of RevErbα

The possibility of RevErbα phosphorylation was investigated by performing an in-gel kinase assay. Freshly isolated human PMNL were incubated with different stimuli such as ionophore (Iono), arachidonic acid (AA), phorbol 12-myristate 13-acetate (PMA), sodium arsenite (SA),

di-buturyl-cAMP (db-cAMP), sucrose and N-formyl-Met-Leu-Phe (fMLP) for 1.5-3 min at 37°C. PMNL were lysed by the addition of 2x SDS-PAGE loading buffer and aliquots of whole cell lysates were loaded on a 10% SDS/polyacrylamide gel that has been polymerized with purified RevErbα (approx. 2 mg/ml). After electrophoresis, proteins were refolded within the gel matrix and incubated in presence of [γ-^{32}P]-ATP for 30 min at 30°C. Gels were washed intensively to remove unbound [γ-^{32}P]-ATP, dried and incubated on an imaging plate for 3 days. As shown in Fig. 4.29, lysates from PMNL cells that have been stimulated with 5 µM ionophore, 40 µM arachidonic acid, 0.1 µM PMA, 100 µM sodium arsenite or 1 µM N-formyl-Met-Leu-Phe gave phosphorylated bands at approximately 40 kDa in the RevErbα containing gels. In contrast, lysates of unstimulated cells or cells incubated with db-cAMP or sucrose lead to no phosphorylation signal.

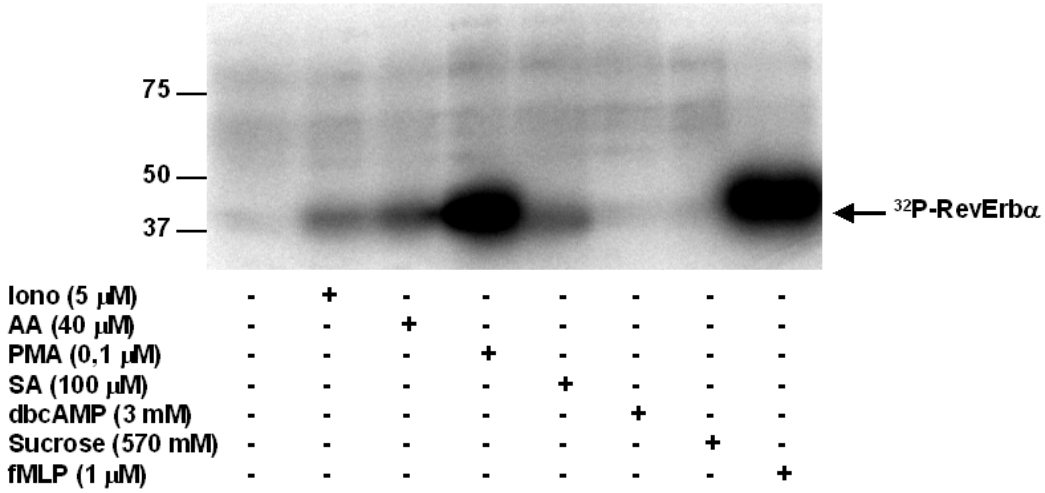

Fig. 4.29: RevErbα is phosphorylated in an in-gel kinase assay. *Total cell extracts of human PMNL (10^6) in PBS containing 1 mg/ml glucose and 1 mM $CaCl_2$ were incubated for 1.5-3 min at 37°C in absence or presence of ionophore (Iono), arachidonic acid (AA), or phorbol 12-myristate 13-acetate (PMA), sodium arsenite (SA), di-buturyl-cAMP (cAMP), sucrose or N-formyl-Met-Leu-Phe (fMLP) in indicated concentrations. Aliquots were electrophoresed on a 10% SDS/polyacrylamide gel, which had been polymerized with approx. 2 mg/ml purified recombinant RevErbα. In-gel kinase assay was performed as described above. Dried gel was incubated on an imaging plate for three days and phosphorylated protein was visualized by scanning with a FLA-3000 IP scanner (Fuji).*

According to the experiments performed with RORα4, the approximate kinase size and the activating stimuli, PMNL cells were pre-treated with the ERK activation inhibitor U0126 (3 µM) for 10 min at 37°C and subsequently stimulated with fMLP, SA, ionophore or PMA. As it was observed for RORα4, pre-incubation with U0126 diminished phosphorylation of RevErbα by the kinase appearing at 40 kDa, irrespective of the used stimulus (Fig. 4.30).

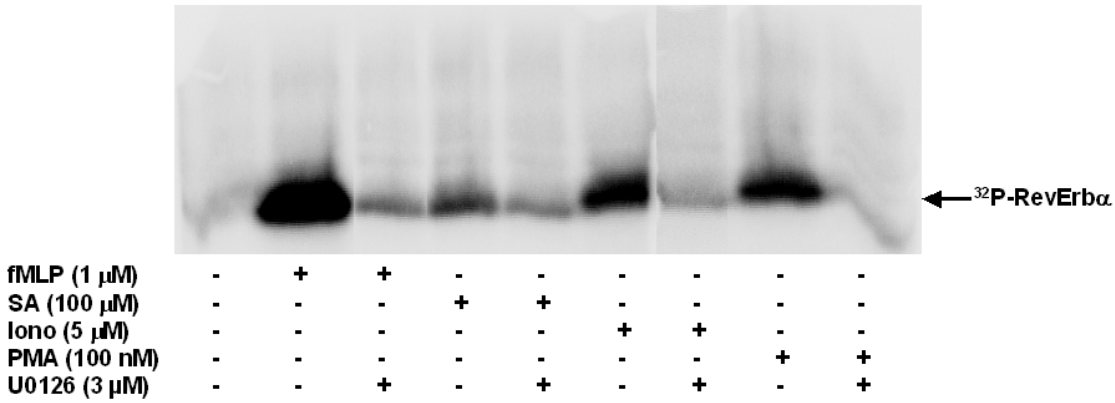

Fig. 4.30: RevErbα phosphorylation is prevented by U0126. *Human PMNL were pre-incubated with 3 µM U0126 for 10 min at 37°C and subsequently stimulated with N-formyl-Met-Leu-Phe (fMLP), sodium arsenite (SA), ionophore (Iono) or phorbol 12-myristate 13-acetate (PMA). Aliquots were electrophoresed on a 10% SDS/polyacrylamide gel, which had been polymerized with 2 mg/ml purified recombinant RevErbα. Gels were analyzed for RevErbα phosphorylation by in-gel kinase assay.*

Purified RevErbα inclusion bodies were refolded exactly as it was described for RORα4 (see chapter 4.1.2). Since the inclusion body recovery was very low and the conditions for RORα4 refolding were suboptimal for RevErbα, cultivation of 1.5 l transformed *E. coli* culture resulted in 170 µg of native RevErbα protein. Most protein loss occurred through precipitation during dialysis against the buffers with descending L-arginine content. Precipitates were removed by centrifugation and the remaining RevErbα solution concentration exceeded hardly 85 µg/ml. Nevertheless, 1 µg of refolded RevErbα was subjected to *in vitro* phosphorylation with ERK-2. As shown in Fig. 4.31 A, ERK was able to phosphorylate purified RevErbα protein, RORα4 was used as positive control.

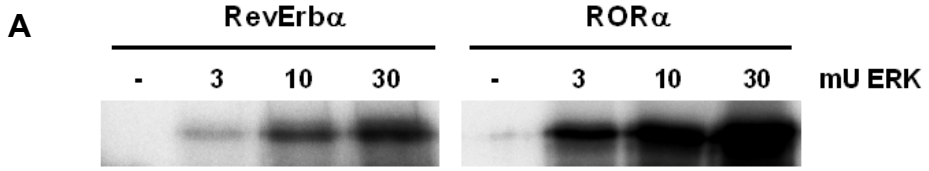

B

```
1    mttldsnnnt ggvityigss qsspsrtspe slysdnsngs fqsltqgcpt yfppsptgsl
61   tqdparsfgs ippslsddgs psssssssss sssfyngspp gslqvameds srvspsksts
121  nitklngmvl lckvcgdvas gfhygvhace gckgffrrsi qqniqykrcl knencsivri
181  nrnrcqqcrf kkclsvgmsr davrfgripk rekqrmlaem qsamnlannq lssqcpletS
241  ptqhptpgpm gpsppapvp splvgfsqfp qqltpprsps peptvedvis qvarahreif
301  tyahdklgss pgnfnanhas gsppattphr wenqgcppap ndnntlaaqr hnealnglrq
361  apssypptwp pgpahhschq snsnghrlcp thvyaapegk apanspqqgn sknvllacpm
421  nmyphgrsgr tvqeiwedfs msftpavrev vefakhipgf rdlsqhdqvt llkagtfevl
481  mvrfaslfnv kdqtvmflsr ttyslqelga mgmgdllsam fdfseklnsl alteeelglf
541  tavvlvsadr sgmensasve qlqetllral ralvlknrpl etsrftklll klpdlrtlnn
601  mhsekllsfr vdaq
```

Fig. 4.31: In vitro phosphorylation of RevErbα. *(A) 1 µg refolded RevErbα protein (or RORα4 as positive control) was incubated with active ERK-2 in presence of [γ-^{32}P]-ATP at 30°C for 30 min. Probes were separated by SDS-PAGE and dried gel was incubated on an imaging plate for 48 hours. Phosphorylated proteins were visualized with a FLA-3000 scanner (Fuji). (B) Amino acid sequence of RevErbα protein, putative ERK recognition motifs are indicated.*

The RevErbα amino acid sequence reveals 18 putative ERK recognition motifs (Fig. 4.31 B), but the actual phosphorylation sites still remain to be determined.

In order to test whether activation of cellular ERK influences RevErbα repressing activity, the two nuclear receptors RORα4 and RevErbα, both *in vitro* phosphorylatable with extracellular-signal regulated kinase, were cotransfected along with the REa23 promoter construct and incubated with 160 nM PMA or the equivalent volume of the solvent DMSO in D-MEM. However, RevErbα repressing activity was not affected by incubation with PMA. In a second experiment, stripped FCS was used. Treatment of FCS with charcoal extracts small lipophilic molecules, which could act as ligands for the nuclear receptors RORα and RevErbα. As shown in Fig. 4.32, usage of a medium supplemented with stripped FCS abrogated the increased activity of the T128A mutant completely, WT and mutant showed very similar activities in presence or absence of RevErbα. However, incubation with the protein kinase C activator PMA diminished entire transactivation, but again had no effect on RevErbα repressing activity.

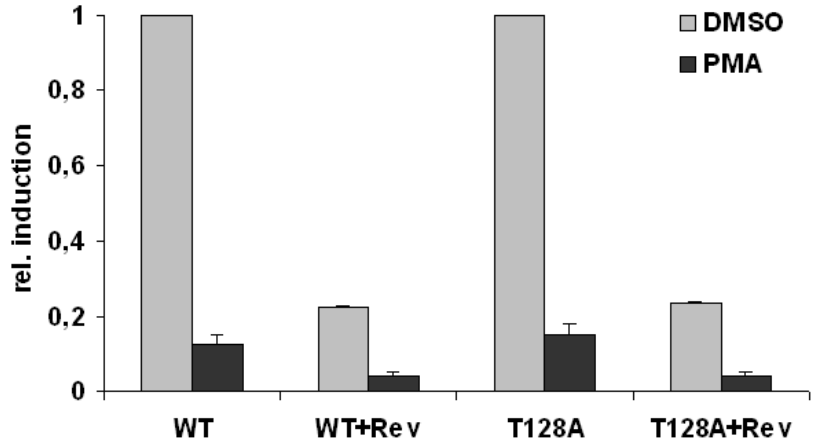

Fig. 4.32: Influence of PMA incubation on transcriptional activity of the two nuclear receptors RORα4 and RevErbα on the REa23 promoter construct. *40 ng pSG5-RORα4-WT or -T128A were cotransfected with 40 ng pSG5- RevErbα or pSG5 empty plasmid in HeLa cells. After 16 h, medium with stripped FCS and 160 nM PMA (or DMSO) were added. Luciferase activity was determined after 24 h of incubation.*

5 DISCUSSION

RORα is a key regulator of a variety of physiological events with putative clinical relevance. Since it is involved in lipid and bone metabolism, where it shows protective effects against atherosclerosis and osteoporosis, and additionally negatively regulates inflammation, RORα is of increasing pharmaceutical interest (summarized in [88]). Little is known about RORα protein regulation or activity modulation by binding of endo- or exogenous ligands. On the basis of a reproducible protein production method and the development of an anti-RORα antibody, studies on RORα signaling pathways were performed.

Overexpression and purification of RORα4

In order to produce recombinant RORα4 protein in *E. coli*, the cDNA of human RORα4 was cloned into pET28a, a bacterial expression vector. The pET28a vector system was chosen for RORα4 expression because it is one of the most powerful tools yet developed for the overexpression of recombinant proteins in *E. coli*. The system is based on the very strong T7 promoter, that, when transformed in a suitable *E. coli* overexpression strain, provides the possibility to active induction of recombinant protein expression by the addition of isopropyl-β-D-thiogalactopyranoside (IPTG) to the culture. Moreover, the pET28a vector facilitated the generation of RORα4 protein fused to a N-terminal polyhistidine tag, which is linked via a thrombin cleavage site and can be removed if required. The polyhistidine tag was localized on the N-terminal site, since fusion to the C-terminal LBD could result in a sterical hindrance of ligand-receptor interaction. *E. coli* BL21(DE3) were transformed with the emerged vector pET28a-RORα4-6xHisN. However, by the use of the T7 expression system, production of target proteins proceeds very rapidly so that the expressed proteins are often misfolded and aggregate as insoluble inclusion bodies [229]. Inclusion bodies are composed of densely packed denatured protein molecules in form of insoluble particles. They consist mostly in only one type of polypeptide, which helps to isolate and purify the protein aggregates to homogeneity. However, to obtain native and bioactive protein, inclusion bodies have to be solubilized and refolded carefully. In the case of RORα4, a variety of experimental conditions were tested to obtain greater solubility, including the use of lower IPTG concentrations, induction at different cell densities (OD_{660} 0.4-1.2), growth at different temperatures, variation of growth media (incl. addition of glucose or ethanol) and the use of diverse *E. coli* strains (Rosetta, BL21(DE3)pLysS), but none of the experimental conditions led to a greater yield of soluble hRORα4. Hence, the methodology focused on conditions to optimize the amount of

insoluble RORα4 inclusion bodies. Finally, 18-22 mg RORα4 inclusion bodies of ~70% purity were obtained per 1 l of cell culture. After isolation and purification of insoluble inclusion bodies, 6 M guanidine as a strong denaturant was used to solubilize the protein at the beginning of the refolding process. Refolding RORα4 into the native form included three phases: i) gradual removal of the denaturant guanidine and simultaneous addition of the adjuvant L-arginine, ii) gradual removal of L-arginine and iii) protein enrichment by dialysis against 50% glycerol. L-arginine is used to enhance the refolding process and to suppress aggregation of folding intermediates, but the mechanism is still intensively discussed. It was supposed that interactions between the guanidinium group of L-arginine and tryptophan side chains of the target protein may be responsible for suppression of protein aggregation (Fig. 5.1) [230,231].

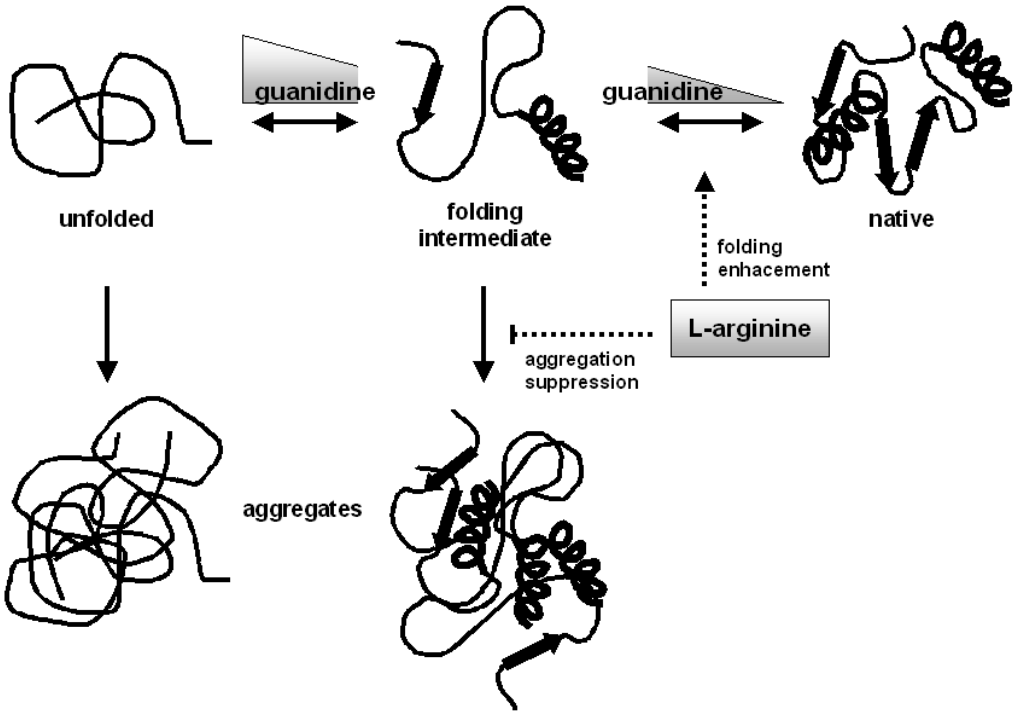

Fig. 5.1: Protein refolding. *Denatured protein is transferred into its native form during gradual removal of denaturant. L-arginine is used as adjuvant suppressing aggregation of folding intermediates.*

Gradual removal of guanidine and L-arginine had to be performed very carefully to prevent reaggregation of solubilized protein. Most critical parameters were time, pH, buffer substances, and protein concentration. The pH had to be between 8 and 9, lower pH values lead to precipitation of recombinant RORα4. Addition of Zn^{2+} ions was necessary for conformational development of the two zinc finger motifs in the DNA binding domain of the

protein. However, precipitation of $Zn(OH)_2$ had to be avoided by keeping the pH below 9.3. The initial protein concentration was adjusted to maximal 20-25 µg/ml, like it was described by others to be a critical parameter to achieve the maximum refolding efficiency [232]. Various combinations of solubilizing agents ($MgSO_4$, Chaps, L-glutamine/L-arginine) [233,234], refolding buffers (Tris-HCl, HEPES, addition of cholesterol) and methods of refolding (dialysis or slow dilution) were tested to improve the refolding efficiency. However, the described conditions were found to be optimal.

The complete process lasted over three days, and after the last step of protein enrichment, the concentration of soluble protein achieved 200-300 µg/ml. At this concentration and solved in 50% glycerol, refolded RORα4 could be stored at –70°C. The RORα4 DNA binding activity was tested by performing an EMSA, where RORα4 binding to a double-stranded, monomeric ROR response element was checked. The EMSA results suggest that the refolded protein is functional and that the N-terminal polyhistidine tag does not prevent correct folding or interferes with DNA binding activity. In order to check specificity of the RORα4-DNA complex, anti-RORα antibody was added to the binding reaction mixture which caused a complete loss of RORα4-DNA binding.

To further increase protein purity, the refolded his-tagged RORα4 protein was loaded onto a nickel affinity column. For optimal protein recovery it was necessary to vary the buffer conditions: involvement of DTT destructed the resin by reduction of Ni^{2+} ions, thus, addition of DTT should be avoided. The pH had to be adjusted to the binding optimum pH 8; moreover, addition of Zn^{2+} ions was omitted, because Zn^{2+} may occupy the His tag so it is not accessible for the Ni-resin. Nevertheless, Zn^{2+} ions are essential for RORα4 activity and had to be added to the elution buffers at the latest. By performing a batch purification procedure, approx. 90% of the applied RORα4 protein bound to the resin. The protein was washed and eluted with an imidazole gradient, elution of RORα4 appeared between 50 and 100 mM imidazole, therefore, the imidazole gradient for column wash is cascaded in a very fine way within this interval. While the loaded sample was colored slightly brown, which was probably caused by insoluble non-protein *E. coli* residues, the eluted fractions were colorless and concentrations from 400 µg/ml could be achieved. However, RORα4 protein dimers, trimers and small fragments, bearing the N-terminal His-tag, possibly formed during sonication, could not be separated by Nickel affinity chromatography.

In summary, a method for the overexpression of human full-length RORα4 in *Escherichia coli* was developed. Production of mg amounts of native RORα4 protein can be performed

easily within 4 days. Although the RORα4 protein was insoluble when expressed in *E. coli*, it could be refolded into an active conformation. Against former skepticism, refolding of insoluble proteins aggregates obtained from overexpression in prokaryotes became a common and accepted method for obtaining large amounts of native recombinant proteins in the past years [235]. Protocols for refolding procedures of a variety of proteins can be found at databases in the internet (http://refold.med.monash.edu.au/). Some general guidelines for developing a refolding procedure are apparent, but a specific protocol must be empirically determined for each protein. However, the functionality of refolded proteins has to be verified and the method is not appropriate for every protein. However, since the refolded RORα4 recombinant protein showed the expected functionality, demonstrating that it was folded properly, it can be used as starting material for further investigative studies on the nuclear receptor RORα.

Anti-RORα antibody

Production of a new monoclonal anti-RORα antibody was achieved by injecting recombinant hRORα4 into Balb/c mice. To prevent the possibility of raising an antibody targeted against the polyhistidine epitope, the fused His-tag was cleaved before injection. Because injection of prokaryotic residues in mice causes an intense immune response, leading to a variety of antibodies targeted against *E. coli* proteins, high RORα4 purity was needed for immunization. This purity was obtained by separation of probe proteins by electrophoresis and subsequent excision of the RORα4 band out of the polyacrylamide gel.

Eight injections with hRORα4 in PBS were sufficient for immunization, and after fusion of mouse lymphocytes with NS-1 cells, the hybridoma cell line 6E8 was identified as anti-RORα antibody donor. The quality of anti-RORα antibody was tested by immunoblotting using lysates of untreated HeLa cells and HeLa cells transfected with pSG5-RORα4. Antibody clone 6E8 showed high specificity and sensitivity and could be used for detecting of both denatured and native RORα4 protein. The antibody epitope was identified by immunoblot using various protein truncation mutants, and amino acids 83-105 of human RORα4 emerged as necessary for antibody recognition. These amino acids lie within the N-terminus of the conserved hinge domain, more precisely in the carboxy-terminal extension (CTE). The two arising advantages of this epitope location are: (i) all four RORα isoforms should be detectable with clone 6E8 and (ii) since the CTE was absolute necessary for monomeric DNA binding [93], binding of clone 6E8 to RORα4 protein diminishes its DNA binding affinity

significantly. Therefore, the anti-RORα antibody was optimal for demonstration of RORα shift specificity in the electrophoretic mobility shift assay (EMSA).

RORα phosphorylation

As mentioned above, activity of steroid as well as non-steroid nuclear receptor is regulated by phosphorylation. Phosphorylation of a nuclear receptor has multiple effects, DNA binding affinity is influenced, ligand-binding, recruitment of cofactors or protein stability. Besides the binding of a ligand, phosphorylation of nuclear receptors is a very important way to take influence on transcriptional activation (summarized in Table 1.7).

Although cholesterol was found within the ligand binding pocket of RORα, it is not yet clear whether cholesterol is the natural ligand for RORα that functions as on-switch. Cholesterol-deficient cells showed a decreased RORα activity which could be retrieved after cholesterol addition [120,121]. However, cholesterol is an essential component of cell membranes, and cell suffering after depletion of cholesterol is not remarkable. Molecular modeling suggest that RORα acts ligand-independent, because the primary amino acid sequence leads to a three-dimensional conformation similar to that of ligand-bound receptor [107]. Altogether, no activating or repressing agent has been doubtlessly identified so far.

On this background, a posttranslational modification such as phosphorylation as activity regulating event was taken into account. In order to find a kinase that phosphorylates RORα, in-gel kinase experiments were performed. RORα4 was polymerized into a gel matrix, refolded within this matrix and subjected to in-gel phosphorylation with kinases provided from cell lysates that were separated over the gel. These cell lysates were prepared from freshly isolated PMNL cells which were stimulated with various substances to respectively activate different kinase groups. After separation of PMNL cell lysates within the RORα4 containing gel matrix and incubation of the gel in a [γ-^{32}P]-ATP buffer, a RORα4 phosphorylating kinase with an apparent molecular weight of approx. 40 kDa was detected. This kinase was activated by arachidonic acid, ionophore, PMA, sucrose or sodium arsenite incubation, these substances can all be considered as cell stressors. The ERK activation inhibitor U0126 suppressed this phosphorylation. PKA and p38 failed to phosphorylate RORα4 *in vitro*. Finally, ERK was found to phosphorylate RORα4 *in vitro* on Thr-128, which is part of an optimal ERK consensus sequence PLTP. Further *in vitro* experiments demonstrated that mutation of Thr-128 to alanine completely prevents phosphorylation of the RORα4 protein by ERK. Although five additional putative ERK recognition sites can be found in the RORα4 amino acid sequence, phosphorylation by ERK could only be

demonstrated for Thr-128. Thr-128 is located in the hinge region, which represents the connecting link between the DNA binding domain and the ligand binding domain, these three segments constitute the conserved part of all four RORα1-RORα4 isoforms, which only differ in their N-terminal A/B domain. Within the nuclear receptor subfamily, the hinge region shows little homology. Besides orientating the DBD and the LBD in a three dimensional conformation to each other, the hinge domain provides the carboxy-terminal extension (CTE) that recognizes the A/T-rich sequence in front of the response element AGGTCA. The proper conformation of both the protein and the DNA within the complex facilitates the interaction of the nuclear receptors with other components of the transcription machinery [14]. Thus, the hinge domain takes influence on DNA binding properties, facilitates a proper conformation by arranging the other receptor domains, and is responsible for the recruitment of cofactors that are necessary for interaction with the transcription machinery.

Thr-128 was replaced by alanine and the resulting mutant T128A was not accessible for RORα4 phosphorylation by ERK *in vitro*. Experiments demonstrated that the RORα4-T128A mutant exhibits a stronger DNA binding affinity than the wild-type protein. This was shown by an electrophoretic mobility shift assay and confirmed when the transcriptional activity was tested in a reporter gene system, where the T128A mutant showed an increased activity when compared to RORα4-WT. Presumably, the increased DNA binding affinity of the T128A mutant led to an enhanced transcriptional activity. Moreover, in competition experiments with RevErbα, the T128A mutant was more resistant to replacement by RevErbα at the RORE. However, there is little evidence that the lack of phosphorylation contributes to the stronger DNA affinity of the T128A mutant. The phosphomimetic mutants, T128D and T128E, displayed an activity that was in the range between that of WT and the T128A mutant, and it remains unclear whether the mutants perform their task as phosphomimetics properly. Physical exchange of amino acid 128 to valine or isoleucine also increased RORα4 transcriptional activity. In contrast, mutation to arginine, bearing a positive charge, attenuated the activity. These results suggest that residue 128 is a sensitive site whose constitution takes influence on RORα4 DNA binding affinity. Residue 128 is located not far from the carboxy-terminal extension (CTE), which comprises amino acids 83-111 and was shown to bind to the A/T-rich sequence preceding the ROREs. In fact, binding of the CTE is absolute necessary for binding of RORα to its response element, because truncation of this domain led to a complete loss of DNA binding abilities *in vitro* [87,93]. Unfortunately, it was not possible to influence

the DNA binding affinity by phosphorylation of RORα4 protein *in vitro*. In an electrophoretic mobility shift assay, phosphorylation by ERK-2 did not affect RORα4 binding affinity.

In order to demonstrate an effect of the actual Thr-128 phosphorylation status on transcriptional activity *in vivo*, cellular kinases were stimulated by incubation of HeLa cells with PMA. PMA incubation of transfected HeLa cells decreased RORα4 activity, and the specific inhibitor of ERK activation U0126 could neutralize this effect. However, the activity of the T128A mutant was modulated in a similar manner, and the additional mutation of one of the other five putative phosphorylation sites gave the same results. This clearly demonstrates that the PMA/U0126 effects are not evoked by stimulation and inhibition of RORα4 phosphorylation by ERK. A direct influence of ERK activation/inhibition on RORα4 transcriptional activity could not be shown. Western Blots of transfected cells demonstrated that incubation with PMA impaired RORα4 expression which could explain the diminished RORα4 transcriptional activation of the TK-promoter in front of the luciferase coding sequence.

MEK1 is the upstream kinase which phosphorylates and thus activates ERK. To particularly activate cellular ERK in transfected HeLa cells, a constitutive active form of MEK1 was cloned and cotransfected. A slight activation of ERK in the cell nuclei was demonstrated by immunoblotting of transfected HeLa cells using an anti-phospho-ERK antibody. However, RORα4 activity was not influenced by cotransfection of ca-MEK1, even a dominant negative form which should suppress ERK activation, did not seem to influence RORα4 activity.

Within the core-clock of mammals, oscillating expression of Bmal1 protein is responsible for impulse generation. RORα seems to constitutively activate Bmal1 expression. RevErbα suppresses RORα transcriptional activation and thus takes the counterpart. Importantly, RevErbα represses its own expression which results in an oscillating appearance of RevErbα nuclear receptor. This oscillating appearance leads to an oscillating RORα antagonism and finally to an oscillating Bmal1 expression. Altogether, the actual pacemaker in the core-clock of mammals is the feedback loop of RevErbα repressing its own transcription. Within the core-clock, there are various further feedback loops. Therefore, another feedback loop between RORα and Bmal1 protein was considered. In fact, cotransfection of Bmal1 enhanced RORα4 activity on the Bmal1 promoter in an isoform-specific manner. Whereas isoform A seemed to have no influence, isoform B induced RORα4 activity up to 150%. However, a correlation between this activity induction and RORα4 phosphorylation status is not immediately apparent, because the T128A mutant was inducible in a similar manner.

In HeLa cells, RORα4 is predominantly located in the cell nucleus [227]. RORα4-WT, -T128A and -T128E were fused to EGFP and transfected HeLa cells were observed in a confocal laser scan microscope. However, mutation of Thr-128 did not influence the cellular distribution pattern. Besides a clear nuclear localization, RORα4 was additionally found as protein clusters at cellular membranes of HEK293 cells, indicating that the nuclear receptor might have further tasks outside the cell nucleus. But again, neither mutation of Thr-128 nor incubation with PMA affected the appearance of the membrane clusters.
Besides directly regulating nuclear receptor activity, phosphorylation was demonstrated to influence protein stability and degradation by the proteasome [46,67]. Experiments on RORα4 long-term stability over 6 days and experiments on RORα4 degradation by the proteasome, showed no correlation to the phosphorylation status. Transfected RORα4 wild-type and the T128A mutant exhibited the same stability over 6 days in HeLa cells.

Altogether, these results indicate that RORα4 is phosphorylated on Thr-128 by ERK *in vitro*, but within our assay systems we could not demonstrate that this phosphorylation has an effect on transcriptional activation, protein stability or cellular distribution in HeLa cells. Further luciferase experiments with HEK293 and MCF-7 cells suggest similar results. Nevertheless, mutation of Thr-128 to Ala changes RORα4 DNA binding affinity and influences the transcriptional activity, probably because of its location nearby the CTE.
There is a high probability for a cellular relevance of an optimal ERK consensus motif that is conserved in all four RORα isoforms. Further studies should be performed to prove an influence on binding affinity to different types of ROR response elements. Alternatively, phosphorylation on the hinge region could be necessary for direct interaction with an unknown protein modulating RORα activity, and the expression level of this co-regulator protein is too low within the artificial conditions of a reporter gene assay. Moreover, phosphorylation was shown to prepare proteins for further modifications, for example for a sumoylation or a second phosphorylation by another kinase. A recent study reported that ERK phosphorylates mCry1 (Ser-247) and mCry2 (Ser-265), two transcription factors necessary for the maintenance of the core-clock rhythm [175]. Phosphorylation on these residues by ERK reduces mCry repressing activity. Interestingly, physiological relevance of a second ERK phosphorylation site in mCry2, Ser-557, was initially unclear. Lately it was demonstrated that phosphorylation on Ser-557 prepares mCry-2 protein for an additional phosphorylation by glycogen synthase kinase-3 beta (GSK-3β), which is needed for an efficient degradation of protein by the proteasome [176].

RevErbα phosphorylation

Because of the obvious sequence homology between RORα and its opponent RevErbα, it was possible to apply the RORα4 overexpression and purification protocol for RevErbα protein production. Although the conditions might be further optimized, the protein was produced in an acceptable quality and quantity by inclusion body separation and protein refolding. Purified RevErbα inclusion bodies were used to prepare the gels for in-gel kinase assays. In analogy to the experiments performed with RORα, it could be demonstrated that RevErbα is also a target for ERK-2 phosphorylation *in vitro*. Analysis of the RevErbα amino acid sequence reveals 18 putative ERK recognition sites. Initial experiments on physiological relevance of this phosphorylation, by incubation of an RORα4-RevErbα interplay on the REa23 promoter with PMA, gave no hints so far.

Herein, it was shown that RORα as transcriptional activator and RevErbα as transcriptional repressor can be both phosphorylated by ERK-2 *in vitro*. The extracellular-signal regulated kinase receives signals from outside of the cell, it is activated via signal cascades that are initiated by growth factors, cytokines, UV- and γ-radiation. Once activated, ERK translocates and thus carries the signal from the cell surface into the nucleus, where it is known to influence gene transcription by phosphorylation of transcription factors. By this way, the cell reacts to environmental signals [183]. Interestingly, ERK activation itself within the SCN underlies a circadian rhythmicity, imposing a connection between RORα phosphorylation and circadian rhythmicity [204]. However, these data do not provide a clear evidence for phosphorylation by ERK as transcriptional activity modulator so far.

RORα4 Sumoylation

The small-ubiquitine-related modifier (SUMO) is a protein moiety that is ligated to lysine residues in a variety of target proteins. It is structurally related to ubiquitine, and the 79 amino acids long molecule features a molecular weight of 11 kDa. The addition of SUMO can modulate the ability of proteins to interact with their partners, alter their patterns of subcellular distribution and control their stability. SUMO influences many different biological processes, but recent data suggest that it is particularly important in the regulation of gene transcription. Several steroid-, e. g. the PR [236], as well as non-steroid nuclear receptors have recently been shown to be sumoylated. Reports have shown that sumoylation of PPARγ results in an increased protein turnover rate [237]. Bmal1 shows a circadian pattern of

sumoylation that parallels its activation, sumoylation stabilizes Bmal1 protein and is necessary for Bmal1 rhythmicity [181,238].

RORα4 sumoylation was taken into account, because Western Blots of RORα4 protein showed three distinct bands differing in approx. 10 kDa molecular weight. The RORα4 amino acid sequence contains four potential SUMO recognition motifs, but mutation of this motif did not eliminate one of the three distinct bands observed on an immunoblot obtained from transfected HeLa cells. According to Tojo et al. [238], SUMO1 was cloned from cDNA and cotransfected with RORα4. However, no additional bands were detected after cotransfection in HeLa cells. Altogether, an evidence for RORα4 modification by sumoylation is not apparent.

RORα4 protein cleavage

There are several hints for a RORα4 protein cleavage in transfected HeLa cells. Immunoblotting of RORα4 and two truncation mutants revealed additional bands that were not detected after transfection of the empty vectors. The monoclonal anti-ROR antibody clone 6E8 detected the fragment containing the first amino acids of the hinge region (aa 83-105, CTE), whereas the polyclonal antibody from Santa Cruz, recognizing epitopes within the ligand binding domain and/or the N-terminal part of the hinge domain, detected the other fragment of RORα. The 55 kDa-sized RORα4 wild-type is cleaved into two fragments of approx. 20 and 35 kDa, the 82 kDa-sized EGFP-RORα4 in 47 and 35 kDa and the 72 kDa-sized EGFP-HI-LBD1 in 37 and 35 kDa. The mass of cleavage fragments and their detection by the respective antibodies, suggest a cleavage site within the first third of the hinge domain. Further investigations will be necessary to reveal the cleavage mechanism and if the cleavage has a consequence on RORα4 signaling.

6 SUMMARY

The retinoic acid related orphan receptor α (RORα) regulates the expression of various target genes by binding to specific response elements in their promoter region. RORα is an interesting pharmaceutical target since it positively affects several pathophysiological processes of clinical relevance. RORα enhances the expression of Apo-AI protein, the major constituent of HDL, which is responsible for the cholesterol transportation. RORα notably contributes to the bone mineralization and generation of the extracellular bone matrix, demonstrating its involvement in osteoporosis, and by up-regulating the gene for IκBα, RORα has anti-inflammatory effects. Moreover, RORα is necessary for cerebellar development and the maintenance of the mammalian day-night periodicity governed by the core-clock within the suprachiasmatic nuclei. RORα receptors have been reported to bind cholesterol, melatonin, or to function ligand-independent. By monomeric binding to the recognition motif AGGTCA preceded by an A/T-rich sequence (ROR response element, RORE), RORα constitutively activates gene transcription. However, RORα activity is passively suppressed by its opponents RevErbα and RevErbβ, which both bind to the same target sequence.

A method for overexpression and purification of RORα4 in *E. coli* was established, facilitating the production of mg amounts of pure RORα4 protein within three days. Although RORα4 was expressed in insoluble and inactive inclusion bodies, the protein could be solubilized with 6 M guanidine and refolded into its native conformation. This was obtained by dialysis against different buffers of descending guanidine content and with help of the adjuvant L-arginine. Despite this rather complex operation, a final protein concentration of 300-400 µg/ml could be achieved. This solution could be stored at –70°C over months without lost of quality.

The functionality of refolded RORα4 protein was proved by performing an electrophoretic mobility shift assay, where RORα4 binding to a double-stranded, monomeric ROR response element was demonstrated. RORα4 was fused to a N-terminal polyhistidine tag which allowed the further purification by Nickel affinity chromatography.

Because of the obvious sequence homology between RORα and its opponent RevErbα, it was possible to apply the RORα4 overexpression and purification protocol for RevErbα protein production. Although the conditions might be further optimized, the protein was produced in

an acceptable quality and passable quantity by inclusion body separation and protein refolding.

In addition to that, an anti-RORα antibody was generated by immunization of Balb/c mice with overexpressed protein. Antibody clone 6E8 showed high specificity and sensitivity and could be used for detecting of both denatured and native RORα4 protein. The antibody epitope was identified by immunoblotting of various RORα4 truncation mutants, and amino acids 83-105 of human RORα4 emerged as necessary for antibody recognition. These amino acids lie within the hinge domain which is conserved throughout all RORα1-α4 isoforms, facilitating the detection of all RORα isoforms by antibody clone 6E8.

Both the overexpression method for RORα and RevErbα, and the anti-RORα antibody were important tools for subsequent investigations on RORα signaling.

Since the activity of many nuclear receptors is regulated by phosphorylation, RORα4 was screened for phosphorylating kinases. For this purpose, RORα4 was polymerized into a gel matrix, refolded within this matrix and subjected to in-gel phosphorylation with kinases provided from cell lysates that were separated over the gel. This experiment revealed a RORα4 phosphorylating kinase with an approx. molecular weight of 40 kDa, which could be identified as extracellular-signal regulated kinase (ERK).

ERK can be activated over signal cascades that are initiated by e. g. growth factors, cytokines, UV- and γ-radiation. Once activated, ERK translocates and thus carries the signal from the cell surface into the nucleus, where it is known to influence gene transcription by phosphorylation of transcription factors. In this way, the cell reacts on requirements of the environment.

ERK phosphorylated RORα4 at Thr-128 *in vitro*. Mutation of Thr-128 to Ala completely suppressed RORα4 phosphorylation by ERK. The T128A mutant revealed an increased transcriptional activity in a reporter gene assay, and in competition experiments with RevErbα, RORα4-T128A was more resistant to replacement by RevErbα on the RORE then the wild-type. However, there is little evidence that the lack of phosphorylation contributes to the stronger DNA binding affinity of the T128A mutant. Physical exchange of Thr-128 to Val or Ile also increased RORα4 transcriptional activity, whereas mutation to Arg led to an attenuation. Two phosphomimetic mutants were generated, T128D and T128E, however, their activities ranged between that of wild-type and RORα4-T128A. Nevertheless, these results suggest that residue 128 is a sensitive site that influences RORα4 DNA binding affinity. Unfortunately, it was not possible to influence the DNA binding affinity in an electrophoretic mobility shift assay by phosphorylation of RORα4 *in vitro*. Cotransfection of a constitutive

active as well as a dominant negative form of MEK1, the ERK activating kinase, did not influence the activities of RORα4 wild type or mutants.
Confocal laser scan microscopy of EGFP-fused RORα4 mutants in HeLa and HEK293 cells revealed that the subcellular distribution pattern is modulated neither by mutation of Thr-128, nor incubation with the kinase activating substance phorbol 12-myristate 13-acetate (PMA).
RORα4 sumoylation as a further posttranslational modification was taken into account, because Western Blots of transfected HeLa cells showed three distinct RORα4 bands differing in approx. 10 kDa molecular weight. Generally, addition of SUMO (small-ubiquitine-related modifier) to nuclear receptors can modulate their ability to interact with their partners, alter their patterns of subcellular distribution and control their stability. The RORα4 amino acid sequence contains four potential SUMO recognition motifs, but mutation of this motif did not eliminate one of the three distinct RORα4 bands observed on an immunoblot obtained from transfected HeLa cells. Moreover, cotransfection of SUMO1 with RORα4 gave no additionally detected bands. Altogether, an evidence for RORα4 modification by sumoylation is not immediately apparent.
In addition to that, there are several hints for a RORα4 protein cleavage in transfected HeLa cells. Immunoblotting of RORα4 and two truncation mutants revealed two additional bands that were not detected after transfection of the empty vectors. The mass of cleavage fragments and their respective detection by two different anti-RORα antibodies suggest a cleavage site within the first third of the hinge domain. Further investigations will be necessary to reveal the cleavage mechanism and if the cleavage has a consequence on RORα4 signaling.

In analogy to the experiments performed with RORα, RevErbα was shown to be target of *in vitro* phosphorylation by ERK. The amino acid sequence of RevErbα revealed 18 putative consensus motifs, but the actual phosphorylation site and the physiological relevance still remain to be clarified. First experiments on the physiological relevance of this phosphorylation by incubation of a RORα4-RevErbα interplay on the RORE in a luciferase assay system with PMA, gave no answers so far.

7 ZUSAMMENFASSUNG

Der Retinoic Acid Related Orphan Recepor α (RORα) ist ein nukleärer Rezeptor, der die Expression verschiedener Targetgene reguliert, indem er an spezifische Erkennungssequenzen in deren Promotorbereiche bindet. Pharmazeutisches Interesse erweckt RORα, weil es einige klinisch relevante pathophysiologische Prozesse positiv beeinflusst. Anti-atherosklerotische Eigenschaften werden RORα nachgesagt, da es die Expression von Apo-AI aktiviert, welches den Hauptbestandteil des Cholesterol-transportierenden HDLs darstellt. Durch die Verstärkung der Knochenmineralisierung und dem Aufbau der extrazellulären Knochenmatrix kann RORα einer Osteoporose entgegenwirken. Außerdem wirkt RORα anti-inflammatorisch, da es die Expression von IκBα verstärkt und damit den NF-κB-Signalweg hemmt. Des weiteren ist RORα an der Gehirnentwicklung und an der Aufrechterhaltung des Tag-Nacht-Rhythmus, der bei Säugetieren in den suprachiasmatischen Nuclei erzeugt wird, beteiligt. Bei Kristallisationsexperimenten wurde Cholesterin in der Ligandenbindungstasche von RORα gefunden, und es wird diskutiert, ob auch Melatonin mit dem nukleären Rezeptor interagiert. Allerdings gibt es ebenso Studien die beweisen, dass RORα auch ohne Ligand in der aktivierten Konformation vorliegt. Durch monomere Bindung an das DNA-Erkennungsmotiv AGGTCA (ROR response element, RORE), welchem eine A/T-reiche Sequenz vorangeht, kann RORα konstitutiv aktivierend wirken. Allerdings kann diese Aktivität durch die Gegenspieler RevErbα und RevErbβ passiv reprimiert werden, da jene die gleichen Motive erkennen und RORα aus seiner Bindung verdrängen können.

Es wurde eine Methode zur Überexpression und Aufreinigung von RORα4 in *E. coli* etabliert, mit der man innerhalb von 3 Teigen reines Protein in mg-Mengen erhalten kann. Obwohl RORα4 in *E. coli* in Form von unlöslichen und inaktiven Einschlusskörpern (Inclusion Bodies) produziert wurde, konnten diese in 6 M Guanidin gelöst und das Protein in seine native Form rückgefaltet werden. Dies wurde durch Dialyse gegen verschiedene Puffer mit absteigenden Guanidinkonzentrationen erreicht, zusätzlich wurde L-Arginin als Hilfsstoff zur Stabilisierung der Faltungsintermediate eingesetzt. Obwohl das Rückfaltungsverfahren relativ aufwändig war und zu Beginn des Prozesses nur sehr geringe Proteinkonzentrationen eingesetzt werden mussten, wurden am Ende Lösungen mit 200-300 µg/ml RORα4 erreicht. Das auf diese Weise rückgefaltete Protein konnte bei –70°C über mehrere Monate gelagert werden, ohne dass ein Qualitätsverlust zu verzeichnen war.

Die Funktionalität des rückgefalteten RORα4-Rezeptors wurde anhand von *in vitro* DNA-Bindungsstudien bewiesen, in denen gezeigt werden konnte, dass das Protein an ein doppelsträngiges Oligonukleotid, welches ein monomeres RORE enthielt, bindet.
An das Protein wurde N-terminal ein Polyhistidin-Rest angebracht, über den RORα4 mittels Nickel-Affinitätschromatographie noch weiter aufgereinigt werden konnte. Je Liter *E. coli*-Kultur konnten auf diese Weise 16-20 mg RORα4 in einer Reinheit von 85% gewonnen werden.
Bedingt durch die hohe Sequenzhomologie zwischen RORα und RevErbα, konnte die Methode zur Überexpression und Aufreinigung von RORα direkt auf RevErbα übertragen werden. Die Konditionen erwiesen sich zwar als optimierungsfähig, dennoch konnte durch Inclusion-Body-Separation, Lösung in 6 M Guanidin und Proteinrückfaltung, reines, funktionsfähiges RevErbα gewonnen werden.
Durch Immunisierung von Balb/c-Mäusen mit überexprimiertem RORα konnte ein Anti-RORα-Antikörper generiert werden. Acht Injektionen über einen Zeitraum von 6 Monaten reichten aus, um die Bildung von Antikörpern zu provozieren. Nachdem einzelne Mauslymphozyten mit NS-1-Zellen fusioniert wurden, konnten aus der Hybridomzelllinie 6E8 Anti-RORα-Antikörper gewonnen werden, die besonders hohe Spezifität und Sensitivität aufwiesen und zur Detektion sowohl von nativem, als auch von denaturiertem Protein verwendet werden konnten. Das Antikörper-Epitop wurde durch Immunoblotting von verschiedenen, verkürzten RORα4-Mutanten bestimmt, wobei sich die Aminosäuren 83-105 von humanem RORα4 als detektierte Region herausstellten. Dieser Bereich liegt innerhalb der Hinge-Domäne, die bei allen RORα1-4-Isoformen in identischer Sequenz vorliegt und daher alle 4 Isoformen mit Klon 6E8 detektierbar sein müssten.
Sowohl die Überexpressionsmethode für RORα bzw. RevErbα, als auch der Anti-RORα-Antikörper stellten wichtige Werkzeuge dar, die sich für weitere Versuche rund um den nukleären Rezeptor RORα4 als unerlässlich erwiesen.

Die Aktivität vieler nukleärer Rezeptoren, sowohl die der Steroid- als auch die der Non-Steroidrezeptoren, wird durch Phosphorylierung reguliert. Diese Art der posttranslationalen Modifikation beeinflusst die Wechselwirkung mit anderen Proteinen, Liganden oder der DNA selbst. Auch kann die Lokalisation innerhalb der Zelle oder die Proteinstabilität verändert werden. Eine Phosphorylierung kann sowohl aktivierende als auch inhibierende Wirkung zeigen.

Auf der Suche nach Kinasen die RORα4 phosphorylieren, wurde RORα4-Protein kovalent in eine SDS-Polyacrylamid-Gelmatrix einpolymerisiert, Zelllysate mit aktivierten Kinasen über dieses Gel aufgetrennt und die Proteine innerhalb der Gelmatrix rückgefaltet. Während der Inkubation dieses Gels in radioaktivem [γ-^{32}P]-ATP, konnten die aufgetrennten Kinasen das im Gel einpolymerisierte RORα4 phosphorylieren. Durch dieses Experiment wurde eine Kinase mit ungefährem Molekulargewicht von 40 kDa entdeckt, die RORα4 phosphorylieren konnte und schließlich als ERK (extracellular-signal regulated kinase) identifiziert wurde.
ERK gehört zu der Familie der MAPK (mitogen activated protein kinases), die sich durch extrazelluläre Signale aktivieren lassen. ERK wird u. a. durch Wachstumsfaktoren, Zytokine und UV- oder γ-Strahlung aktiviert. Die aktivierte ERK transloziert zum Zellkern und kann dort verschiedene nukleäre Rezeptoren phosphorylieren. Auf diese Weise ist ERK in der Lage, den Stoffwechsel der Zelle an die Anforderungen der Zellumgebung anzupassen.
In *in vitro*-Versuchen wurde Thr-128 des RORα4-Rezeptors als ERK-Phosphorylierungsstelle bestimmt. Die Mutation von Thr-128 zu Ala verstärkte die Transkriptionsaktivität von RORα4 im Reportergenassay, der mit Hilfe von zwei unterschiedlichen Promotorkonstrukten durchgeführt wurde. Der REa23-Promoter enthält drei RORE, die kurz vor einen Thymidinkinasepromotor geschaltet wurden. Das zweite Konstrukt enthält an der gleichen Stelle den humanen Bmal1-Promoter, der für die Generation des zirkadianen Rhythmus im suprachiasmatischen Nucleus verantwortlich ist. Auf beiden Promotoren wirkt RORα4 aktivierend, während RevErbα die RORα4-vermittelte Transkriptionsaktivität durch Verdrängung des Rezeptors vom RORE aufhebt. In Kompetitionsexperimenten mit dem Gegenspieler RevErbα ließ sich RORα-T128A auf beiden Promotoren weniger leicht vom RORE verdrängen als der Wildtyp. Allerdings gibt es wenige Hinweise darauf, dass die verstärkte Aktivität der T128A-Mutante tatsächlich auf die fehlende Phosphorylierung zurückzuführen ist. Mutation von Thr-128 zu Val oder Ile verstärkte ebenso die Aktivität des Rezeptors, während Austausch zum positiv geladenen Arg sie verringerte. Es wurden zwei phosphomimetische Mutanten erzeugt, indem Thr-128 gegen Asp oder Glu ausgetauscht wurde, die von der Struktur her einem phosphoryliertem Thr ähneln. Allerdings lag die Aktivität der beiden phosphomimetischen Mutanten zwischen den Aktivitäten von Wildtyp und Ala-Mutante. Diese Ergebnisse zeigen, dass die Aminosäure an Position 128 eine sensitive Stelle ist, deren Konstitution Einfluss auf die DNA-Bindungseigenschaften des RORα4-Rezeptors nimmt. Thr-128 ist in der Nähe der Carboxy-terminalen Extension (CTE) lokalisiert, von der gezeigt wurde, dass sie für die monomere Bindung von RORα an das RORE essentiell ist. Es war jedoch nicht möglich, die DNA-Bindungseigenschaften von

RORα4 in einem EMSA (electrophoretic mobility shift assay) durch vorherige *in vitro* Phosphorylierung zu verändern.

Verschiedene Versuche wurden unternommen, um die zelluläre ERK von transfizierten HeLa-Zellen zu aktivieren. Inkubation mit dem unspezifischen Kinaseaktivator Phorbol-12-myristat-13-acetat (PMA) führte zu einer Verringerung der Aktivität von RORα4, die durch den spezifischen Inhibitor der ERK-Aktivierung U0126 wieder aufgehoben werden konnte. Dieser Effekt wurde allerdings nicht durch eine ERK-Phosphorylierung verursacht, denn die T128A-Mutante ließ sich in ähnlicher Weise von PMA und U0126 manipulieren.

MEK1 phosphoryliert und aktiviert somit ERK. Eine konstitutiv aktive Form von MEK1 führt zu einer Daueraktivierung von ERK, wogegen eine dominant negative MEK1 die Aktivierung verhindert. Cotransfektion von einer konstitutiv aktiven, sowie einer dominant negativen MEK1 zusammen mit entweder dem RORα4 Wildtyp oder der T128A-Mutante veränderte deren Transkriptionsaktivitäten nicht.

Der Einfluss der Phosphorylierung auf die subzellulare Lokalisation von RORα4 wurde durch konfokale Laserscan-Mikroskopie von EGFP-getaggtem RORα4 und Mutanten in transfizierten HeLa und HEK293 untersucht. Hinsichtlich der Verteilung innerhalb der Zelle konnten keine Unterschiede beobachtet werden, auch Inkubation mit PMA hatte keinen Effekt auf die zelluläre Lokalisation der Proteine.

Für den Wildtyp und die T128A-Mutante wurden Studien zur Proteinstabilität durchgeführt. Frühere Ergebnisse zeigten, dass RORα erst ubiquitinyliert und anschließend durch das Proteasom abgebaut wird. Da der Proteasominhibitor MG-132 stets zu einer verringerten Aktivität führte wurde spekuliert, ob der Abbau durch das Proteasom für den Start der Transkription essentiell ist. Inkubation von transfizierten HeLa-Zellen mit MG-132 beeinflusste die T128A-Mutante jedoch in gleichem Maße wie den Wildtyp. Auch Proteinstabilitätsexperimente über einen Zeitraum von 6 Tagen zeigten keine Unterschiede zwischen Ala-Mutante und Wildtyp.

Neben der Phosphorylierung wurden auch die Möglichkeit weiterer posttranslationaler Modifikationen untersucht. Western Blots von transfizierten HeLa-Zellen zeigten RORα4 als eine Ansammlung von 3 Banden, die sich in einem Molekulargewicht von ca. 10 kDa unterschieden. Daher wurde eine Modifikation durch Sumoylierung in Betracht gezogen. Das Anfügen eines SUMO-Restes (small ubiquitine-related modifier) an einen nukleären Rezeptor kann zu vielerlei Effekten führen, z. B. kann die Interaktion mit anderen Proteinen beeinflusst werden, ebenso die zelluläre Verteilung oder die Proteinstabilität. Die Primärsequenz von RORα4 weist 4 potentielle Sumoylierungsstellen auf, die alle einzeln mutiert wurden.

Allerdings führte keine der Mutationen zum Verschwinden einer der drei Banden, die typischerweise für RORα4 in transfizierten HeLa-Zellen gefunden werden. Auch eine Cotransfektion eines SUMO1-Überexpressionsvektors führte zu keiner additiv detektierten Bande. Bisher liegen demnach keine Hinweise darauf vor, dass RORα4 sumoyliert wird.
Eine weitere posttranslationale Modifikation könnte eine Spaltung von RORα4 sein. Auf Blots von transfizierten HeLa-Zellen waren neben den drei erwähnten Banden zwei weitere Banden zu erkennen, deren Molekulargewichtssumme stets das Molekulargewicht des Gesamtproteins ergaben. Dies konnte außer für den RORα4-Wildtyp für zwei weitere, verkürzte RORα4-Formen nach Transfektion in HeLa-Zellen beobachtet werden. Transfektion eines leeren Expressionsvektors hingegen zeigte keiner dieser detektierten Banden. Manche Fragmente ließen sich nur mit dem monoklonalen anti-RORα-Antikörper 6E8 detektieren, andere hingegen nur mit dem polyklonalen RORα-Antikörper der Firma Santa Cruz. Anhand der Fragmentgrößen und der Detektion durch einen bestimmten Antikörper ließ sich das erste Drittel der Hinge-Domäne als ungefähre Schnittstelle berechnen. Weitere Experimente sind notwendig, um den Spaltungsmechanismus und die genaue Stelle zu untersuchen.

In Analogie zu den Experimenten die mit RORα durchgeführt wurden, konnte auch für den Gegenspieler RevErbα eine Phosphorylierung durch ERK nachgewiesen werden. Die Aminosäuresequenz von RevErbα enthält 18 potentielle ERK-Phosphorylierungsmotive, die tatsächliche Stelle ist allerdings noch nicht bekannt. Erste Studien zur physiologischen Relevanz der RevErbα-Phosphorylierung wurden vorgenommen, dabei wurde ein RORα4-RevErbα Kompetitionsexperiment im Reportergen-Assay mit PMA inkubiert. Allerdings konnte bisher keine Auswirkung der unspezifischen Kinasenaktivierung auf die Aktivität von RevErbα gezeigt werden.

8 ABBREVIATIONS

A	alanine
AA	arachidonic acid
ACTR	acetyl transferase
AF-1/2	activation function 1/2
AIB	amplified in breast cancer
AKBA	O-acetyl 11-keto boswellic acid
Ala	alanine
Apo	apolipoprotein
AR	androgen receptor
Arg	arginine
Asp	aspartic acid
ATP	adenosine triphosphate
Bcip	5-bromo 4-chloro 3-indolylphosphate
Bmal	brain-muscle-Arnt-like protein
bp	base pairs
BSA	bovine serum albumin
ca	constitutive active
CaMK	calcium-calmodulin dependent kinase
cAMP	cyclic adenosine monophosphate
CBP	CREB-binding protein
cdk	cyclin-dependent kinase
cDNA	coding DNA
cds	coding sequence
CKIε	casein kinase I epsilon
CMV	cytomegalie virus
COX	cyclooxygenase
Cry	cryptochrome
CTE	C-terminal extension
D	aspartic acid
dbcAMP	di-buturyl-cAMP
DBD	DNA binding domain
D-MEM	Dulbecco´s modified eagle medium
DMSO	dimethylsulfoxide
dn	dominant negative
DRIP	VDR-interacting protein
DTT	dithiothreitol
E	glutamic acid
EDTA	ethylenediaminetetraacetic acid
EGFP	enhanced green fluorescent protein
EGTA	ethylene glycol-bis(2-aminoethylether)-N,N,N´,N´-tetraacetic acid
ELISA	enzyme-linked immunosorbent assay
EMSA	electrophoretic mobility shift assay
ER	estrogen receptor
ERK	extracellular signal-regulated kinase
FASPS	familiar advanced sleep-phase syndrome
FCS	fetal calf serum
fMLP	N-formyl-Met-Leu-Phe

Glu	glutamic acid
GPCR	G protein coupled receptor
GR	glucocorticoid receptor
GRIP	GR-interacting protein
GSK3β	glycogen synthase kinase 3 beta
GST	glutathione-S-transferase
H	helix
hASMC	human aortic smooth muscle cells
HDL	high density lipoprotein
HEK	human embryonic kidney cells
HeLa	epithelial cells derived from cervix carcinoma
HEPES	4-(2-hydroxyethyl)piperazine-1-ethanesulfonic acid
HepG2	human hepatoma cell line
hr	hairless
HRE	hormone response element
HUVEC	human umbilical vein endothelial cells
IL	interleukin
Ile	isoleucine
i. p.	intraperitoneal
IPTG	isopropyl-β-D-thiogalactopyranoside
IR	infrared
IκBα	NF-κB inhibiting protein alpha
JNK	c-jun NH_2-terminal kinase
ko	knockout
LBD	ligand binding domain
LPS	lipoplysaccharide
LU	light units
MAPK	mitogen activated protein kinase
MBP	myelin basic protein
MCF-7	human mammary gland epithelial cells
MEK	MAPK kinase
MEKK	MAPK kinase kinase
MT	melatonin receptor
NBT	nitroblue-tetrazolium chloride
NCoR	nuclear receptor corepressor
NF-κB	nuclear factor kappa B
NGFI-B	NGF induced clone B
NMDA	N-methyl-D-aspartate
PAF	platelet activating factor
PBP	PPAR-binding protein
PBS	phosphate buffered saline
Pcp	Purkinje cell specific protein
PCR	polymerase chain reaction
PEG	polyethylene glycol
Per	period
PKA	protein kinase A
PKC	protein kinase C
PMA	phorbol 12-myristate 13-acetate
PMNL	polymorphonuclear leukocytes
PMSF	phenylmethanesulfonyl fluoride
PPAR	peroxisome proliferator activated receptor

PR	progesterone receptor
PRMT	protein arginine N-methyltransferase
PVDF	polyvinylidendifluoride
RAC	receptor-associated coactivator
RAR	retinoic acid receptor
RE	response element
RevErb	reverse erbA receptor
RLU	relative light units
ROR	retinoic acid related orphan receptor
RORE	ROR response element
RXR	retinoid X receptor
RZR	retinoid Z receptor
SA	sodium arsenite
SCN	suprachiasmatic nuclei
SCOP	SCN circadian oscillatory protein
SDS	sodium dodecylsulfate
SDS-PAGE	SDS-polyacrylamide gel electrophoresis
SEAP	secreted alkaline phosphatase
SF/FTZ-F	steroidogenic factor/Fushi Tarazu factor
sg	staggerer
SHP	small heterodimeric partner
SMRT	silencing mediator of retinoid and thyroid receptors
SRC	steroid receptor coactivator
STI	soybean trypsin inhibitor
SUMO	small ubiquitine-related modifier
TFIIH	transcription/DNA repair factor II
TIF	transcriptional intermediary factor
TK	thymidin kinase
TNFα	tumor necrosis factor
TR	thyroid hormone receptor
TRAM	TR activator molecule
TRAP	TR-associated protein
Val	valine
VDR	vitamin D receptor
WB	Western Blot

9 REFERENCES

[1] A. Revelli, M. Massobrio, J. Tesarik, Nongenomic actions of steroid hormones in reproductive tissues, Endocr. Rev. 19 (1998) 3-17.

[2] V. Laudet, Evolution of the nuclear receptor superfamily: early diversification from an ancestral orphan receptor, J Mol Endocrinol 19 (1997) 207-226.

[3] V. Giguere, Orphan nuclear receptors: from gene to function, Endocr. Rev. 20 (1999) 689-725.

[4] A. Tremblay, G.B. Tremblay, F. Labrie, V. Giguere, Ligand-independent recruitment of SRC-1 to estrogen receptor beta through phosphorylation of activation function AF-1, Mol Cell 3 (1999) 513-519.

[5] C.E. Juge-Aubry, E. Hammar, C. Siegrist-Kaiser, A. Pernin, A. Takeshita, W.W. Chin, A.G. Burger, C.A. Meier, Regulation of the transcriptional activity of the peroxisome proliferator-activated receptor alpha by phosphorylation of a ligand-independent trans-activating domain, J. Biol. Chem. 274 (1999) 10505-10510.

[6] D. Shao, S.M. Rangwala, S.T. Bailey, S.L. Krakow, M.J. Reginato, M.A. Lazar, Interdomain communication regulating ligand binding by PPAR-gamma, Nature 396 (1998) 377-380.

[7] B.F. Luisi, W.X. Xu, Z. Otwinowski, L.P. Freedman, K.R. Yamamoto, P.B. Sigler, Crystallographic analysis of the interaction of the glucocorticoid receptor with DNA, Nature 352 (1991) 497-505.

[8] J.W. Schwabe, L. Chapman, J.T. Finch, D. Rhodes, The crystal structure of the estrogen receptor DNA-binding domain bound to DNA: how receptors discriminate between their response elements, Cell 75 (1993) 567-578.

[9] J.W. Schwabe, L. Fairall, L. Chapman, J.T. Finch, R.N. Dutnall, D. Rhodes, The cocrystal structures of two zinc-stabilized DNA-binding domains illustrate different ways of achieving sequence-specific DNA recognition, Cold Spring Harb Symp Quant Biol 58 (1993) 141-147.

[10] K. Umesono, R.M. Evans, Determinants of target gene specificity for steroid/thyroid hormone receptors, Cell 57 (1989) 1139-1146.

[11] T.E. Wilson, R.E. Paulsen, K.A. Padgett, J. Milbrandt, Participation of non-zinc finger residues in DNA binding by two nuclear orphan receptors, Science 256 (1992) 107-110.

[12] A. Aranda, A. Pascual, Nuclear hormone receptors and gene expression, Physiol. Rev. 81 (2001) 1269-1304.

[13] C.K. Glass, Differential recognition of target genes by nuclear receptor monomers, dimers, and heterodimers, Endocr. Rev. 15 (1994) 391-407.

[14] L.D. McBroom, G. Flock, V. Giguere, The nonconserved hinge region and distinct amino-terminal domains of the ROR alpha orphan nuclear receptor isoforms are required for proper DNA bending and ROR alpha-DNA interactions, Mol. Cell. Biol. 15 (1995) 796-808.

[15] T. Michigami, A. Suga, M. Yamazaki, C. Shimizu, G. Cai, S. Okada, K. Ozono, Identification of amino acid sequence in the hinge region of human vitamin D receptor that transfers a cytosolic protein to the nucleus, J. Biol. Chem. 274 (1999) 33531-33538.

[16] T.A. Jackson, J.K. Richer, D.L. Bain, G.S. Takimoto, L. Tung, K.B. Horwitz, The partial agonist activity of antagonist-occupied steroid receptors is controlled by a novel hinge domain-binding coactivator L7/SPA and the corepressors N-CoR or SMRT, Mol. Endocrinol. 11 (1997) 693-705.

[17] J.M. Wurtz, W. Bourguet, J.P. Renaud, V. Vivat, P. Chambon, D. Moras, H. Gronemeyer, A canonical structure for the ligand-binding domain of nuclear receptors, Nat. Struct. Biol. 3 (1996) 87-94.

[18] C.K. Glass, M.G. Rosenfeld, The coregulator exchange in transcriptional functions of nuclear receptors, Genes Dev. 14 (2000) 121-141.

[19] N.J. McKenna, B.W. O'Malley, Combinatorial control of gene expression by nuclear receptors and coregulators, Cell 108 (2002) 465-474.

[20] J.D. Chen, Steroid/nuclear receptor coactivators, Vitam Horm 58 (2000) 391-448.

[21] G.J. Narlikar, H.Y. Fan, R.E. Kingston, Cooperation between complexes that regulate chromatin structure and transcription, Cell 108 (2002) 475-487.

[22] T. Kouzarides, Histone methylation in transcriptional control, Curr Opin Genet Dev 12 (2002) 198-209.

[23] D. Chen, H. Ma, H. Hong, S.S. Koh, S.M. Huang, B.T. Schurter, D.W. Aswad, M.R. Stallcup, Regulation of transcription by a protein methyltransferase, Science 284 (1999) 2174-2177.

[24] K. Merienne, S. Pannetier, A. Harel-Bellan, P. Sassone-Corsi, Mitogen-regulated RSK2-CBP interaction controls their kinase and acetylase activities, Mol. Cell. Biol. 21 (2001) 7089-7096.

[25] Y. Shang, M. Myers, M. Brown, Formation of the androgen receptor transcription complex, Mol Cell 9 (2002) 601-610.

[26] F.J. Dilworth, P. Chambon, Nuclear receptors coordinate the activities of chromatin remodeling complexes and coactivators to facilitate initiation of transcription, Oncogene 20 (2001) 3047-3054.

[27] T.H. Bugge, J. Pohl, O. Lonnoy, H.G. Stunnenberg, RXR alpha, a promiscuous partner of retinoic acid and thyroid hormone receptors, EMBO J. 11 (1992) 1409-1418.

[28] S.A. Kliewer, K. Umesono, D.J. Mangelsdorf, R.M. Evans, Retinoid X receptor interacts with nuclear receptors in retinoic acid, thyroid hormone and vitamin D3 signalling, Nature 355 (1992) 446-449.

[29] D.J. Mangelsdorf, R.M. Evans, The RXR heterodimers and orphan receptors, Cell 83 (1995) 841-850.

[30] T.E. Wilson, T.J. Fahrner, J. Milbrandt, The orphan receptors NGFI-B and steroidogenic factor 1 establish monomer binding as a third paradigm of nuclear receptor-DNA interaction, Mol. Cell. Biol. 13 (1993) 5794-5804.

[31] P. Chambon, A decade of molecular biology of retinoic acid receptors, FASEB J. 10 (1996) 940-954.

[32] M.P. Cosma, Ordered recruitment: gene-specific mechanism of transcription activation, Mol Cell 10 (2002) 227-236.

[33] B. Durand, M. Saunders, C. Gaudon, B. Roy, R. Losson, P. Chambon, Activation function 2 (AF-2) of retinoic acid receptor and 9-cis retinoic acid receptor: presence of a conserved autonomous constitutive activating domain and influence of the nature of the response element on AF-2 activity, EMBO J. 13 (1994) 5370-5382.

[34] S. Hahn, Structure and mechanism of the RNA polymerase II transcription machinery, Nat Struct Mol Biol 11 (2004) 394-403.

[35] C. Rochette-Egly, Dynamic combinatorial networks in nuclear receptor-mediated transcription, J. Biol. Chem. 280 (2005) 32565-32568.

[36] J. Xu, Q. Li, Review of the in vivo functions of the p160 steroid receptor coactivator family, Mol. Endocrinol. 17 (2003) 1681-1692.

[37] J.W. Lee, Y.C. Lee, S.Y. Na, D.J. Jung, S.K. Lee, Transcriptional coregulators of the nuclear receptor superfamily: coactivators and corepressors, Cell Mol Life Sci 58 (2001) 289-297.

[38] D.Y. Lee, C. Teyssier, B.D. Strahl, M.R. Stallcup, Role of protein methylation in regulation of transcription, Endocr. Rev. 26 (2005) 147-170.

[39] B.A. Lewis, D. Reinberg, The mediator coactivator complex: functional and physical roles in transcriptional regulation, J Cell Sci 116 (2003) 3667-3675.

[40] G.B. Atkins, X. Hu, M.G. Guenther, C. Rachez, L.P. Freedman, M.A. Lazar, Coactivators for the orphan nuclear receptor RORalpha, Mol. Endocrinol. 13 (1999) 1550-1557.

[41] Z. Nawaz, B.W. O'Malley, Urban renewal in the nucleus: is protein turnover by proteasomes absolutely required for nuclear receptor-regulated transcription?, Mol. Endocrinol. 18 (2004) 493-499.

[42] E. Kopf, J.L. Plassat, V. Vivat, H. de The, P. Chambon, C. Rochette-Egly, Dimerization with retinoid X receptors and phosphorylation modulate the retinoic acid-induced degradation of retinoic acid receptors alpha and gamma through the ubiquitin-proteasome pathway, J. Biol. Chem. 275 (2000) 33280-33288.

[43] D.M. Lonard, B.W. O'Malley, Expanding functional diversity of the coactivators, Trends Biochem Sci 30 (2005) 126-132.

[44] A.P. Dennis, B.W. O'Malley, Rush hour at the promoter: how the ubiquitin-proteasome pathway polices the traffic flow of nuclear receptor-dependent transcription, J Steroid Biochem Mol Biol 93 (2005) 139-151.

[45] M. Muratani, W.P. Tansey, How the ubiquitin-proteasome system controls transcription, Nat. Rev. Mol. Cell. Biol. 4 (2003) 192-201.

[46] M. Gianni, A. Bauer, E. Garattini, P. Chambon, C. Rochette-Egly, Phosphorylation by p38MAPK and recruitment of SUG-1 are required for RA-induced RAR gamma degradation and transactivation, EMBO J. 21 (2002) 3760-3769.

[47] C. Rochette-Egly, Nuclear receptors: integration of multiple signalling pathways through phosphorylation, Cell Signal 15 (2003) 355-366.

[48] D.A. Lannigan, Estrogen receptor phosphorylation, Steroids 68 (2003) 1-9.

[49] T. Shen, K.B. Horwitz, C.A. Lange, Transcriptional hyperactivity of human progesterone receptors is coupled to their ligand-dependent down-regulation by mitogen-activated protein kinase-dependent phosphorylation of serine 294, Mol. Cell. Biol. 21 (2001) 6122-6131.

[50] S. Hauser, G. Adelmant, P. Sarraf, H.M. Wright, E. Mueller, B.M. Spiegelman, Degradation of the peroxisome proliferator-activated receptor gamma is linked to ligand-dependent activation, J. Biol. Chem. 275 (2000) 18527-18533.

[51] N. Bruck, J. Bastien, G. Bour, A. Tarrade, J.L. Plassat, A. Bauer, S. Adam-Stitah, C. Rochette-Egly, Phosphorylation of the retinoid x receptor at the omega loop, modulates the expression of retinoic-acid-target genes with a promoter context specificity, Cell Signal. 17 (2005) 1229-1239.

[52] V. Perissi, A. Aggarwal, C.K. Glass, D.W. Rose, M.G. Rosenfeld, A corepressor/coactivator exchange complex required for transcriptional activation by nuclear receptors and other regulated transcription factors, Cell 116 (2004) 511-526.

[53] S.H. Yang, A.D. Sharrocks, A.J. Whitmarsh, Transcriptional regulation by the MAP kinase signaling cascades, Gene 320 (2003) 3-21.

[54] C.A. Hazzalin, L.C. Mahadevan, MAPK-regulated transcription: a continuously variable gene switch?, Nat. Rev. Mol. Cell. Biol. 3 (2002) 30-40.

[55] C. Rochette-Egly, S. Adam, M. Rossignol, J.M. Egly, P. Chambon, Stimulation of RAR alpha activation function AF-1 through binding to the general transcription factor TFIIH and phosphorylation by CDK7, Cell 90 (1997) 97-107.

[56] M.H. Delmotte, A. Tahayato, P. Formstecher, P. Lefebvre, Serine 157, a retinoic acid receptor alpha residue phosphorylated by protein kinase C in vitro, is involved in RXR.RARalpha heterodimerization and transcriptional activity, J. Biol. Chem. 274 (1999) 38225-38231.

[57] C. Rochette-Egly, M. Oulad-Abdelghani, A. Staub, V. Pfister, I. Scheuer, P. Chambon, M.P. Gaub, Phosphorylation of the retinoic acid receptor-alpha by protein kinase A, Mol. Endocrinol. 9 (1995) 860-871.

[58] J. Bastien, S. Adam-Stitah, T. Riedl, J.M. Egly, P. Chambon, C. Rochette-Egly, TFIIH interacts with the retinoic acid receptor gamma and phosphorylates its AF-1-activating domain through cdk7, J. Biol. Chem. 275 (2000) 21896-21904.

[59] R. Taneja, C. Rochette-Egly, J.L. Plassat, L. Penna, M.P. Gaub, P. Chambon, Phosphorylation of activation functions AF-1 and AF-2 of RAR alpha and RAR gamma is indispensable for differentiation of F9 cells upon retinoic acid and cAMP treatment, EMBO J. 16 (1997) 6452-6465.

[60] J.C. Hsieh, P.W. Jurutka, S. Nakajima, M.A. Galligan, C.A. Haussler, Y. Shimizu, N. Shimizu, G.K. Whitfield, M.R. Haussler, Phosphorylation of the human vitamin D receptor by protein kinase C. Biochemical and functional evaluation of the serine 51 recognition site, J. Biol. Chem. 268 (1993) 15118-15126.

[61] J.C. Hsieh, H.T. Dang, M.A. Galligan, G.K. Whitfield, C.A. Haussler, P.W. Jurutka, M.R. Haussler, Phosphorylation of human vitamin D receptor serine-182 by PKA

suppresses 1,25(OH)2D3-dependent transactivation, Biochem. Biophys. Res. Commun. 324 (2004) 801-809.

[62] P.W. Jurutka, J.C. Hsieh, S. Nakajima, C.A. Haussler, G.K. Whitfield, M.R. Haussler, Human vitamin D receptor phosphorylation by casein kinase II at Ser-208 potentiates transcriptional activation, Proc. Natl. Acad. Sci. U S A 93 (1996) 3519-3524.

[63] P.M. Barger, A.C. Browning, A.N. Garner, D.P. Kelly, p38 mitogen-activated protein kinase activates peroxisome proliferator-activated receptor alpha: a potential role in the cardiac metabolic stress response, J. Biol. Chem. 276 (2001) 44495-44501.

[64] J.P. Gray, K.A. Burns, T.L. Leas, G.H. Perdew, J.P. Vanden Heuvel, Regulation of peroxisome proliferator-activated receptor alpha by protein kinase C, Biochemistry 44 (2005) 10313-10321.

[65] E. Hu, J.B. Kim, P. Sarraf, B.M. Spiegelman, Inhibition of adipogenesis through MAP kinase-mediated phosphorylation of PPARgamma, Science 274 (1996) 2100-2103.

[66] M. Adams, M.J. Reginato, D. Shao, M.A. Lazar, V.K. Chatterjee, Transcriptional activation by peroxisome proliferator-activated receptor gamma is inhibited by phosphorylation at a consensus mitogen-activated protein kinase site, J. Biol. Chem. 272 (1997) 5128-5132.

[67] L. Yin, J. Wang, P.S. Klein, M.A. Lazar, Nuclear receptor Rev-erbalpha is a critical lithium-sensitive component of the circadian clock, Science 311 (2006) 1002-1005.

[68] S. Adam-Stitah, L. Penna, P. Chambon, C. Rochette-Egly, Hyperphosphorylation of the retinoid X receptor alpha by activated c-Jun NH2-terminal kinases, J. Biol. Chem. 274 (1999) 18932-18941.

[69] H.Y. Lee, Y.A. Suh, M.J. Robinson, J.L. Clifford, W.K. Hong, J.R. Woodgett, M.H. Cobb, D.J. Mangelsdorf, J.M. Kurie, Stress pathway activation induces phosphorylation of retinoid X receptor, J. Biol. Chem. 275 (2000) 32193-32199.

[70] M.D. Krstic, I. Rogatsky, K.R. Yamamoto, M.J. Garabedian, Mitogen-activated and cyclin-dependent protein kinases selectively and differentially modulate transcriptional enhancement by the glucocorticoid receptor, Mol. Cell. Biol. 17 (1997) 3947-3954.

[71] I. Rogatsky, S.K. Logan, M.J. Garabedian, Antagonism of glucocorticoid receptor transcriptional activation by the c-Jun N-terminal kinase, Proc. Natl. Acad. Sci. U S A 95 (1998) 2050-2055.

[72] S. Chen, Y. Xu, X. Yuan, G.J. Bubley, S.P. Balk, Androgen receptor phosphorylation and stabilization in prostate cancer by cyclin-dependent kinase 1, Proc. Natl. Acad. Sci. U S A 103 (2006) 15969-15974.

[73] Z. Zhu, R.R. Becklin, D.M. Desiderio, J.T. Dalton, Identification of a novel phosphorylation site in human androgen receptor by mass spectrometry, Biochem. Biophys. Res. Commun. 284 (2001) 836-844.

[74] H.K. Lin, S. Yeh, H.Y. Kang, C. Chang, Akt suppresses androgen-induced apoptosis by phosphorylating and inhibiting androgen receptor, Proc. Natl. Acad. Sci. U S A 98 (2001) 7200-7205.

[75] D. Gioeli, B.E. Black, V. Gordon, A. Spencer, C.T. Kesler, S.T. Eblen, B.M. Paschal, M.J. Weber, Stress kinase signaling regulates androgen receptor phosphorylation, transcription, and localization, Mol. Endocrinol. 20 (2006) 503-515.

[76] T.A. Knotts, R.S. Orkiszewski, R.G. Cook, D.P. Edwards, N.L. Weigel, Identification of a phosphorylation site in the hinge region of the human progesterone receptor and additional amino-terminal phosphorylation sites, J. Biol. Chem. 276 (2001) 8475-8483.

[77] Y. Zhang, C.A. Beck, A. Poletti, J.P.t. Clement, P. Prendergast, T.T. Yip, T.W. Hutchens, D.P. Edwards, N.L. Weigel, Phosphorylation of human progesterone receptor by cyclin-dependent kinase 2 on three sites that are authentic basal phosphorylation sites in vivo, Mol. Endocrinol. 11 (1997) 823-832.

[78] M. Qiu, A. Olsen, E. Faivre, K.B. Horwitz, C.A. Lange, Mitogen-activated protein kinase regulates nuclear association of human progesterone receptors, Mol. Endocrinol. 17 (2003) 628-642.

[79] I. Rogatsky, J.M. Trowbridge, M.J. Garabedian, Potentiation of human estrogen receptor alpha transcriptional activation through phosphorylation of serines 104 and 106 by the cyclin A-CDK2 complex, J. Biol. Chem. 274 (1999) 22296-22302.

[80] S. Kato, T. Kitamoto, Y. Masuhiro, J. Yanagisawa, Molecular mechanism of a cross-talk between estrogen and growth-factor signaling pathways, Oncology 55 (1998) 5-10.

[81] S.F. Arnold, J.D. Obourn, H. Jaffe, A.C. Notides, Phosphorylation of the human estrogen receptor by mitogen-activated protein kinase and casein kinase II: consequence on DNA binding, J Steroid Biochem Mol Biol 55 (1995) 163-172.

[82] D. Chen, P.E. Pace, R.C. Coombes, S. Ali, Phosphorylation of human estrogen receptor alpha by protein kinase A regulates dimerization, Mol. Cell. Biol. 19 (1999) 1002-1015.

[83] S.F. Arnold, J.D. Obourn, H. Jaffe, A.C. Notides, Phosphorylation of the human estrogen receptor on tyrosine 537 in vivo and by src family tyrosine kinases in vitro, Mol. Endocrinol. 9 (1995) 24-33.

[84] M. Becker-Andre, E. Andre, J.F. DeLamarter, Identification of nuclear receptor mRNAs by RT-PCR amplification of conserved zinc-finger motif sequences, Biochem. Biophys. Res. Commun. 194 (1993) 1371-1379.

[85] C. Chauvet, B. Bois-Joyeux, J.L. Danan, Retinoic acid receptor-related orphan receptor (ROR) alpha4 is the predominant isoform of the nuclear receptor RORalpha in the liver and is up-regulated by hypoxia in HepG2 human hepatoma cells, Biochem. J. 364 (2002) 449-456.

[86] S. Besnard, C. Heymes, R. Merval, M. Rodriguez, J.P. Galizzi, J.A. Boutin, J. Mariani, A. Tedgui, Expression and regulation of the nuclear receptor RORalpha in human vascular cells, FEBS Lett. 511 (2002) 36-40.

[87] V. Giguere, M. Tini, G. Flock, E. Ong, R.M. Evans, G. Otulakowski, Isoform-specific amino-terminal domains dictate DNA-binding properties of ROR alpha, a novel family of orphan hormone nuclear receptors, Genes Dev. 8 (1994) 538-553.

[88] F. Boukhtouche, J. Mariani, A. Tedgui, The "CholesteROR" protective pathway in the vascular system, Arterioscler. Thromb. Vasc. Biol. 24 (2004) 637-643.

[89] P. Lau, P. Bailey, D.H. Dowhan, G.E. Muscat, Exogenous expression of a dominant negative RORalpha1 vector in muscle cells impairs differentiation: RORalpha1 directly interacts with p300 and myoD, Nucleic Acids Res. 27 (1999) 411-420.

[90] H.P. Harding, G.B. Atkins, A.B. Jaffe, W.J. Seo, M.A. Lazar, Transcriptional activation and repression by RORalpha, an orphan nuclear receptor required for cerebellar development, Mol. Endocrinol. 11 (1997) 1737-1746.

[91] A.N. Moraitis, V. Giguere, C.C. Thompson, Novel mechanism of nuclear receptor corepressor interaction dictated by activation function 2 helix determinants, Mol. Cell. Biol. 22 (2002) 6831-6841.

[92] R. Retnakaran, G. Flock, V. Giguere, Identification of RVR, a novel orphan nuclear receptor that acts as a negative transcriptional regulator, Mol. Endocrinol. 8 (1994) 1234-1244.

[93] V. Giguere, L.D. McBroom, G. Flock, Determinants of target gene specificity for ROR alpha 1: monomeric DNA binding by an orphan nuclear receptor, Mol. Cell. Biol. 15 (1995) 2517-2526.

[94] E. Raspe, H. Duez, P. Gervois, C. Fievet, J.C. Fruchart, S. Besnard, J. Mariani, A. Tedgui, B. Staels, Transcriptional regulation of apolipoprotein C-III gene expression by the orphan nuclear receptor RORalpha, J. Biol. Chem. 276 (2001) 2865-2871.

[95] B. Bois-Joyeux, C. Chauvet, H. Nacer-Cherif, W. Bergeret, N. Mazure, V. Giguere, V. Laudet, J.L. Danan, Modulation of the far-upstream enhancer of the rat alpha-fetoprotein gene by members of the ROR alpha, Rev-erb alpha, and Rev-erb beta groups of monomeric orphan nuclear receptors, DNA Cell Biol 19 (2000) 589-599.

[96] P. Delerive, D. Monte, G. Dubois, F. Trottein, J. Fruchart-Najib, J. Mariani, J.C. Fruchart, B. Staels, The orphan nuclear receptor ROR alpha is a negative regulator of the inflammatory response, EMBO Rep. 2 (2001) 42-48.

[97] H. Migita, J. Morser, K. Kawai, Rev-erbalpha upregulates NF-kappaB-responsive genes in vascular smooth muscle cells, FEBS Lett. 561 (2004) 69-74.

[98] T.K. Sato, S. Panda, L.J. Miraglia, T.M. Reyes, R.D. Rudic, P. McNamara, K.A. Naik, G.A. FitzGerald, S.A. Kay, J.B. Hogenesch, A functional genomics strategy reveals ROR alpha as a component of the mammalian circadian clock., Neuron 43 (2004) 527-537.

[99] M. Downes, A.J. Carozzi, G.E. Muscat, Constitutive expression of the orphan receptor, Rev-erbA alpha, inhibits muscle differentiation and abrogates the expression of the myoD gene family, Mol. Endocrinol. 9 (1995) 1666-1678.

[100] E. Raspe, G. Mautino, C. Duval, C. Fontaine, H. Duez, O. Barbier, D. Monte, J. Fruchart, J.C. Fruchart, B. Staels, Transcriptional regulation of human Rev-erbalpha gene expression by the orphan nuclear receptor retinoic acid-related orphan receptor alpha, J. Biol. Chem. 277 (2002) 49275-49281.

[101] P. Delerive, W.W. Chin, C.S. Suen, Identification of Reverb(alpha) as a novel ROR(alpha) target gene, J. Biol. Chem. 277 (2002) 35013-35018.

[102] G. Adelmant, A. Begue, D. Stehelin, V. Laudet, A functional Rev-erb alpha responsive element located in the human Rev-erb alpha promoter mediates a repressing activity, Proc. Natl. Acad. Sci. U S A 93 (1996) 3553-3558.

[103] M. Becker-Andre, I. Wiesenberg, N. Schaeren-Wiemers, E. Andre, M. Missbach, J.H. Saurat, C. Carlberg, Pineal gland hormone melatonin binds and activates an orphan of the nuclear receptor superfamily, J. Biol. Chem. 269 (1994) 28531-28534.

[104] I. Wiesenberg, M. Missbach, J.P. Kahlen, M. Schrader, C. Carlberg, Transcriptional activation of the nuclear receptor RZR alpha by the pineal gland hormone melatonin and identification of CGP 52608 as a synthetic ligand, Nucleic Acids Res. 23 (1995) 327-333.

[105] M. Missbach, B. Jagher, I. Sigg, S. Nayeri, C. Carlberg, I. Wiesenberg, Thiazolidine diones, specific ligands of the nuclear receptor retinoid Z receptor/retinoid acid receptor-related orphan receptor alpha with potent antiarthritic activity, J. Biol. Chem. 271 (1996) 13515-13522.

[106] D. Steinhilber, M. Brungs, O. Werz, I. Wiesenberg, C. Danielsson, J.P. Kahlen, S. Nayeri, M. Schrader, C. Carlberg, The nuclear receptor for melatonin represses 5-lipoxygenase gene expression in human B lymphocytes, J. Biol. Chem. 270 (1995) 7037-7040.

[107] J.M. Harris, P. Lau, S.L. Chen, G.E. Muscat, Characterization of the retinoid orphan-related receptor-alpha coactivator binding interface: a structural basis for ligand-independent transcription, Mol. Endocrinol. 16 (2002) 998-1012.

[108] R.L. Sidman, P.W. Lane, M.M. Dickie, Staggerer, a new mutation in the mouse affecting the cerebellum, Science 137 (1962) 610-612.

[109] N. Hadj-Sahraoui, F. Frederic, H. Zanjani, N. Delhaye-Bouchaud, K. Herrup, J. Mariani, Progressive atrophy of cerebellar Purkinje cell dendrites during aging of the heterozygous staggerer mouse (Rora(+/sg)), Brain Res. Dev. Brain Res. 126 (2001) 201-209.

[110] F. Boukhtouche, M. Doulazmi, F. Frederic, I. Dusart, B. Brugg, J. Mariani, RORalpha, a pivotal nuclear receptor for Purkinje neuron survival and differentiation: from development to ageing, Cerebellum 5 (2006) 97-104.

[111] F. Boukhtouche, S. Janmaat, G. Vodjdani, V. Gautheron, J. Mallet, I. Dusart, J. Mariani, Retinoid-related orphan receptor alpha controls the early steps of Purkinje cell dendritic differentiation, J. Neurosci. 26 (2006) 1531-1538.

[112] F. Boukhtouche, G. Vodjdani, C.I. Jarvis, J. Bakouche, B. Staels, J. Mallet, J. Mariani, Y. Lemaigre-Dubreuil, B. Brugg, Human retinoic acid receptor-related orphan receptor alpha1 overexpression protects neurones against oxidative stress-induced apoptosis, J Neurochem 96 (2006) 1778-1789.

[113] M. Doulazmi, F. Frederic, F. Capone, M. Becker-Andre, N. Delhaye-Bouchaud, J. Mariani, A comparative study of Purkinje cells in two RORalpha gene mutant mice: staggerer and RORalpha(-/-), Brain Res. Dev. Brain Res. 127 (2001) 165-174.

[114] T. Matsui, Transcriptional regulation of a Purkinje cell-specific gene through a functional interaction between ROR alpha and RAR, Genes Cells 2 (1997) 263-272.

[115] B.A. Hamilton, W.N. Frankel, A.W. Kerrebrock, T.L. Hawkins, W. FitzHugh, K. Kusumi, L.B. Russell, K.L. Mueller, V. van Berkel, B.W. Birren, L. Kruglyak, E.S. Lander, Disruption of the nuclear hormone receptor RORalpha in staggerer mice, Nature 379 (1996) 736-739.

[116] T. Meyer, M. Kneissel, J. Mariani, B. Fournier, In vitro and in vivo evidence for orphan nuclear receptor RORalpha function in bone metabolism, Proc. Natl. Acad. Sci. U S A 97 (2000) 9197-9202.

[117] A. Mamontova, S. Seguret-Mace, B. Esposito, C. Chaniale, M. Bouly, N. Delhaye-Bouchaud, G. Luc, B. Staels, N. Duverger, J. Mariani, A. Tedgui, Severe atherosclerosis and hypoalphalipoproteinemia in the staggerer mouse, a mutant of the nuclear receptor RORalpha, Circulation 98 (1998) 2738-2743.

[118] N. Vu-Dac, P. Gervois, T. Grotzinger, P. De Vos, K. Schoonjans, J.C. Fruchart, J. Auwerx, J. Mariani, A. Tedgui, B. Staels, Transcriptional regulation of apolipoprotein A-I gene expression by the nuclear receptor RORalpha, J. Biol. Chem. 272 (1997) 22401-22404.

[119] F. Bitsch, R. Aichholz, J. Kallen, S. Geisse, B. Fournier, J.M. Schlaeppi, Identification of natural ligands of retinoic acid receptor-related orphan receptor alpha ligand-binding domain expressed in Sf9 cells--a mass spectrometry approach, Anal. Biochem. 323 (2003) 139-149.

[120] J. Kallen, J.M. Schlaeppi, F. Bitsch, I. Delhon, B. Fournier, Crystal structure of the human RORalpha ligand binding domain in complex with cholesterol sulfate at 2.2 A, J. Biol. Chem. 279 (2004) 14033-14038. Epub 12004 Jan 14013.

[121] J.A. Kallen, J.M. Schlaeppi, F. Bitsch, S. Geisse, M. Geiser, I. Delhon, B. Fournier, X-ray structure of the hRORalpha LBD at 1.63 A: structural and functional data that cholesterol or a cholesterol derivative is the natural ligand of RORalpha, Structure (Camb) 10 (2002) 1697-1707.

[122] E. Trenkner, M.K. Hoffmann, Defective development of the thymus and immunological abnormalities in the neurological mouse mutation "staggerer", J. Neurosci. 6 (1986) 1733-1737.

[123] B. Kopmels, J. Mariani, N. Delhaye-Bouchaud, F. Audibert, D. Fradelizi, E.E. Wollman, Evidence for a hyperexcitability state of staggerer mutant mice macrophages, J Neurochem 58 (1992) 192-199.

[124] S.J. Tapscott, H. Weintraub, MyoD and the regulation of myogenesis by helix-loop-helix proteins, J Clin Invest 87 (1991) 1133-1138.

[125] H. Weintraub, V.J. Dwarki, I. Verma, R. Davis, S. Hollenberg, L. Snider, A. Lassar, S.J. Tapscott, Muscle-specific transcriptional activation by MyoD, Genes Dev. 5 (1991) 1377-1386.

[126] S. Besnard, J. Bakouche, Y. Lemaigre-Dubreuil, J. Mariani, A. Tedgui, D. Henrion, Smooth muscle dysfunction in resistance arteries of the staggerer mouse, a mutant of the nuclear receptor RORalpha, Circ. Res. 90 (2002) 820-825.

[127] M. Akashi, T. Takumi, The orphan nuclear receptor RORalpha regulates circadian transcription of the mammalian core-clock Bmal1, Nat. Struc. Mol. Biol. 12 (2005) 441-448.

[128] M.H. Hastings, A.B. Reddy, E.S. Maywood, A clockwork web: circadian timing in brain and periphery, in health and disease, Nat. Rev. Neurosci. 4 (2003) 649-661.

[129] M. Akashi, E. Nishida, Involvement of the MAP kinase cascade in resetting of the mammalian circadian clock, Genes Dev. 14 (2000) 645-649.

[130] A. Balsalobre, F. Damiola, U. Schibler, A serum shock induces circadian gene expression in mammalian tissue culture cells, Cell 93 (1998) 929-937.

[131] F. Delaunay, V. Laudet, Circadian clock and microarrays: mammalian genome gets rhythm, Trends Genet. 18 (2002) 595-597.

[132] B.M. Forman, J. Chen, B. Blumberg, S.A. Kliewer, R. Henshaw, E.S. Ong, R.M. Evans, Cross-talk among ROR alpha 1 and the Rev-erb family of orphan nuclear receptors, Mol. Endocrinol. 8 (1994) 1253-1261.

[133] W. Yu, M. Nomura, M. Ikeda, Interactivating feedback loops within the mammalian clock: BMAL1 is negatively autoregulated and upregulated by CRY1, CRY2, and PER2, Biochem. Biophys. Res. Commun. 290 (2002) 933-941.

[134] L.P. Shearman, S. Sriram, D.R. Weaver, E.S. Maywood, I. Chaves, B. Zheng, K. Kume, C.C. Lee, G.T. van der Horst, M.H. Hastings, S.M. Reppert, Interacting molecular loops in the mammalian circadian clock, Science 288 (2000) 1013-1019.

[135] H.R. Ueda, S. Hayashi, W. Chen, M. Sano, M. Machida, Y. Shigeyoshi, M. Iino, S. Hashimoto, System-level identification of transcriptional circuits underlying mammalian circadian clocks, Nat. Genet. 37 (2005) 187-192.

[136] D.P. King, Y. Zhao, A.M. Sangoram, L.D. Wilsbacher, M. Tanaka, M.P. Antoch, T.D. Steeves, M.H. Vitaterna, J.M. Kornhauser, P.L. Lowrey, F.W. Turek, J.S. Takahashi, Positional cloning of the mouse circadian clock gene, Cell 89 (1997) 641-653.

[137] M.K. Bunger, L.D. Wilsbacher, S.M. Moran, C. Clendenin, L.A. Radcliffe, J.B. Hogenesch, M.C. Simon, J.S. Takahashi, C.A. Bradfield, Mop3 is an essential component of the master circadian pacemaker in mammals, Cell 103 (2000) 1009-1017.

[138] K. Bae, X. Jin, E.S. Maywood, M.H. Hastings, S.M. Reppert, D.R. Weaver, Differential functions of mPer1, mPer2, and mPer3 in the SCN circadian clock, Neuron 30 (2001) 525-536.

[139] G.T. van der Horst, M. Muijtjens, K. Kobayashi, R. Takano, S. Kanno, M. Takao, J. de Wit, A. Verkerk, A.P. Eker, D. van Leenen, R. Buijs, D. Bootsma, J.H. Hoeijmakers, A. Yasui, Mammalian Cry1 and Cry2 are essential for maintenance of circadian rhythms, Nature 398 (1999) 627-630.

[140] B. Zheng, U. Albrecht, K. Kaasik, M. Sage, W. Lu, S. Vaishnav, Q. Li, Z.S. Sun, G. Eichele, A. Bradley, C.C. Lee, Nonredundant roles of the mPer1 and mPer2 genes in the mammalian circadian clock, Cell 105 (2001) 683-694.

[141] S. Honma, T. Kawamoto, Y. Takagi, K. Fujimoto, F. Sato, M. Noshiro, Y. Kato, K. Honma, Dec1 and Dec2 are regulators of the mammalian molecular clock, Nature 419 (2002) 841-844.

[142] M.J. Zylka, L.P. Shearman, D.R. Weaver, S.M. Reppert, Three period homologs in mammals: differential light responses in the suprachiasmatic circadian clock and oscillating transcripts outside of brain, Neuron 20 (1998) 1103-1110.

[143] M. Reick, J.A. Garcia, C. Dudley, S.L. McKnight, NPAS2: an analog of clock operative in the mammalian forebrain, Science 293 (2001) 506-509.

[144] S. Mitsui, S. Yamaguchi, T. Matsuo, Y. Ishida, H. Okamura, Antagonistic role of E4BP4 and PAR proteins in the circadian oscillatory mechanism, Genes Dev. 15 (2001) 995-1006.

[145] J. Wuarin, U. Schibler, Expression of the liver-enriched transcriptional activator protein DBP follows a stringent circadian rhythm, Cell 63 (1990) 1257-1266.

[146] N. Preitner, F. Damiola, L. Lopez-Molina, J. Zakany, D. Duboule, U. Albrecht, U. Schibler, The orphan nuclear receptor REV-ERBalpha controls circadian transcription within the positive limb of the mammalian circadian oscillator, Cell 110 (2002) 251-260.

[147] H.R. Ueda, W. Chen, A. Adachi, H. Wakamatsu, S. Hayashi, T. Takasugi, M. Nagano, K. Nakahama, Y. Suzuki, S. Sugano, M. Iino, Y. Shigeyoshi, S. Hashimoto, A

transcription factor response element for gene expression during circadian night, Nature 418 (2002) 534-539.

[148] T. Hirota, Y. Fukada, Resetting mechanism of central and peripheral circadian clocks in mammals, Zoolog Sci 21 (2004) 359-368.

[149] J.P. Etchegaray, C. Lee, P.A. Wade, S.M. Reppert, Rhythmic histone acetylation underlies transcription in the mammalian circadian clock, Nature 421 (2003) 177-182.

[150] E. Harms, S. Kivimae, M.W. Young, L. Saez, Posttranscriptional and posttranslational regulation of clock genes, J. Biol. Rhythms 19 (2004) 361-373.

[151] V.J. Poirel, C. Cailotto, D. Streicher, P. Pevet, M. Masson-Pevet, F. Gauer, MT1 melatonin receptor mRNA tissular localization by PCR amplification, Neuro Endocrinol Lett 24 (2003) 33-38.

[152] J. Arendt, D.J. Skene, Melatonin as a chronobiotic, Sleep Med Rev 9 (2005) 25-39.

[153] P. Pevet, L. Agez, B. Bothorel, M. Saboureau, F. Gauer, V. Laurent, M. Masson-Pevet, Melatonin in the multi-oscillatory mammalian circadian world, Chronobiol Int 23 (2006) 39-51.

[154] J. Redman, S. Armstrong, K.T. Ng, Free-running activity rhythms in the rat: entrainment by melatonin, Science 219 (1983) 1089-1091.

[155] C. von Gall, D.R. Weaver, J. Moek, A. Jilg, J.H. Stehle, H.W. Korf, Melatonin plays a crucial role in the regulation of rhythmic clock gene expression in the mouse pars tuberalis, Ann N Y Acad Sci 1040 (2005) 508-511.

[156] L. Agez, V. Laurent, P. Pevet, M. Masson-Pevet, F. Gauer, Melatonin affects nuclear orphan receptors mRNA in the rat suprachiasmatic nuclei, Neuroscience 144 (2007) 522-530.

[157] S. Kojima, M. Hirose, K. Tokunaga, Y. Sakaki, H. Tei, Structural and functional analysis of 3' untranslated region of mouse Period1 mRNA, Biochem. Biophys. Res. Commun. 301 (2003) 1-7.

[158] J.E. Baggs, C.B. Green, Nocturnin, a deadenylase in Xenopus laevis retina: a mechanism for posttranscriptional control of circadian-related mRNA, Curr Biol 13 (2003) 189-198.

[159] C. Lee, J.P. Etchegaray, F.R. Cagampang, A.S. Loudon, S.M. Reppert, Posttranslational mechanisms regulate the mammalian circadian clock, Cell 107 (2001) 855-867.

[160] C. Crosio, N. Cermakian, C.D. Allis, P. Sassone-Corsi, Light induces chromatin modification in cells of the mammalian circadian clock, Nat Neurosci 3 (2000) 1241-1247.

[161] Y. Naruse, K. Oh-hashi, N. Iijima, M. Naruse, H. Yoshioka, M. Tanaka, Circadian and light-induced transcription of clock gene Per1 depends on histone acetylation and deacetylation, Mol. Cell. Biol. 24 (2004) 6278-6287.

[162] K. Yagita, F. Tamanini, M. Yasuda, J.H. Hoeijmakers, G.T. van der Horst, H. Okamura, Nucleocytoplasmic shuttling and mCRY-dependent inhibition of ubiquitylation of the mPER2 clock protein, EMBO J. 21 (2002) 1301-1314.

[163] M. Akashi, Y. Tsuchiya, T. Yoshino, E. Nishida, Control of intracellular dynamics of mammalian period proteins by casein kinase I epsilon (CKIepsilon) and CKIdelta in cultured cells, Mol. Cell. Biol. 22 (2002) 1693-1703.

[164] R.V. Kondratov, M.V. Chernov, A.A. Kondratova, V.Y. Gorbacheva, A.V. Gudkov, M.P. Antoch, BMAL1-dependent circadian oscillation of nuclear CLOCK: posttranslational events induced by dimerization of transcriptional activators of the mammalian clock system, Genes Dev. 17 (2003) 1921-1932.

[165] P.L. Lowrey, K. Shimomura, M.P. Antoch, S. Yamazaki, P.D. Zemenides, M.R. Ralph, M. Menaker, J.S. Takahashi, Positional syntenic cloning and functional characterization of the mammalian circadian mutation tau, Science 288 (2000) 483-492.

[166] K.L. Toh, C.R. Jones, Y. He, E.J. Eide, W.A. Hinz, D.M. Virshup, L.J. Ptacek, Y.H. Fu, An hPer2 phosphorylation site mutation in familial advanced sleep phase syndrome, Science 291 (2001) 1040-1043.

[167] E. Vielhaber, E. Eide, A. Rivers, Z.H. Gao, D.M. Virshup, Nuclear entry of the circadian regulator mPER1 is controlled by mammalian casein kinase I epsilon, Mol. Cell. Biol. 20 (2000) 4888-4899.

[168] A. Takano, Y. Isojima, K. Nagai, Identification of mPer1 phosphorylation sites responsible for the nuclear entry, J. Biol. Chem. 279 (2004) 32578-32585.

[169] E.J. Eide, M.F. Woolf, H. Kang, P. Woolf, W. Hurst, F. Camacho, E.L. Vielhaber, A. Giovanni, D.M. Virshup, E. Vielhaber, E. Eide, A. Rivers, Z.H. Gao, Control of mammalian circadian rhythm by CKIepsilon-regulated proteasome-mediated PER2 degradation, Mol. Cell. Biol. 25 (2005) 2795-2807.

[170] C. Lee, D.R. Weaver, S.M. Reppert, Direct association between mouse PERIOD and CKIepsilon is critical for a functioning circadian clock, Mol. Cell. Biol. 24 (2004) 584-594.

[171] M.H. Vitaterna, C.P. Selby, T. Todo, H. Niwa, C. Thompson, E.M. Fruechte, K. Hitomi, R.J. Thresher, T. Ishikawa, J. Miyazaki, J.S. Takahashi, A. Sancar, Differential regulation of mammalian period genes and circadian rhythmicity by cryptochromes 1 and 2, Proc. Natl. Acad. Sci. U S A 96 (1999) 12114-12119.

[172] K. Kume, M.J. Zylka, S. Sriram, L.P. Shearman, D.R. Weaver, X. Jin, E.S. Maywood, M.H. Hastings, S.M. Reppert, mCRY1 and mCRY2 are essential components of the negative limb of the circadian clock feedback loop, Cell 98 (1999) 193-205.

[173] E.A. Griffin, Jr., D. Staknis, C.J. Weitz, Light-independent role of CRY1 and CRY2 in the mammalian circadian clock, Science 286 (1999) 768-771.

[174] E.J. Eide, E.L. Vielhaber, W.A. Hinz, D.M. Virshup, The circadian regulatory proteins BMAL1 and cryptochromes are substrates of casein kinase Iepsilon, J. Biol. Chem. 277 (2002) 17248-17254.

[175] K. Sanada, Y. Harada, M. Sakai, T. Todo, Y. Fukada, Serine phosphorylation of mCRY1 and mCRY2 by mitogen-activated protein kinase, Genes Cells 9 (2004) 697-708.

[176] Y. Harada, M. Sakai, N. Kurabayashi, T. Hirota, Y. Fukada, Ser-557-phosphorylated mCRY2 is degraded upon synergistic phosphorylation by glycogen synthase kinase-3 beta, J. Biol. Chem. 280 (2005) 31714-31721.

[177] E. Iwahana, M. Akiyama, K. Miyakawa, A. Uchida, J. Kasahara, K. Fukunaga, T. Hamada, S. Shibata, Effect of lithium on the circadian rhythms of locomotor activity and glycogen synthase kinase-3 protein expression in the mouse suprachiasmatic nuclei, Eur. J. Neurosci. 19 (2004) 2281-2287.

[178] T. Tamaru, Y. Isojima, G.T. van der Horst, K. Takei, K. Nagai, K. Takamatsu, Nucleocytoplasmic shuttling and phosphorylation of BMAL1 are regulated by circadian clock in cultured fibroblasts, Genes Cells 8 (2003) 973-983.

[179] J. Hirayama, I. Fukuda, T. Ishikawa, Y. Kobayashi, T. Todo, New role of zCRY and zPER2 as regulators of sub-cellular distributions of zCLOCK and zBMAL proteins, Nucleic Acids Res. 31 (2003) 935-943.

[180] K. Sanada, T. Okano, Y. Fukada, Mitogen-activated protein kinase phosphorylates and negatively regulates basic helix-loop-helix-PAS transcription factor BMAL1, J. Biol. Chem. 277 (2002) 267-271.

[181] L. Cardone, J. Hirayama, F. Giordano, T. Tamaru, J.J. Palvimo, P. Sassone-Corsi, Circadian clock control by SUMOylation of BMAL1, Science 309 (2005) 1390-1394.

[182] M.H. Cobb, E.J. Goldsmith, How MAP kinases are regulated, J. Biol. Chem. 270 (1995) 14843-14846.

[183] L. Chang, M. Karin, Mammalian MAP kinase signalling cascades, Nature 410 (2001) 37-40.

[184] M.H. Cobb, MAP kinase pathways, Prog Biophys Mol Biol 71 (1999) 479-500.

[185] R.J. Davis, The mitogen-activated protein kinase signal transduction pathway, J. Biol. Chem. 268 (1993) 14553-14556.

[186] J. Avruch, X.F. Zhang, J.M. Kyriakis, Raf meets Ras: completing the framework of a signal transduction pathway, Trends Biochem Sci 19 (1994) 279-283.

[187] C.F. Zheng, K.L. Guan, Activation of MEK family kinases requires phosphorylation of two conserved Ser/Thr residues, EMBO J. 13 (1994) 1123-1131.

[188] M. Yan, D.J. Templeton, Identification of 2 serine residues of MEK-1 that are differentially phosphorylated during activation by raf and MEK kinase, J. Biol. Chem. 269 (1994) 19067-19073.

[189] S.J. Mansour, W.T. Matten, A.S. Hermann, J.M. Candia, S. Rong, K. Fukasawa, G.F. Vande Woude, N.G. Ahn, Transformation of mammalian cells by constitutively active MAP kinase kinase, Science 265 (1994) 966-970.

[190] S. Cowley, H. Paterson, P. Kemp, C.J. Marshall, Activation of MAP kinase kinase is necessary and sufficient for PC12 differentiation and for transformation of NIH 3T3 cells, Cell 77 (1994) 841-852.

[191] D.M. Payne, A.J. Rossomando, P. Martino, A.K. Erickson, J.H. Her, J. Shabanowitz, D.F. Hunt, M.J. Weber, T.W. Sturgill, Identification of the regulatory phosphorylation sites in pp42/mitogen-activated protein kinase (MAP kinase), EMBO J. 10 (1991) 885-892.

[192] N.G. Anderson, J.L. Maller, N.K. Tonks, T.W. Sturgill, Requirement for integration of signals from two distinct phosphorylation pathways for activation of MAP kinase, Nature 343 (1990) 651-653.

[193] T.W. Sturgill, L.B. Ray, E. Erikson, J.L. Maller, Insulin-stimulated MAP-2 kinase phosphorylates and activates ribosomal protein S6 kinase II, Nature 334 (1988) 715-718.

[194] L.L. Lin, M. Wartmann, A.Y. Lin, J.L. Knopf, A. Seth, R.J. Davis, cPLA2 is phosphorylated and activated by MAP kinase, Cell 72 (1993) 269-278.

[195] K. Takishima, I. Griswold-Prenner, T. Ingebritsen, M.R. Rosner, Epidermal growth factor (EGF) receptor T669 peptide kinase from 3T3-L1 cells is an EGF-stimulated "MAP" kinase, Proc. Natl. Acad. Sci. U S A 88 (1991) 2520-2524.

[196] M. Cheng, T.G. Boulton, M.H. Cobb, ERK3 is a constitutively nuclear protein kinase, J. Biol. Chem. 271 (1996) 8951-8958.

[197] G. Zhou, Z.Q. Bao, J.E. Dixon, Components of a new human protein kinase signal transduction pathway, J. Biol. Chem. 270 (1995) 12665-12669.

[198] A.S. Zervos, L. Faccio, J.P. Gatto, J.M. Kyriakis, R. Brent, Mxi2, a mitogen-activated protein kinase that recognizes and phosphorylates Max protein, Proc. Natl. Acad. Sci. U S A 92 (1995) 10531-10534.

[199] C. Lechner, M.A. Zahalka, J.F. Giot, N.P. Moller, A. Ullrich, ERK6, a mitogen-activated protein kinase involved in C2C12 myoblast differentiation, Proc. Natl. Acad. Sci. U S A 93 (1996) 4355-4359.

[200] S. Mertens, M. Craxton, M. Goedert, SAP kinase-3, a new member of the family of mammalian stress-activated protein kinases, FEBS Lett. 383 (1996) 273-276.

[201] Y. Jiang, C. Chen, Z. Li, W. Guo, J.A. Gegner, S. Lin, J. Han, Characterization of the structure and function of a new mitogen-activated protein kinase (p38beta), J. Biol. Chem. 271 (1996) 17920-17926.

[202] H. Dziema, B. Oatis, G.Q. Butcher, R. Yates, K.R. Hoyt, K. Obrietan, The ERK/MAP kinase pathway couples light to immediate-early gene expression in the suprachiasmatic nucleus, Eur. J. Neurosci. 17 (2003) 1617-1627.

[203] K. Obrietan, S. Impey, D.R. Storm, Light and circadian rhythmicity regulate MAP kinase activation in the suprachiasmatic nuclei, Nat. Neurosci. 1 (1998) 693-700.

[204] G.Q. Butcher, B. Lee, K. Obrietan, Temporal regulation of light-induced extracellular signal-regulated kinase activation in the suprachiasmatic nucleus, J. Neurophysiol. 90 (2003) 3854-3863. Epub 2003 Aug 3820.

[205] A.N. Coogan, H.D. Piggins, Circadian and photic regulation of phosphorylation of ERK1/2 and Elk-1 in the suprachiasmatic nuclei of the Syrian hamster, J. Neurosci. 23 (2003) 3085-3093.

[206] A.N. Coogan, H.D. Piggins, MAP kinases in the mammalian circadian system--key regulators of clock function, J. Neurochem. 90 (2004) 769-775.

[207] M. Nakaya, K. Sanada, Y. Fukada, Spatial and temporal regulation of mitogen-activated protein kinase phosphorylation in the mouse suprachiasmatic nucleus, Biochem. Biophys. Res. Commun. 305 (2003) 494-501.

[208] G.A. Pizzio, E.C. Hainich, G.A. Ferreyra, O.A. Coso, D.A. Golombek, Circadian and photic regulation of ERK, JNK and p38 in the hamster SCN, Neuroreport 14 (2003) 1417-1419.

[209] H.S. Lee, J.L. Nelms, M. Nguyen, R. Silver, M.N. Lehman, The eye is necessary for a circadian rhythm in the suprachiasmatic nucleus, Nat Neurosci 6 (2003) 111-112.

[210] T. Hamada, J. LeSauter, J.M. Venuti, R. Silver, Expression of Period genes: rhythmic and nonrhythmic compartments of the suprachiasmatic nucleus pacemaker, J. Neurosci. 21 (2001) 7742-7750.

[211] D.A. Golombek, M.R. Ralph, KN-62, an inhibitor of Ca2+/calmodulin kinase II, attenuates circadian responses to light, Neuroreport 5 (1994) 1638-1640.

[212] S. Yokota, M. Yamamoto, T. Moriya, M. Akiyama, K. Fukunaga, E. Miyamoto, S. Shibata, Involvement of calcium-calmodulin protein kinase but not mitogen-activated protein kinase in light-induced phase delays and Per gene expression in the suprachiasmatic nucleus of the hamster, J Neurochem 77 (2001) 618-627.

[213] K. Nomura, Y. Takeuchi, S. Yamaguchi, H. Okamura, K. Fukunaga, Involvement of calcium/calmodulin-dependent protein kinase II in the induction of mPer1, J Neurosci Res 72 (2003) 384-392.

[214] H.J. Chen, M. Rojas-Soto, A. Oguni, M.B. Kennedy, A synaptic Ras-GTPase activating protein (p135 SynGAP) inhibited by CaM kinase II, Neuron 20 (1998) 895-904.

[215] Y. Hayashi, K. Sanada, Y. Fukada, Circadian and photic regulation of MAP kinase by Ras- and protein phosphatase-dependent pathways in the chick pineal gland, FEBS Lett. 491 (2001) 71-75.

[216] K. Shimizu, M. Okada, K. Nagai, Y. Fukada, Suprachiasmatic nucleus circadian oscillatory protein, a novel binding partner of K-Ras in the membrane rafts, negatively regulates MAPK pathway, J. Biol. Chem. 278 (2003) 14920-14925.

[217] J. Sambrook, D.W. Russel, Molecular cloning: A Laboratory Manual, 2nd Ed, Cold Spring Harbour Laboratory, Cold Spring Harbour, NY (2001).

[218] M.M. Bradford, A rapid and sensitive method for the quantitation of microgram quantities of protein utilizing the principle of protein-dye binding, Anal. Biochem. 72 (1976) 248-254.

[219] O. Werz, J. Klemm, B. Samuelsson, O. Rådmark, 5-lipoxygenase is phosphorylated by p38 kinase-dependent MAPKAP kinases, Proc. Natl. Acad. Sci. U S A 97 (2000) 5261-5266.

[220] K.M. Brand, C. Klein, I. Zundorf, T. Dingermann, W. Knoss, Generation and characterisation of monoclonal antibodies to oleanolic acid, Planta Med. 70 (2004) 986-992.

[221] D.T. Dudley, L. Pang, S.J. Decker, A.J. Bridges, A.R. Saltiel, A synthetic inhibitor of the mitogen-activated protein kinase cascade, Proc. Natl. Acad. Sci. U S A 92 (1995) 7686-7689.

[222] J.V. Duncia, J.B. Santella, 3rd, C.A. Higley, W.J. Pitts, J. Wityak, W.E. Frietze, F.W. Rankin, J.H. Sun, R.A. Earl, A.C. Tabaka, C.A. Teleha, K.F. Blom, M.F. Favata, E.J. Manos, A.J. Daulerio, D.A. Stradley, K. Horiuchi, R.A. Copeland, P.A. Scherle, J.M. Trzaskos, R.L. Magolda, G.L. Trainor, R.R. Wexler, F.W. Hobbs, R.E. Olson, MEK inhibitors: the chemistry and biological activity of U0126, its analogs, and cyclization products, Bioorg. Med. Chem. Lett. 8 (1998) 2839-2844.

[223] F. Guillaumond, H. Dardente, V. Giguere, N. Cermakian, Differential control of Bmal1 circadian transcription by REV-ERB and ROR nuclear receptors, J. Biol. Rhythms 20 (2005) 391-403.

[224] S.J. Mansour, J.M. Candia, J.E. Matsuura, M.C. Manning, N.G. Ahn, Interdependent domains controlling the enzymatic activity of mitogen-activated protein kinase kinase 1, Biochemistry 35 (1996) 15529-15536.

[225] I. Suzuma, K. Suzuma, K. Ueki, Y. Hata, E.P. Feener, G.L. King, L.P. Aiello, Stretch-induced retinal vascular endothelial growth factor expression is mediated by phosphatidylinositol 3-kinase and protein kinase C (PKC)-zeta but not by stretch-induced ERK1/2, Akt, Ras, or classical/novel PKC pathways, J. Biol. Chem. 277 (2002) 1047-1057.

[226] B.S. Li, Veeranna, J. Gu, P. Grant, H.C. Pant, Activation of mitogen-activated protein kinases (Erk1 and Erk2) cascade results in phosphorylation of NF-M tail domains in transfected NIH 3T3 cells, Eur J Biochem 262 (1999) 211-217.

[227] A. Aschrafi, N. Meindl, B. Firla, R.P. Brandes, D. Steinhilber, Intracellular localization of RORalpha is isoform and cell line-dependent, Biochim. Biophys. Acta 1763 (2006) 805-814.

[228] A.N. Moraitis, V. Giguere, The co-repressor hairless protects RORalpha orphan nuclear receptor from proteasome-mediated degradation, J. Biol. Chem. 278 (2003) 52511-52518. Epub 52003 Oct 52521.

[229] J.T. Moore, A. Uppal, F. Maley, G.F. Maley, Overcoming inclusion body formation in a high-level expression system, Protein Expr. Purif. 4 (1993) 160-163.

[230] K. Tsumoto, M. Umetsu, I. Kumagai, D. Ejima, J.S. Philo, T. Arakawa, Role of arginine in protein refolding, solubilization, and purification, Biotechnol Prog 20 (2004) 1301-1308.

[231] K. Tsumoto, D. Ejima, Y. Kita, T. Arakawa, Review: Why is arginine effective in suppressing aggregation?, Protein Pept Lett 12 (2005) 613-619.

[232] R. Rudolph, H. Lilie, In vitro folding of inclusion body proteins, FASEB J. 10 (1996) 49-56.

[233] S.E. Bondos, A. Bicknell, Detection and prevention of protein aggregation before, during, and after purification, Anal. Biochem. 316 (2003) 223-231.

[234] A.P. Golovanov, G.M. Hautbergue, S.A. Wilson, L.Y. Lian, A simple method for improving protein solubility and long-term stability, J. Am. Chem. Soc. 126 (2004) 8933-8939.

[235] K.L. Maxwell, D. Bona, C. Liu, C.H. Arrowsmith, A.M. Edwards, Refolding out of guanidine hydrochloride is an effective approach for high-throughput structural studies of small proteins, Protein Sci. 12 (2003) 2073-2080.

[236] A. Chauchereau, L. Amazit, M. Quesne, A. Guiochon-Mantel, E. Milgrom, Sumoylation of the progesterone receptor and of the steroid receptor coactivator SRC-1, J. Biol. Chem. 278 (2003) 12335-12343.

[237] Z.E. Floyd, J.M. Stephens, Control of peroxisome proliferator-activated receptor gamma2 stability and activity by SUMOylation, Obes Res 12 (2004) 921-928.

[238] M. Tojo, K. Matsuzaki, T. Minami, Y. Honda, H. Yasuda, T. Chiba, H. Saya, Y. Fujii-Kuriyama, M. Nakao, The aryl hydrocarbon receptor nuclear transporter is modulated by the SUMO-1 conjugation system, J. Biol. Chem. 277 (2002) 46576-46585.

10 APPENDIX

Antibody (developed in)	Purchased from	Working dilution	Buffer
anti-RORα (goat)	Santa Cruz	2 µg/ml	TBS+0.3% Tween 20+0.05% NaN_3
anti-RORα (mouse)	-	2 µg/ml	TBS+0.3% Tween 20+0.05% NaN_3
anti-RevErbα	US Biologicals	EMSA: pure	-
anti-RevErbα	Perseus Proteomics	WB: 1 µg/ml	TBS+0.3% Tween 20+0.05% NaN_3
anti-Bmal1 (rabbit, antiserum)	Abcam	1:100	PBS+0.05% NaN_3
anti-GFP (mouse, antiserum)	Sigma	1:2000	TBS+0.3% Tween 20+0.05% NaN_3
anti-MEK1	QED Bioscience	1 µg/ml	PBS+0.05% NaN_3
anti-ERK (rabbit)	New England Biolabs	1:1000	5% low-fat milk powder in PBS+0.3% Tween 20
anti-P-ERK (mouse)	New England Biolabs	1:1000	5% low-fat milk powder in PBS+0.3% Tween 20
anti-rabbit (goat, alkaline phosphatase conjugated)	Sigma	1:1000	5% low-fat milk powder in TBS
anti-mouse (goat, alkaline phosphatase conjugated)	Sigma	1:1000	5% low-fat milk powder in TBS
anti-goat (rabbit, alkaline phosphatase conjugated)	Sigma	1:1000	5% low-fat milk powder in TBS

Table 10.1: Antibodies used for Immunoblotting or Electrophoretic Mobility Shift Assay.

Substance	Purchased from	Working dilution
U0126	Alexis	10 mM in DMSO
PMA	Sigma	100 µM in DMSO
MG-132	Calbiochem	10 mM in DMSO

Table 10.2: Substances used for incubation of transfected HeLa cells.

Mutant	Primer	Sequence (5´ to 3´)
T128A	T128A-for	GTTGTAGGTGGGCGCCAGCGGCTCAGC
	T128A-rev	GCTGAGCCGCTGGCGCCCACCTACAAC
T153A	T153A-for	CATTGACGGGCACGCACCTGAGG
	T153A-rev	CCTCAGGTGCGTGCCCGTCAATG
S173A	S173A-for	CATACAGCCTGCACCAGACCAG
	S173A-rev	CTGGTCTGGTGCAGGCTGTATG
T193A	T193A-for	CAATATGTGACTACGCCCCAGCATCAG
	T193A-rev	CTGATGCTGGGGCGTAGTCACATATTG
S210A	S210A-for	GACACAGTTGGTGCAGTCTCGCCGTTG
	S210A-rev	CAACGGCGAGACTGCACCAACTGTGTC
S332A	S332A-for	CGTCGGGTGCGGCATACTTC
	S332A-rev	GAAGTATGCCGCACCCGACG
T128D	T128D-for	TGAGCCGCTGGATCCCACCTAC
	T128D-rev	GTAGGTGGGATCCAGCGGCTCA
T128E	T128E–for	TGAGCCGCTGGAGCCCACCTAC
	T128E–rev	GTAGGTGGGCTCCAGCGGCTCA

Table 10.3: Primers used for site directed mutagenesis on pET28a-RORα4 or pSG5-RORα4 in order to mutate putative ERK phosphorylation sites.

Fragment	Primer	Sequence (5´ to 3´)
Bmal1-prom	Bmal1-MluI-for	GATAACGCGTCCCAGAGAAGAGGGACATCCCGG
	Bmal1-XhoI-rev	GATACTCGAGCGCGCCCGCACTCGGATCCCGC
Bmal1-iso A	B_A_EcoRI-for	TAGAGAATTCATGGCAGACCAGAGAATGGAC
	B_BglII-rev	TAGGAGATCTTTACAGCGGCCATGGCAAGTC
Bmal1-iso B	B_B_EcoRI-for	TAGAGAATTCATGATTAATATAGAAAGCATGGACACAG
	B_BglII-rev	TAGGAGATCTTTACAGCGGCCATGGCAAGTC

Table 10.4: Primers used for cloning of the Bmal1-promoter and Bmal1 protein isoforms A and B from genomic DNA and cDNA of Mono Mac 6 cells, respectively.

Fragment	Primer	Sequence (5´ to 3´)
HI-LBD-1	HI-LBD-1-HindIII-for	GCTCAAGCTTGTCTCGAGATGCTGTAAAATTTGGC
HI-LBD-2	HI-LBD-2-HindIII-for	GCTCAAGCTTGCAGAAACACCGGATGCAGCAG
HI-LBD-3	HI-LBD-3-HindIII-for	GCTCAAGCTTGACGCCCACCTACAACATCTCG
HI-LBD-4	HI-LBD-4-HindIII-for	GCTCAAGCTTGGACGGGCACACCCCTGAGG
HI-LBD-5	HI-LBD-5-HindIII-for	GCTCAAGCTTGCCTTCCCCAGACCAGTCAGGTC
HI-LBD-6	HI-LBD-6-HindIII-for	GCTCAAGCTTGCCAGCATCAGGCTTCTTTCCC
HI-LBD-1-6	HI-LBD-Acc65l-rev	ATCTGGTACCTTACAGCCATGAGCGATCTGCTG

Table 10.5: Primers used for the generation of RORα truncation mutants for determination of anti-RORα antibody epitope.

Mutant	Primer	Sequence (5´ to 3´)
K89A	K89A-for	GATGCTGTAGCATTTGGCCGAATG
	K89A-rev	CATTCGGCCAAATGCTACAGCATC
K185A	K185A-for	CAATGGAATCGCTCCAGAACCAATATG
	K185A-rev	CATATTGGTTCTGGAGCGATTCCATTG
K302A	K302A-for	CAAATTGTGCTTCTAGCTGCAGGTTCTC
	K302A-rev	GAGAACCTGCAGCTAGAAGCACAATTTG
T193A	K386A-for	GAAAAGGTAGCAATTGAAAAACTGCAACAG
	K386A-rev	CTGTTGCAGTTTTTCAATTGCTACCTTTTC

Table 10.6: Primers used for site directed mutagenesis on pSG5-RORα4 in order to mutate putative sumoylation motifs.

Primer	Sequence (5´ to 3´)
SUMO1-SpeI-for	GCCACCACTAGTATGTCTGACCAGGAGGCAAAACCTTC
SUMO1-HindIII-rev	GCCACCAAGCTTAACTGTTGAATGACCCCCCGTTTG

Table 10.7: Primers used for cloning of SUMO1 on cDNA of Mono Mac 6 cells.

Fragment	Primer	Sequence (5´ to 3´)
MEK1-481	MEK1-481-HindIII-for	ACTTAAGCTTATGCCCAAGAAGAAGCCGAC
	MEK1-481-EcoRV-rev	GTTCAGGAATTCTTCCAGCTTTC
MEK1-701	MEK1-701EcoRV-for	GAAAGCTGGAAGAATTCCTGAAC
	MEK1-701XhoI-rev	TAGACTCGAGTTAGACGCCAGCAGCATGGG

Table 10.8: Primers used for cloning of MEK1 on cDNA of Mono Mac 6 cells.

Mutant	Primer	Sequence (5´ to 3´)
MEK1-S218E	S218E-for	GACATCTGGGAGATGGGACTG
	S218E-rev	CAGTCCCATCTCCCAGATGTC
MEK1-S218E-S222D = ca-MEK1	S222D-for	GATGGGACTGGATCTGGTAGAGATG
	S222D-rev	CATCTCTACCAGATCCAGTCCCATC
MEK1-K97M = dn-MEK1	K97M-for	GTCATGGCCAGAATGCTAATTCATC
	K97M-rev	GATGAATTAGCATTCTGGCCATGAC

Table 10.9: Primers used for site directed mutagenesis on pSG5-MEK1 in order to generate a constitutive active (ca) and a dominant negative (dn) MEK1.

11 PUBLICATIONS

Publication I

Lechtken A., Zündorf I., Dingermann T., Firla B., Steinhilber D., Overexpression, refolding, and purification of polyhistidine-tagged human retinoic acid related orphan receptor RORalpha4. Protein Expr. Purif. 49 (2006) 114-120.

Publication II

Lechtken A., Hörnig M., Werz O., Corvey N., Brandes R., Zündorf I., Dingermann T., Steinhilber D., Extracellular signal-regulated kinase-2 phosphorylates RORα4 *in vitro*. Biochem. Biophys. Res. Commun. 358 (2007) 890-896.

12 CURRICULUM VITAE

Persönliches

Adriane Lechtken
geboren am 13. Juni 1977 in Erlangen

Schul- und Hochschulausbildung

seit Jan 2007	Stipendiatin des EU-Graduiertenkollegs "Role of Eicosanoids in Biology and Medicine"
seit Aug 2003	Durchführung der Promotionsarbeit am Institut für Pharmazeutische Chemie der Universität Frankfurt/Main unter der Leitung von Prof. Dr. D. Steinhilber
Juni 2003	Dritte Pharmazeutische Prüfung und Erteilung der Approbation als Apothekerin
Nov 2002 - April 2003	Praktikum in der galenischen Entwicklung der Pfizer GmbH Arzneimittelwerk Gödecke in Freiburg
Mai 2002 - Okt 2002	Praktikum in der Apotheke an der Bergstraße in Weinheim
April 2002	Zweite Pharmazeutische Prüfung
April 1998 - März 2002	Studium der Pharmazie an der Ruprecht Karls-Universität Heidelberg
Mai 1997	Allgemeine Hochschulreife
1988 -1997	Wilhelm von Humboldt Gymnasium Ludwigshafen
1984-1988	Robert Schumann Grundschule Frankenthal

Kongressbeiträge mit Abstract und Poster

2006	„RORα4 is phosphorylated by extracellular-signal regulated kinase", Jahrestagung der DPhG und GdCh in Frankfurt/Main
2005	„Overexpression and Refolding of the Retinoic Acid Related Orphan Receptor alpha", DPhG Doktorandentagung in Mainz

Publikationen

- Lechtken A., Zündorf I., Dingermann T., Firla B., Steinhilber D., Overexpression, refolding, and purification of polyhistidine-tagged human retinoic acid related orphan receptor RORalpha4. Protein Expr. Purif. 49 (2006) 114-120.
- Lechtken A., Hörnig M., Werz O., Corvey N., Brandes R., Zündorf I., Dingermann T., Steinhilber D., Extracellular signal-regulated kinase-2 phosphorylates RORα4 *in vitro*. Biochem. Biophys. Res. Commun. 358 (2007) 890-896.

Praktika, Weiterbildung, Lehrtätigkeit

seit 2004	Vertretungen in der Apotheke an der Berstraße in Weinheim
seit Aug 2003	Fortbildung zur Fachapothekerin für Pharmazeutische Analytik bei der Landesapothekerkammer Hessen
Aug 2003 – Jan 2007	Betreuung von Pharmaziestudenten des 4. Semesters im Praktikum „Instrumentelle Analytik“
Mär-Nov 2001	Hilfswissenschaftlerin in der Krankenhausapotheke des Universitätsklinikums Heidelberg
Mär/Apr 2001	Werksstudentin (5-wöchig) bei Abbott in Ludwigshafen
Jul 1997	Praktikum (3-wöchig) in der BASF AG Ludwigshafen

Akademische Lehrer

Meine akademische Lehrer neben Herrn Prof. Dr. Dieter Steinhilber waren:

Prof. Dr. R. Claus	Prof. Dr. G. Fricker
Prof. Dr. M. Wiessler	Dr. R. Dillmann-Marschner
Prof. Dr. H.-P. Deigner	Dr. G. Reich
Prof. Dr. T. Lindel	Prof. Dr. R. Zawatzky
Prof. Dr. M. Wink	Prof. Dr. H. Ludwig
Prof. Dr. J. Reichling	Prof. Dr. R. H. A. Fink
Prof. Dr. U. Hilgenfeldt	Prof. Dr. D. Krüger

13 DANKSAGUNG

An dieser Stelle möchte ich mich ganz herzlichen bedanken bei

...Prof. Dieter Steinhilber für die Aufnahme in seinen Arbeitskreis, die stets freundliche und geduldige Betreuung, für die Freiheit allen eigenen Ideen nachkommen zu dürfen, der Unterstützung und dem entgegengebrachten Vertrauen beim (nicht immer leichten) Wachsen zur absoluten Selbstständigkeit;
...Prof. Oliver Werz für den sehr netten und unkomplizierten Umgang, das Interesse an meiner Arbeit, die „zündenden" Ideen und das Überlassen der Wohnung;
...Prof. Theo Dingermann und Ilse Zündorf für das Impfen der kleinen Mäuschen und das Geschick und den Fleiß bei der Herstellung eines perfekten Antikörpers;
...Prof. Ralf Brandes für das stundenlange und gewissenhafte EGFP-Mikroskopieren und das kollegiale Miteinander;
...Beate Firla für die Starthilfe zu Beginn meiner Arbeit;
...Nadine Meindl, die mir das eigenverantwortliche Arbeiten und das Generieren von neuen Ideen beigebracht hat;
...Astrid Brüggerhoff für ihren Fleiß beim Präparieren von Maxis und Ansetzen der Zellen;
...Brigitte Welter für das Besorgen von Literatur, das Korrekturlesen und die Gespräche über die süßen und sauren Seiten des Lebens;
...Michael Hörnig für die in-gels, die netten Gespräche über knifflige Methoden und die Sprungbereitschaft bei Computerkrankheiten;
...Nicole Schnur für die stets geduldige Hilfe bei allen möglichen und unmöglichen Labor- und Lebensproblemen;
...Kirsten Stoffers, ohne die ich niemals nach Frankfurt gekommen wäre;
...Sabine Lindner und Marika Hoffmann für die angenehme Labornachbarschaft;
...meinem Mitstreiter Michael Ermisch für die in-gels, für seine Begeisterungsfähigkeit für das zickigste Protein der Welt und das ausdauernde Hochhalten der RORα-Flagge;
...Lars Tausch für seine Geduld mit mir in schweren Zeiten, dem gemeinsamen „in die Schule gehen" und den Feierabend-Bierchen;
...Christian Feißt für allerschönste Kaffeepausen in der Sonne, die Einführung in das Frankfurter Nachtleben und die mallorquinischen Strände, die ehrliche Beratung zu allen Lebensfragen und die beste Freundschaft;

...den Assistenten des vierten Semesters Sandra Hoffmann, Carsten Corvey, Malte Schürken, und Benjamin Rietschel für die lustige Zeit im Praktikum, beim Korrigieren von Klausuren und Protokollen; Ute Bahr für die perfekte Semesterleitung und das mir entgegengebrachte Vertrauen im Umgang mit Studenten; Daniel Engelhard für das Einfüllen der Analysen;
...meinen Studenten, die mir eine willkommene Abwechslung zum alltäglichen Forscherfrust waren, sowohl innerhalb als auch außerhalb der Praktikumszeiten;
...allen derzeitigen und ehemaligen Mitgliedern des Arbeitskreises für die unterhaltsamen Diskussionen in der Kaffee- und 11.30 h-Mittagspause, den Freitags-Sekt, Stammtischen und Dichtrunden;
...allen Mitarbeitern der Frankfurter Pharmazie für ihre freundliche Aufnahme.

Mein ganz besonderer Dank gilt meinen Eltern, meiner Schwester Annette und meinen Freunden, die stets geduldig mit mir waren, die mich in guten wie in schwierigen Zeiten tatkräftig unterstützt und nie den Glauben an mich verloren haben.